Centro Universitario de la Región Este, Universidad de la República

Uruguay

ROLE OF THE DOMINANT PRIMARY PRODUCER AND THE ASSOCIATED TROPHIC STRUCTURE ON CARBON FLUXES (CO_2 AND CH_4) IN SHALLOW LAKES

ROL DEL PRODUCTOR PRIMARIO DOMINANTE Y DE LA ESTRUCTURA TRÓFICA ASOCIADA, SOBRE LOS FLUJOS DE CARBONO (CO_2 Y CH_4) EN LAGOS SOMEROS

Autora: Maite Colina

Orientadoras: Mariana Meerhoff y Sarian Kosten

Maldonado, Uruguay

(Octubre 2022)

El formato de presentación de esta tesis es por compendio de artículos, constando de tres artículos que se corresponden a los capítulos 2, 3 y 4. Dos de los artículos (capítulos 2 y 3) ya se encuentran publicados en revistas arbitradas, y el último artículo (capítulo 4) será sometido luego de la defensa de tesis.

A continuación, se detalla las referencias e información correspondiente a las revistas (área temática y ranking) para los dos artículos publicados, así como la información sobre la revista donde se planea someter el último artículo.

Capítulo 2:

Colina, M., S. Kosten, N. Silvera, J. M. Clemente, & M. Meerhoff, 2021. Carbon fluxes in subtropical shallow lakes: contrasting regimes differ in CH4 emissions. Hydrobiologia. DOI: 10.1007/s10750-021-04752-1.

Scope Aquatic Science

Ranking Q1

Capítulo 3:

Colina, M., M. Meerhoff, G. Pérez, A. J. Veraart, P. L. E. Bodelier, & S. Kosten, 2021. Trophic and non-trophic effects of fish and macroinvertebrates on carbon emissions. Freshwater Biology 66: 1831–1845. DOI: 10.1111/fwb.13795.

Scope Aquatic Science

Ranking Q1

Capítulo 4:

Colina, M., Meerhoff, M., Kosten, S. Experimental warmer conditions promote stronger carbon dioxide uptake by freshwater pelagic communities dominated by cyanobacteria, with poor incorporation of carbon into the classic trophic web.

A someter en: Inland Waters

Scope Aquatic Science

Ranking Q1

AGRADECIMIENTOS

Esta tesis fue posible en el marco del Programa para el Desarrollo de las Ciencias Básica (Geociencias, PEDECIBA, Uruguay).

La Agencia Nacional de Investigación e Innovación (ANII, Uruguay) otorgó la beca de posgrado que me permitió dedicarme a esta tesis durante los primeros 3 años de trabajo. Así como, una beca de Movilidad que me permitió realizar en 2019 una estancia de 6 meses en los Países Bajos y llevar adelante uno de los experimentos fundamentales de la tesis.

El trabajo de campo en Uruguay fue posible gracias al Academy Ecology Fund 2018, otorgado por la Royal Netherlands Academy of Arts and Sciences (KNAW).

El último experimento realizado para esta tesis fue posible gracias a los apoyos financieros (alícuotas) de PEDECIBA y a la financiación otorgada por la International Society of Limnology (SIL), Tonolli Award 2020.

Todo el trabajo comprendido en esta tesis nunca hubiese sido posible sin el apoyo y la participación de muchas personas que de una forma u otra formaron parte de las diferentes etapas de este proceso, y a las que me gustaría agradecer:

Mis supervisoras, Mariana y Sarian, fueron ambas una guía y apoyo fantástico durante todo el proceso de la tesis. Les agradezco mucho todas las horas, la energía y el cariño que ellas también volcaron en cada etapa. Me ayudaron a crecer, no solo a través del conocimiento científico que aportaron, sino también al transmitirme su confianza y entusiasmo. Ambas me enseñaron, por sobre todas las cosas, a disfrutar de la aventura de hacer ciencia.

Los integrantes del Grupo de Ecología y Rehabilitación de Ecosistemas Acuáticos del CURE de Maldonado. Muy especialmente Margeny, Maite, Lucía, Clementina y Miriam, con quienes además de compartir en el laboratorio o en el campo también compartimos muchos cierres de jornada con ricas cenas y charlas sobre la vida fuera de la ciencia.

Los integrantes del IWWR de Radboud, que me hicieron sentir muy bienvenida durante mi estadía en Nijmegen, entre ellos Janneke Roelofs, Ralph Aben, Sarian, Gijs van Dijk, Leon Lamers.

El grupo el trabajo con quienes compartí este último año: Coti, Lea, Flor, Clemen y Emi. Las muchas horas de campo de Ponderful no hubiesen sido lo mismo sin este super equipo de gente.

Las amigas de la vida: Vicky, Valen, Romi y Franca.

Martín, que a pesar de que la vida nos encuentra ahora en un lugar diferente de cuando empecé el doctorado, sé que con él voy a poder contar siempre como aliado y amigo. Gracias por convencerme de que, en lugar de abandonar la idea de hacer ciencia, me animara a iniciar la aventura que fue esta tesis.

Mi familia que siempre apoya todos los planes que se me ocurren, y especialmente a mi sobrina Inés que nació en la etapa final de la escritura.

TABLE OF CONTENTS

RESUMEN

En los últimos años se ha evidenciado el rol que los ecosistemas de agua dulce pueden tener sobre el ciclo global del carbono y por tanto sobre el clima. En particular, los lagos someros pueden actuar como fuente o sumidero de gases de efecto invernadero (GEI, como dióxido de carbono (CO_2) y metano (CH_4)), cuya producción y consumo está determinada por la interacción entre factores abióticos (e.g., temperatura y disponibilidad de oxígeno) y bióticos (e.g., estructura e interacciones biológicas). Esta tesis pretende contribuir a comprender cómo regímenes relativamente estables y contrastantes en lagos someros afectan los flujos de CO_2 y CH_4, combinando análisis a diferentes escalas y bajo el escenario de cambio global actual. Se analizaron los flujos totales de CO_2 y CH_4 entre lagos subtropicales con regímenes contrastantes (i.e., dominancia de macrófitas sumergidas, de fitoplancton, o la casi ausencia de productores primarios) comparados a nivel de hábitat y ecosistema, registrándose las mayores emisiones de CH_4 en condiciones de dominancia de fitoplancton. Mediante un experimento a escala de mesocosmos se evaluaron las emisiones de carbono en función de la actividad de peces a nivel de la columna de agua y del sedimento, evidenciando un rol preponderante de los procesos bentónicos sobre los pelágicos. Por último, los cambios en el balance entre fijación y emisión de CO_2 en condiciones eutróficas y como respuesta al calentamiento climático, se evaluaron en un experimento a escala de microcosmos con foco en procesos pelágicos. Comunidades planctónicas con composiciones de fitoplancton contrastantes (i.e., dominancia de algas verdes o cianobacterias) mostraron un aumento de la fijación de CO_2 ante mayores temperaturas, fundamentalmente en aquellas dominadas por cianobacterias. Sin embargo, una muy baja proporción del carbono fijado resultó ser incorporado a la vía trófica planctónica, quedando disponible para su potencial mineralización. Mediante los abordajes empleados evidenciamos la importancia del acoplamiento entre zonas o hábitats de los lagos someros (e.g., pelágico-litoral, pelágico-bentónico) sobre los flujos de carbono, y que si bien, escenarios eutróficos y más cálidos facilitarían la fijación de CO_2 podrían en contrapartida potenciar las emisiones de CH_4. Los resultados generados contribuyen a mejorar las predicciones sobre el rol de los ecosistemas de agua dulce someros al balance global del carbono.

Palabras clave: lagos someros, productores primarios, estructura trófica, dióxido de carbono, metano

ABSTRACT

Shallow lakes can act as sources or sinks of greenhouse gasses (GHG), such as carbon dioxide (CO_2) and methane (CH_4). Their production and consumption in aquatic ecosystems are determined by the interaction between abiotic (e.g., temperature and oxygen availability) and biotic (e.g., structure of biological communities and their interactions) factors. In shallow lakes, different levels of anthropogenic impact (i.e., nutrients input) can promote different regimes characterized by different dominant primary producers and associated trophic structures. This thesis aims to contribute to the understanding of how the combination of physical, chemical and biological factors, associated with different regimes, affects the fluxes of CO_2 and CH_4 in shallow lakes. Thus, through combining analyzes at different scales and under the consideration of the current global scenario of worldwide eutrophication and climate warming. Clear differences in total CH_4 fluxes were found between subtropical shallow lakes with contrasting regimes (i.e., dominated by submerged macrophytes, phytoplankton, or almost absence of primary producers) compared at the habitat and ecosystem level, with the highest emissions at phytoplankton-dominated regime. Trophic and non-trophic effects of fish in the water column and at the water-sediment interface were evaluated in a mesocosm experiment, where a preponderant role of benthic processes over pelagic ones was evidenced. The potential changes in the metabolic balance (i.e., CO_2 uptake: efflux) in eutrophic ecosystems subjected to warmer temperatures, were evaluated in a microcosm experiment with contrasting phytoplankton compositions (i.e., chlorophytes-dominated versus cyanobacteria-dominated). A clear increase in CO_2 fixation was observed with warmer temperatures, mainly for cyanobacteria-dominated systems. However, an extremely low proportion of the fixed carbon was potentially incorporated towards the biomass of plankton communities. The different approaches in this thesis stress out the relevant role on carbon fluxes of the coupling between the different zones in shallow lakes (e.g., pelagic-littoral, pelagic-benthic). Besides, even when eutrophic and warmer scenarios might facilitate CO_2 uptake in shallow lakes, might also enhance CH_4 emissions. The results generated will help improve predictions about the contribution of shallow lakes to the global carbon balance.

Key words: shallow lakes, primary producers, trophic structure, carbon dioxide, methane.

CHAPTER 1

GENERAL INTRODUCTION

The role of freshwater ecosystems on the global carbon balance

Just in the first two decades of the XXI century, Earth's mean surface temperature increased by 0.99ºC compared to the previous 150 years. By the end of the century a mean temperature rise higher than 4ºC is further expected (IPCC, 2021). Since CO_2 and CH_4 are the main greenhouse gases (GHG) in driving global climate, understanding and quantifying their contributions from the different compartments – including terrestrial and aquatic - on Earth is highly relevant in order to generate accurate predictions on climate change and to plan the most effective mitigation measures. Including GHG contributions (i.e. both emissions and retention) by freshwater ecosystems is increasingly recommended by the IPCC for the elaboration of GHG national inventories (IPCC, 2006, 2013, 2019).

Mainly over the last decade, massive empirical evidence has contributed to changing the general perception about freshwater ecosystems being passive conduits in the global carbon cycle (Forbes, 1887; Salonen et al., 1983; Tranvik, 1988), i.e. transporting carbon from land to the sea, to the current vision positioning these ecosystems as highly active compartments (Cole et al., 2007; Tranvik et al., 2009, 2018). Nowadays, it is widely recognized that large quantities of carbon are received, transformed, stored, and emitted into the atmosphere by freshwaters all around the globe (Tranvik et al., 2009; Cole, 2013; DelSontro et al., 2018). Gross estimations suggest that the amount of organic carbon annually buried in the sediments of freshwater ecosystems exceeds the amount of organic carbon sequestered by the ocean floor (Tranvik et al., 2009; Cole, 2013), thus highlighting their role as an important global reservoir of carbon. But in fact, freshwaters do also act as relevant sources of carbon to the atmosphere. GHG emitted from freshwater ecosystems, such as carbon dioxide (CO_2) and methane (CH_4), account for approximately 75% of the total GHG sequestered by land ecosystems (excluding inland waters). The emissions of CH_4 alone, which has a radiative forcing 34 times stronger than CO_2 in a 100 years horizon (Myhre et al., 2013), counteracts around the 25% of the GHG terrestrial sink (Bastviken et al., 2011; DelSontro et al., 2018).

Production, consumption and fluxes of CO_2 and CH_4 in shallow lakes

Despite shallow lakes and ponds only represent 8.6% of the Earth's surface covered by inland waters, these ecosystems are the most abundant and widely distributed among fresh waters (Meerhoff & Jeppesen, 2009; Downing, 2010; Verpoorter et al., 2014). Their shallow depth potentially allows for light penetration to the bottom in most of if not the entire lake (Meerhoff & Jeppesen, 2009). Particularly in small lakes, the low water volume also allows for a high concentration of terrestrial inputs of organic matter and nutrients (Wetzel, 2001; Cole et al., 2006; Downing, 2010). In consequence, high productivity and high recycling of matter often occurs in ponds and shallow lakes, which translates into a disproportional contribution in terms of carbon emissions, representing around 15% of the CO_2 and more than 40% of the CH_4

emissions from lentic freshwater ecosystems globally (Holgerson & Raymond, 2016; DelSontro et al., 2018).

Despite much attention has been devoted to understand the main factors behind the provision of ecosystem services such as biodiversity hotspots, water supply, nutrient retention, cultural and aesthetic values, and hydrological cycle regulation, among others (Montoya & Raffaelli, 2010; Schallenberg et al., 2013; Hilt et al., 2017; Janssen et al., 2020), the main factors driving the role of these ecosystems as potential sources or sinks of CO_2 and CH_4 are still insufficiently known (e.g. Williamson et al., 2009; Moss, 2010; Hilt et al., 2017).

The exchange or flux (i.e., net uptake and/or release) of CO_2 and CH_4 between any aquatic ecosystem and the atmosphere occurs through different pathways, being the magnitude and the direction of the fluxes related to the combination of physical, chemical, and biological factors (Bastviken et al., 2008). The incorporation of CO_2 relies on the primary production of aquatic plants, algae, and cyanobacteria (gross primary production – GPP), whereas the release of CO_2 occurs by the respiration of all biological communities (ecosystem respiration – ER) (Odum, 1956; Trolle et al., 2012; Cole, 2013) (Fig.1). Commonly, shallow lakes are often characterized as net heterotrophic ecosystems and as net CO_2 sources (Cole et al., 2006), given that trophic webs have been traditionally assumed as mainly sustained through allochthonous organic (Cole et al., 1994; Jansson et al., 2007) and inorganic carbon (Weyhenmeyer et al., 2015). In shallow waters with a well oxygenated water-sediment interface, a large proportion of the organic carbon deposited into the sediments will be mineralized through aerobic decomposition and can significantly contribute to total CO_2 emissions (Kortelainen et al., 2006). Under conditions of no significant inputs of terrestrial carbon, however, net ecosystem CO_2 uptake can occur as has been previously reported (Laas et al., 2012; Pacheco et al., 2014; Jeppesen et al., 2016).

The production and consumption of CH_4 is conducted entirely by components of the microbiota (Fig. 1). Mainly in organic matter-rich sediments, and mainly under anoxic conditions, CH_4 can be produced by methanogenic Archaea (Biderre-Petit et al., 2011; Borrel et al., 2011). Although recent evidence has shown that, probably with minor relative contributions to total emission, oxic CH_4 production can also occur (Günthel et al., 2019), and the role of cyanobacteria in this production has been recently proposed (Bizic et al., 2018; Bižić et al., 2020). Under oxic conditions, methane oxidizing bacteria (MOB) oxidize CH_4 to CO_2 in the water column or in oxygenated water-sediment interfaces (Biderre-Petit et al., 2011; Borrel et al., 2011). Although dissolved CH_4 can be oxidized in the water column before reaching the atmosphere, in shallow waters a large proportion of the CH_4 produced in the sediments can actually reach the surface and diffusion can also contribute significantly to total CH_4 emissions (Bastviken et al., 2004, 2008; Holgerson & Raymond, 2016). In addition, as diffusion strongly depends on wind action on water surface, carbon emission (of both CH_4 and CO_2) through diffusion will be facilitated in large and wind-exposed shallow lakes (Cole & Caraco, 1998; Bastviken et al., 2004). CH_4 can also be emitted from shallow waters through plant mediated emissions, and through ebullition. The first process occurs mainly in vegetated littoral zones with rooted emergent plants, which might transport CH_4 from the sediments to the atmosphere through their tissues (Villa et al.,

2020; Bodmer et al., 2021). Ebullition, in contrast, occurs mainly in open waters and comprise the release of gas bubbles from highly productive sediments. Recent evidence suggests that ebullition usually may represent the major proportion of the total CH_4 emissions in shallow lakes, being a more relevant pathway than in deep lakes where hydrostatic pressure prevents bubble release (Bastviken et al., 2004, 2011) and rising bubbles may largely dissolve before reaching the surface (Bastviken et al., 2008).

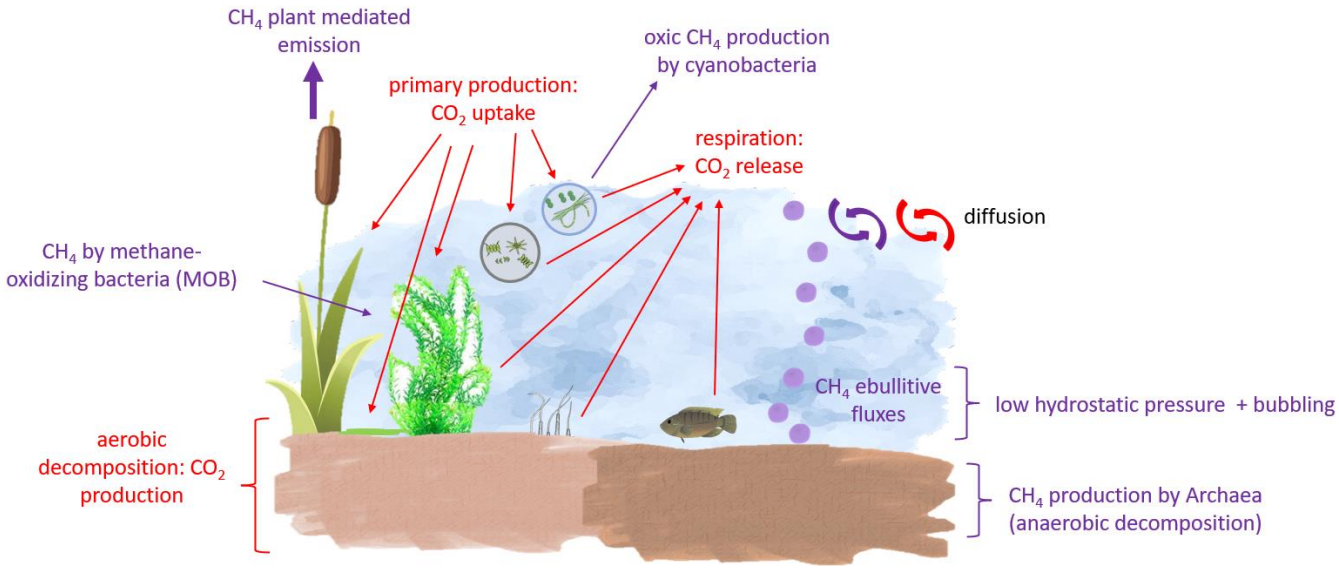

Figure 1. Schematic summary of the main pathways for CO_2 (in red) and CH_4 (in violet) fluxes in shallow lakes. Drawing: M. Colina (except for fish, drawn by Javier Gorga).

The behavior of shallow lakes in the carbon cycle may strongly vary according to their dominant regime. Commonly as a function of nutrient concentrations (typically total phosphorous), shallow lakes can occur at alternative equilibria or (relatively) stable regimes characterized by contrasting configurations in their trophic structures (Scheffer et al., 1993, 2003). These alternative regimes strongly differ in their general functioning, affecting several ecosystem services and processes, among them, general lake metabolism and the in-lake carbon processing (Hilt et al., 2017; Janssen et al., 2020), with consequences for the carbon fluxes (CO_2 and CH_4) between the aquatic ecosystem and the atmosphere (Xing et al., 2006; Brothers et al., 2013). The presence of stable and well-developed submerged macrophyte beds promote the perpetuation of clear water conditions in shallow lakes, through reducing nutrient availability for phytoplankton growth, and by limiting light and sediment resuspension (Scheffer et al., 1993). In addition, submerged macrophytes often provide habitat and refuge for large-bodied zooplankton and to small planktivorous fish and macroinvertebrates, particularly in the temperate zone (Meerhoff et al., 2007a, 2007b), enhancing the diversity of consumers and carbon assimilation by higher trophic levels (Kosten et al., 2009).

Regarding carbon fluxes, different effects have been reported as a consequence of the presence of submerged macrophytes. Intense primary production by submerged macrophytes during daytime and particularly during the warm seasons, with significant CO_2 uptake, has been reported (Natchimuthu et al., 2014; Davidson et al., 2015). However, a wide diversity of consumers and well oxygenated sediments can fuel ecosystem respiration and net CO_2 efflux (Brothers et al., 2013; Jeppesen et al., 2016). In turn, plant leaves (in the water column) and roots (at the sediments, through the radial oxygen loss – ROL; Lemoine et al., 2012) can enhance dissolved oxygen (O_2) availability, facilitating CH_4 oxidation and hampering CH_4 production. Therefore, even when macrophytes tissues might contribute with organic matter substrate for CH_4 production (Grasset et al., 2019), less total CH_4 emissions might occur in the presence than in the absence of submerged macrophytes (Sorrell et al., 2002; Sorrell & Downes, 2004; Yoshida et al., 2014).

Due to their low volume: surface ratio, shallow lakes are extremely vulnerable to external stressors, not least terrestrial inputs of nutrients and other contaminants that promote anthropogenic eutrophication (Smith et al., 1999). In this context, after certain (climate dependent) thresholds in TP loadings, and often after a perturbation event, the development of phytoplankton or free-floating plants may preclude submerged macrophytes (Scheffer et al., 2003; de Tezanos Pinto & O'Farrell, 2014). Particularly without nutrient limitation, cyanobacteria may became the dominant taxonomic group in phytoplankton-dominated ecosystems (Moss, 2011; O'Neil et al., 2012). Given the poor-quality food for zooplankton, plus their potential toxicity (Ahlgren et al., 1990; DeMott, 1999; Paerl & Paul, 2012; Colina et al., 2016), cyanobacterial-dominance promotes the pauperizing of the entire trophic web and lower carbon assimilation by high trophic levels (Ger et al., 2014). In consequence, even when intense primary production with an intense CO_2 uptake can occur (Balmer & Downing, 2011; Pacheco et al., 2014), the also high organic matter accumulation on the sediments and consequent anoxic conditions might fuel CH_4 production and emissions (Yan et al., 2017; Beaulieu et al., 2019; Yang et al., 2019). On top, the recently found potential role of cyanobacteria producing CH_4 during photosynthesis (Bižić et al., 2020), indicating the occurrence of positive feedbacks with climate warming.

Carbon processing inside shallow lakes: relevance of habitats

Three habitats or zones are usually recognized in shallow lakes: the littoral, the pelagic and the benthic zones (Wetzel, 2001; Scheffer, 2004), with potentially a strong interconnection in terms of energy, nutrients, organisms, and information fluxes (Schindler & Scheuerell, 2002; Meerhoff & Jeppesen, 2009; Kosten & Meerhoff, 2014). The strength of the interconnection and the relative importance of each habitat for the whole lake functioning strongly depends on the dominant regime (Liboriussen & Jeppesen, 2003, 2006). For example, pelagic fish and zooplankton can use littoral vegetated zones for refuge, reproduction, or feeding areas, even temporarily during different ontogenetic stages or at a diel basis (Meerhoff et al., 2007; Meerhoff

& Jeppesen, 2009; Kosten & Meerhoff, 2014). Particularly, fish can represent and important link between the different lake zones, given their ontogenetic and diel changes in the use of the space, mobility and wide feeding habits and resource use (Schindler & Scheuerell, 2002; Vander Zanden & Vandeboncoeur, 2002; Kosten & Meerhoff, 2014).

Understanding such interconnection is also needed to understand and predict carbon processing, and to predict CO_2 and CH_4 fluxes. Vegetated littoral zones comprise the interface between the terrestrial and the aquatic ecosystems and may receive relatively high inputs or carbon from the surrounding lands (Wetzel, 1992; Juutinen et al., 2003; Jansson et al., 2007). Depending on the aerial extent of this habitat, the relative contribution of autochthonous carbon to the food web of shallow lakes increases from the littoral to the pelagic habitat (Marczak et al., 2007; Doi, 2009). It could thus be expected that a stronger carbon processing takes place in the littoral than in the pelagic zone, and correspondingly stronger CO_2 and CH_4 emissions occur in the littoral area (Juutinen et al., 2003). Such littoral-pelagic coupling is, however, expected to weaken under eutrophic conditions with high phytoplankton biomasses and poorly developed vegetated zones.

Benthic-pelagic coupling is also crucial in shallow waters (Vadeboncoeur et al., 2002; Van de Bogert et al., 2007; Kosten & Meerhoff, 2014). Primary and secondary production are often largely sustained by interactions between both lake zones. Decomposition in the pelagic zone supplies organic matter to the benthos, whereas carbon and nutrient remineralization in the sediments sustain production processes at the water column (Schindler & Scheuerell, 2002; Chumchal & Drenner, 2004; Geurts et al., 2010). This interplay between benthic and pelagic processes might be crucial for carbon processing and water-atmosphere fluxes (CO_2 and CH_4).

Fish feeding activities at the different lake zones can directly and indirectly affect carbon processing and overall ecosystem fluxes. In the pelagic zone, trophic cascade effects from planktivorous fish feeding on large-bodied zooplankton might facilitate an increase in MOB biomass, by weakening zooplankton grazing impact on bacteria (Devlin et al., 2015). In consequence, CH_4 oxidation in the water column could be enhanced (Devlin et al., 2015). This highlights that fish feeding activity in the pelagic habitat might deeply affect the recycling of CH_4, often produced in the lake sediments, into the pelagic food web (Bastviken et al., 2003; Jones & Grey, 2011; Sanseverino et al., 2012; Devlin et al., 2015). Besides promoting turbid conditions by uprooting submerged macrophytes and releasing nutrients and suspended solids from the sediments (Zambrano et al., 2001; Datta et al., 2009; Rahman, 2015), fish feeding on benthic resources can indirectly affect carbon fluxes through their effect on O_2 availability in the sediment-water interface, and in consequence affect the main carbon mineralization pathway (i.e., aerobic versus anaerobic). Fish predation upon burrowing benthic macroinvertebrates, such as tubifex worms, can hamper the bioirrigation or the water-sediment interface that occurs when tubifex worms pump oxygenated water into their burrows (Leal et al., 2007; Baranov et al., 2016). In addition, fish mechanical disturbance of the sediments can also increase the release of bubbles, increasing CH_4 ebullition (Bhattacharyya et al., 2013; Ma et al., 2018). However, intense bioturbation pressures have also been linked to sediment-water interface oxygenation and a reduction in total CH_4 emissions (Oliveira Junior et al., 2019) and potentially

an increase in CO_2 emissions due to aerobic decomposition in the sediments (Baranov et al., 2016). The net outcome on overall lake carbon fluxes of fish, and particularly of different fish guilds, is therefore still unclear.

The role of shallow lakes in the carbon cycle, under a climatic warming scenario

Climate change, and particularly the current warming processes, is strongly dependent on the carbon cycle, and in turn, the carbon cycle is affected by the effects of climate change on the local biota (Battin et al., 2009). Particularly for shallow lakes due to their high sensitivity to external conditions, changes in the frequency and intensity of rains and storms might have strong effects on the general regimes and in the interconnection between lake zones, that ultimately will affect CO_2 and CH_4 fluxes. In addition, synergistic effects between climate warming and eutrophication are increasingly reported, where climate change might reinforce eutrophication and their manifestations around the globe (Paerl & Huisman, 2008; Moss, 2010; Kosten et al., 2012; Paerl & Paul, 2012; Lürling et al., 2018), and vice-versa (Moss, 2011; Yan et al., 2017; Bižić et al., 2020; Meerhoff et al., 2022). More frequent and intense storms, as predicted for some regions, would promote water column mixing (Carey et al., 2018), as well as nutrients supply from the watershed through runoff (Jeppesen et al., 2009; Ockenden et al., 2017). Meanwhile, lower precipitation and higher evaporation would promote water-column stratification, with frequent anoxia at the water-sediment interface (Søndergaard et al., 2013), facilitating the internal nutrient release from the sediments (Jeppesen et al., 2009; Søndergaard et al., 2013).

The more eutrophic conditions expected under warmer scenarios would also have associated higher CH_4 total emissions (Davidson et al., 2018; Beaulieu et al., 2019; Yang et al., 2019). Besides, as microbial activity is expected to increase with warming, strong temperature effects on CH_4 production and total emissions (Yvon-Durocher et al., 2011, 2014), and particularly CH_4 ebullition (Aben et al., 2017), are also expected. With increasing temperature, a decrease in carbon CO_2 sequestration, while increasing CO_2 emission has been observed (Kosten et al., 2010; Moss, 2010; Yvon-Durocher et al., 2010, 2011; Pacheco et al., 2014), which can be explained because respiration rates tend to increase faster with temperature than photosynthesis (i.e., with a reduction in the ratio between GPP and ER) (Allen et al., 2005; Acuña et al., 2008; Yvon-Durocher et al., 2011). However, eutrophic and warmer conditions would also intensified primary production, mainly by phytoplankton, and under particular conditions support CO_2 uptake (Pacheco et al., 2014) or at least lead to a net decrease in CO_2 emissions (Davidson et al., 2015; Junger et al., 2019).

The increase in ambient temperature might promote changes in the structure of biological communities and in the strength of trophic interactions. Stronger trophic cascade effects favoring the top predator are expected in temperate climates (Hansson et al., 2012), while latitudinal comparisons suggest that interactions between intermediate consumers (e.g., the link zooplanktivorous fish-zooplankton) are stronger in warmer climates (Meerhoff et al., 2012).

The effect on net carbon emissions as a function of the number of trophic levels and food web complexity is, however, recently analyzed in temperate systems (Hansson et al., 2012). Such processes are even less understood in tropical and subtropical lakes, where communities are structured in comparatively more complex and shorter trophic webs (Meerhoff et al., 2007a; Teixeira de Mello et al., 2009; Iglesias et al., 2017; Lacerot et al., 2021). Besides, the modulating role of macrophytes is weaker (Meerhoff et al., 2006, 2007b, 2007a), as well as the cascading effects reaching phytoplankton (Meerhoff et al., 2012; Attayde et al., 2021; Lacerot et al., 2021), than in similar temperate systems.

In summary, how the interplay between the composition of biological communities and the abiotic factors determines CO_2 and CH_4 fluxes in shallow lakes is still unclear, not least under a scenario of warming due to climate change. In addition, tropical and subtropical systems are far less studied than temperate and boreal regions with respect to carbon processing, as well as for the south compared to the north hemisphere (Cole et al., 2007; Holgerson & Raymond, 2016; Aben et al., 2017; Sanches et al., 2019).

Outline of the thesis

General objective:

This thesis aims to contribute to the understanding of how the combination of physical, chemical and biological factors associated with different general regimes in shallow lakes drive carbon fluxes (CO_2 and CH_4), and particularly under the consideration of the current scenario of global changes, such as widespread eutrophication and climate warming.

The main hypothesis is that the general dominant regime in shallow lakes (such as the dominance by submerged macrophytes or by phytoplankton, or the nearly absence of primary producers) and the typically distinct structure of biological communities (such as dominance of omni-planktivorous fish or by benthivorous fish) promotes clearly differentiated conditions for the in-lake carbon processing (e.g., GPP:ER ratio, oxygen availability and strength of the links between different lake zones as well as distinct trophic cascades effects). Consequently, we predict that dominant regimes in shallow lakes will result in different CO_2 and CH_4 fluxes between the aquatic ecosystem and the atmosphere, as elaborated below.

To address the different components of the general hypothesis, three different specific objectives were proposed as described below.

Specific objective 1 (Chapter 2):

To estimate and compare CO_2 and CH_4 fluxes between three natural subtropical shallow lakes with contrasting regimes (i.e., clear-vegetated lake dominated by submerged macrophytes, phytoplankton-turbid lake, and with an extremely low primary production) at the habitat and the

ecosystem levels. Secondly, to compare the estimated fluxes in subtropical shallow lakes with already published data for temperate and boreal lakes.

Predictions at ecosystem level: As net carbon fluxes are expected to strongly depend on the general regime, mainly represented by the dominant primary producer, we hypothesized that: the differences between regimes in the metabolic balance, oxygen, and organic matter availability would promote differences in CO_2 and CH_4 fluxes. In this line, among high productive ecosystems, submerged macrophyte-dominated lakes are expected to emit less CH_4 than phytoplankton-dominated lakes, and ecosystems with low productivity (mainly sustained by allochthonous carbon) are expected to sustain the lowest CH_4 emissions. Patters regarding to CO_2 fluxes are harder to predict, given that will depend in ecosystem and seasonal conditions, as for example the rate of aerobic organic matter mineralization and the amount of allochthonous organic and inorganic carbon inputs (Fig. 2A).

Predictions at habitat level: Within lakes, the differences in the spatial distribution of the different primary producers, i.e., in littoral and pelagic zones, would promote stronger carbon processing and CO_2 and CH_4 fluxes in the littoral than in the pelagic zones. However, differences between zones are expected to decrease in eutrophic ecosystems dominated by phytoplankton of in extremely low productive ecosystems, where aquatic vegetation is expected to be poorly developed.

Predictions on general patterns: The higher rates in primary production, respiration and decomposition expected with the higher mean temperatures in subtropical lakes would support more intense carbon fluxes than in similar systems located in temperate and boreal regions, as reported in the literature.

Specific objective 2 (Chapter 3):

To experimentally unravel the trophic and non-trophic effects of fish on CO_2 and CH_4 fluxes, analyzing the potential variability of fish impacts on both water column and sediment processes using sticklebacks (mostly zooplanktivorous) and carps (mostly benthivorous). In addition, we assessed the potential differentiated effects of predation pressure and bioturbation, through the comparison between systems with the permanent presence or intermittent presence of fish.

Predictions: Given the differences in the spatial use and trophic activity, the different fish composition would promote different CO_2 and CH_4 fluxes in the following way: trophic cascade effects occurring at the water column will deplete MOB, hampering CH_4 oxidation and facilitating CH_4 diffusion. At the sediment level, moderate fish bioturbation would release already aggregated gas bubbles and enhance CH_4 ebullition, but intense bioturbation would oxygenate sediments and reduce total CH_4 emissions and increase CO_2 emissions. Indirect effects on dissolved O_2 availability in the water-sediment interface, promoted by fish predation upon burrowing macroinvertebrates are expected to decrease CO_2 emissions but increase CH_4 emissions (Fig.2B).

Specific objective 3 (Chapter 4):

To unravel how the metabolic balance (CO_2 uptake: CO_2 efflux ratio) in pelagic freshwater ecosystems, would change under warmer conditions with a likely higher frequency of cyanobacterial dominance, which is expected to occur in freshwaters world-wide.

Prediction: Given cyanobacteria competitive advantages and their low palatability for zooplankton compared to other phytoplankton groups (such as chlorophytes), under eutrophic and warmer conditions it is expected that: cyanobacteria would develop higher biomasses and sustain higher CO_2 uptake than chlorophytes. However, a lower proportion of the fixed carbon is expected to be incorporated to the classic trophic web through zooplankton grazing in cyanobacteria-dominated communities than in chlorophytes-dominated communities. Thus, under cyanobacteria-dominance, large amounts of organic matter are expected to sediment and to be available for mineralization into CO_2 or CH_4.

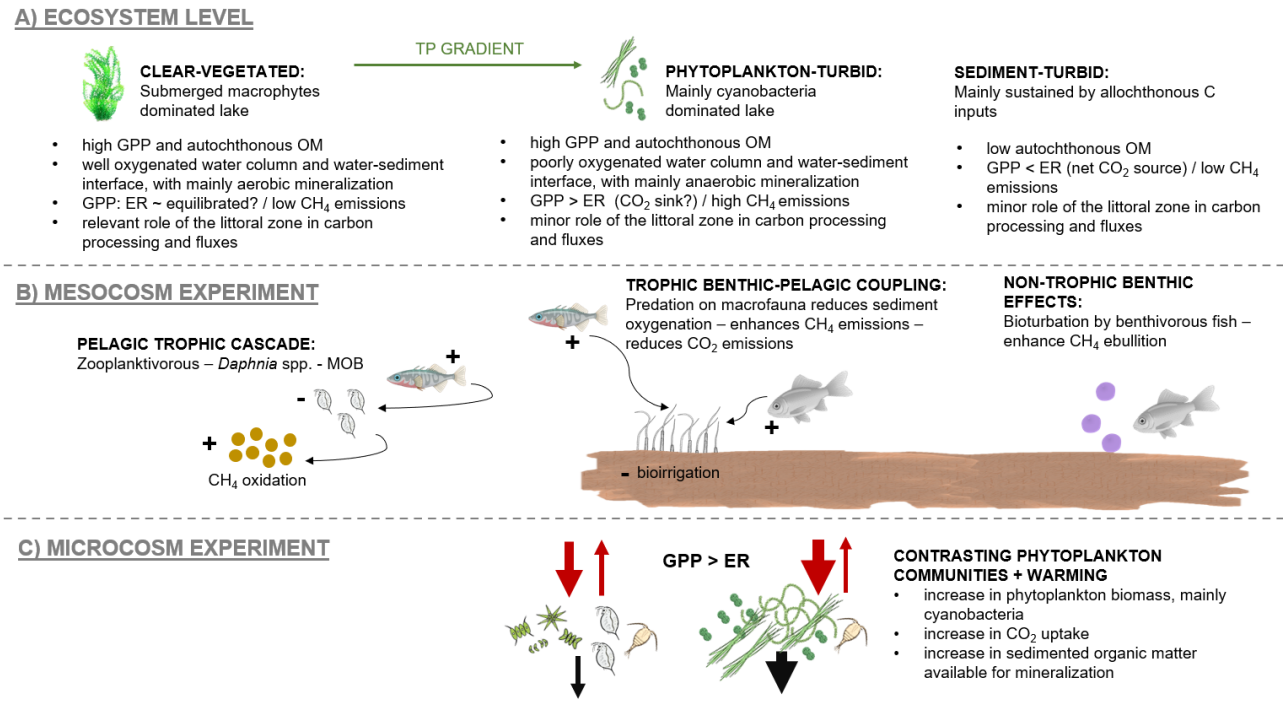

Figure 2. Summary of the main hypotheses related to the different scales at which biological systems were studied in this PhD thesis: A) lake ecosystem, B) mesocosm indoor experiment focusing on pelagic and benthic processes, and C) microcosm indoor experiment focusing on planktonic processes. In A) green arrow indicates increasing total phosphorous (TP) concentration as an indicator of eutrophication, in B) black curved arrows indicate trophic (feeding) effects, and in C) red arrows indicate CO_2 uptake or efflux and black straight arrows indicate organic matter (OM) sedimentation, being the size of the arrows relative to the expected amount of exchanged carbon. Abbreviations: GPP: gross primary production; ER: ecosystem respiration. Drawing credits as before.

General approach followed in this thesis

Different spatial and temporal scales of analysis were applied through this thesis: i) habitat and ecosystem scale analyses allowed us to compare CO_2 and CH_4 fluxes among natural subtropical shallow lakes during summer, and to follow seasonal changes in a clear-vegetated lake; ii) a three-month long indoor mesocosm experiment allowed us to evaluate trophic and non-trophic effects of fish at different mimicked habitats (i.e., at water column and in the water-sediment interface), on total CO_2 and CH_4 emissions; and iii) a 19-days long indoor microcosm experiment allowed us to analyze the role of warming on the metabolic balance (CO_2 uptake: CO_2 efflux) in contrasting eutrophic planktonic (i.e., chlorophyte-dominated versus cyanobacteria-dominated) communities subjected to experimental warming.

Although they are presented in each chapter in detail, a summarizing overview of the main methods applied for the estimation of CO_2 and CH_4 diffusive fluxes (at field and experimental scale), and CH_4 ebullition, together with an overview of their potential constrains, is presented below (Fig. 3).

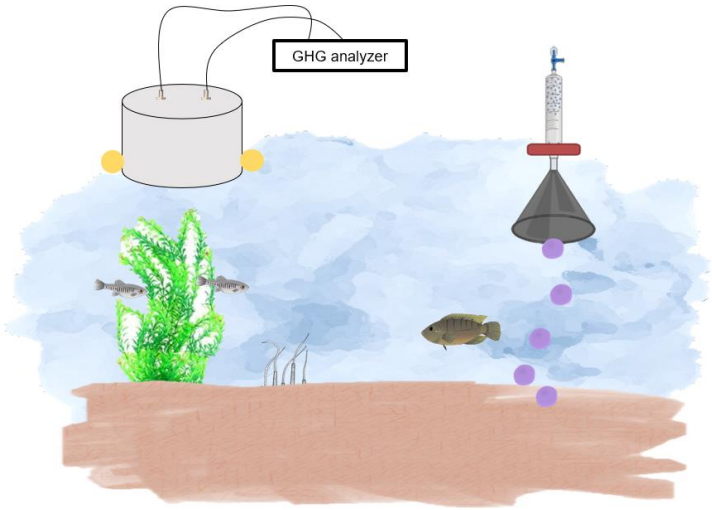

Figure 3. Summary of the main sampling methods for CO_2 and CH_4 fluxes typically used in shallow lakes. Drawing credits as above.

1.Direct methods, for diffusive fluxes of CO_2 and CH_4, consist on measuring the rate of change in the GHG concentrations (CO_2 or CH_4) over a certain period of time (usually 5-10 min), in an enclosing portion of air inside a chamber that floats on the water surface. According to the rate of change in GHG concentration, the total volume and total surface covered by the chamber and the ideal gas law, the GHG diffusive flux can be estimated using the bellow equation (Almeida et al., 2016):

$$\mathrm{F} = \frac{V}{A} * \mathrm{slope} * \frac{(P * F1 * F2)}{(R * T)}$$

Where: F is the GHG flux (usually in $mg.m^{-2}.day^{-1}$), V is the chamber volume (in m^3), A is the chamber surface (in m^2), slope is the rate of change of GHG over time (in $ppm.sec^{-1}$), P is the atmospheric pressure (in atm), F1 is the molecular weight of the gas (44 $g.mol^{-1}$ for CO_2 or 16 $g.mol^{-1}$ for CH_4), F2 is the conversion factor from seconds to days (86400 sec^{-1}), R is the gas constant (0.08205746 $L.atm.mol^{-1}.K^{-1}$) and T is the air temperature (in Kelvin).

The GHG concentration inside the chamber is measured by connecting the chamber to a portable gas analyzer or by periodically taking gas samples, and analyzing the concentration in a gas chromatographer in the laboratory (IHA, 2010).

2.Indirect diffusive flux estimations (for CO_2 and CH_4) can be performed according to the difference in GHG concentration between the water surface and the atmosphere, and the GHG specific gas transfer velocity (KL) (Cole et al., 1994, 2010; IHA, 2010).

$$F = KL * (pGHGwater - pGHGair)$$

Where: F is the GHG flux (usually in $mg.m^{-2}.day^{-1}$), KL is the gas transfer velocity (in $m.d^{-1}$), and pGHG is the partial pressure of the GHG (ppm of CO_2 or CH_4) in water and air, respectively.

KL can be defined as the height of the water that is in equilibrium with the atmosphere per unit of time, for a given gas and at a given temperature (Cole & Caraco, 1998), and can be estimated for the specific lake or experimental system or extrapolated according to wind speed and temperature (Wanninkhof, 1992; Tribe et al., 1995). The estimation of KL based on wind speed only allows for rough approximations, as it implies an oversimplification of all the factors that might affect the gas transfer velocity between compartments, being usually a relevant source of uncertainty in estimations (Cole et al., 2010).

Headspace gas chromatography can be used to estimate the concentration of dissolved GHG in the water. This technique is based on the equilibration of GHG concentrations between a known volume of gas (usually an inert gas, such as nitrogen -N_2) and a known volume of water sample, and analyzing by gas chromatography the resulting GHG concentration in the gas portion (IHA, 2010; Magen et al., 2014). Dissolved GHG concentrations are latter calculated according to Henry´s lay (Sander, 2015). Particularly for CO_2, dissolved concentrations can also be estimated based on pH, alkalinity, and water temperature according to the carbonic balance in freshwaters (Kling et al., 1992; Cole et al., 1994).

3.The ebullitive flux of CH_4 (i.e., bubbling from sediments), can also be sampled through different approaches. In this thesis, the use of bubble traps, adapted to the different field and experimental scale, were used. Bubble traps consist on an inverted funnel connected to a -preferable glass- bottle filled with water. When gas bubbles enter the trap, a volume of water equal to the bubble volume is expelled from inside the bottle. A subsample of the trapped gas

is then analyzed by gas chromatography. The ebullitive flux can be estimated by multiplying the measured CH_4 concentration by the total trapped gas volume, divided by the funnel area and trap deployment time (IHA, 2010), as follows:

$$\text{Eb } CH_4 = \frac{[CH_4] \ * \ \text{total V}}{\text{funnel A} \ * \text{time}}$$

Where: Eb CH_4 is the ebullitive flux (usually in $mg.m^{-2}.day^{-1}$), $[CH_4]$ is the concentration of gas (in $mg.m^{-3}$), total V is the total volume trapped in the bottle (in m^3), funnel A is the total area covered by the funnel (m^2) and time is the sampling period or time where the bubble trap was deployed in the ecosystem (in days).

Given ebullition is an episodic event, it may be hard to capture by common short-term measurements. It is thus hard to get accurate estimations at the ecosystem scale. Excluding this emission pathway might generate important underestimations on CH_4 total emissions (Bastviken et al., 2004, 2011; Sanches et al., 2019).

In all cases, the main potential biases and constrains in GHG flux estimations are that measurements are time consuming and highly technology demanding, and it is thus difficult to get estimations at a large spatial and temporal scales, comprising different zones of habitats within each ecosystem, as well as capturing season and diel changes.

As general considerations for this thesis:

-positive fluxes are considered when the GHG is released into the atmosphere and negative fluxes when that gas is incorporated into the aquatic ecosystem.

-to summarize and compare the contribution of the different GHGs, in this case CO_2 and CH_4, individual fluxes are usually expressed as CO_2 equivalents (CO_2-eq). CO_2-eq corresponds to the amount of CO_2 that would cause the same integrative radiative forcing, on a given time horizon, as an emitted amount of certain GHG or mixture of GHG (Myhre et al., 2013). For example, CO_2-eq for CH_4 is obtained by multiplying the emission of CH_4 by 34, which is its Global Warming Potential (GWP) in a 100-year horizon time. The GWP is defined as an index that measures the radiative forcing following an emission of a unit mass of a given substance, accumulated over a chosen time horizon, relative to that of the reference substance, i.e. CO_2 (Myhre et al., 2013). Total CO_2-eq flux can be then estimated as the sum of CO_2-eq of each gas (in this thesis: CO_2 and CH_4).

CHAPTER 2

CARBON FLUXES IN SUBTROPICAL SHALLOW LAKES: CONTRASTING REGIMES DIFFER IN CH_4 EMISSIONS

Maite Colina[1], Sarian Kosten[2], Nicolás Silvera[1], Juan M. Clemente[1†], Mariana Meerhoff[1,3]

[1] Departamento de Ecología y Gestión Ambiental, Centro Universitario Regional del Este, Universidad de la República, Tacuarembó s/n CP 20000, Maldonado, Uruguay.

[2] Department of Aquatic Ecology and Environmental Biology, Institute of Water and Wetland Research, Radboud University, P.O. Box 9010, 6500 GL Nijmegen, the Netherlands.

[3] Department of Bioscience, Aarhus University, Silkeborg, Denmark.

Published:

Colina, M., S. Kosten, N. Silvera, J. M. Clemente, & M. Meerhoff, 2021. Carbon fluxes in subtropical shallow lakes: contrasting regimes differ in CH_4 emissions. Hydrobiologia. DOI: 10.1007/s10750-021-04752-1.

Abstract

Fluxes of carbon dioxide (CO_2) and methane (CH_4) in shallow lakes are strongly affected by dominant primary producers which mostly has been studied in temperate and boreal regions. We compared summer CO_2 and CH_4 fluxes (diffusion and ebullition) in littoral and pelagic zones of three subtropical shallow lakes with contrasting regimes: clear-vegetated, phytoplankton-turbid, and sediment-turbid, and assessed fluxes in different seasons in the clear-vegetated system. Significant differences among the lakes occurred only for CH_4 fluxes. In the sediment-turbid lake we found undersaturated CH_4 concentrations were below atmospheric equilibrium, implying CH_4 uptake (<0 $mg.m^{-2}.day^{-1}$), likely due to low availability of organic matter. Differences between zones occurred in the clear-vegetated and phytoplankton-turbid lakes, with higher total CH_4 emissions in the littoral than in the pelagic zones (mean: 4342±895 and 983±801 $mg.m^{-2}.day^{-1}$, respectively). CO_2 uptake (<<0 $mg.m^{-2}.day^{-1}$) occurred in the littoral of the phytoplankton-turbid lake (in summer), and in the pelagic of the clear-vegetated lake even in winter, likely associated with submerged macrophytes dominance. Our work highlights the key role of different primary producers regulating carbon fluxes in shallow lakes and points out that, also in the subtropics, submerged macrophyte dominance may decrease carbon emissions to the atmosphere.

Keywords: carbon dioxide, methane, submerged macrophytes, phytoplankton, alternative regimes

Introduction

Shallow lakes are increasingly recognised as hot spots for carbon processing and exchange of large amounts of greenhouse gases (GHG), such as carbon dioxide (CO_2) and methane (CH_4), with the atmosphere (Cole et al., 2007; Cole, 2013; Tranvik et al., 2018). In addition, shallow lakes are the most abundant freshwater ecosystems across the world (Downing et al., 2006) and also are extremely vulnerable to anthropogenic and climatic pressures (Moss et al., 2011). Knowledge of how currently warm ecosystems behave regarding carbon fluxes may improve our understanding of the future effects of climate warming on currently colder ecosystems. However, there are still gaps in our understanding of the main drivers of CO_2 and CH_4 fluxes from shallow lakes, and there is a regional bias in the available knowledge with comparatively scarce field data on tropical and subtropical regions (Cole et al., 2007; Holgerson & Raymond, 2016; DelSontro et al., 2018; Janssen et al., 2020).

Air-water gas exchange through diffusion is the main pathway for CO_2 fluxes. Methane can also be emitted through emergent sections of plants and through gas bubbles formed in the sediment (ebullition) (Bastviken et al., 2004, 2011; Aben et al., 2017). At ecosystem level, CO_2 is incorporated through primary production and is produced by the respiration of all biological communities (Odum, 1956). Methane production and oxidation, in contrast, are processes conducted by different microorganisms; the CH_4 is mainly produced in anoxic and organic matter-rich sediments and oxidised at both the water-sediment interface and in the water column (Bastviken et al., 2004; Biderre-Petit et al., 2011).

Carbon processing within the ecosystem, as well as the CO_2 and CH_4 exchange with the atmosphere, is therefore strongly linked to the biomass and composition of biological communities and their trophic interactions as well as to abiotic conditions such as oxygen (O_2) availability (Atwood et al., 2013; Brothers et al., 2013; Cole, 2013; Janssen et al., 2020; Li et al., 2021). Without significant external inputs of carbon, ecosystems with high primary production/respiration ratios take up CO_2. In turn, CH_4 emissions depend on the fate of the primary producers. There is a tendency to low CH_4 production when primary producers are incorporated in the biomass of consumers and are partially respired again. High anaerobic decomposition with high CH_4 production and emissions occurs when organic matter sedimentation rates are high (Sobek et al., 2012; Brothers et al., 2013; Beaulieu et al., 2019). This also suggests that when sedimentation rates are low, CH_4 emissions may be modest.

Carbon processing may strongly differ among and within systems. Littoral zones, for instance, receive relatively high carbon inputs from the terrestrial surroundings (Wetzel, 1992; Juutinen et al., 2003; Jansson et al., 2007), whereas the importance of autochthonous carbon produced-by phytoplankton or macrophytes tends to be higher in the pelagic zone (Wetzel, 1992; Marczak et al., 2007; Doi, 2009). Indeed, carbon processing is largely influenced by the dominant primary producer, or regime, and the associated trophic structure in the system (Jeppesen et al., 2016; Hilt et al., 2017; Li et al., 2019).

The dominance of submerged macrophytes, possible under low to moderated nutrient concentrations, sustains clear water conditions in shallow lakes through various physical, chemical and biological processes (Scheffer et al., 1993). In the warm seasons and during daytime, the photosynthetic activity of macrophytes can result in high net CO_2 uptake (Natchimuthu et al., 2014; Davidson et al., 2015). However, net CO_2 emissions have also been reported in clear-vegetated lakes in temperate regions, fuelled by high aerobic decomposition of allochthonous or autochthonous organic carbon, which may further be stimulated by radial oxygen loss (ROL) (Lemoine et al., 2012) and respiration of a wide diversity of consumers (Brothers et al., 2013; Jeppesen et al., 2016). On the other hand, ROL and oxygenation of the water column through submerged macrophyte primary production can enhance CH_4 oxidation and hamper CH_4 emissions (Sorrell et al., 2002; Sorrell & Downes, 2004; Yoshida et al., 2014). Under increasing nutrient concentrations, and typically after a perturbation event, shallow lakes might shift to free-floating plant or phytoplankton-turbid regimes (Scheffer et al., 2003; de Tezanos Pinto & O'Farrell, 2014). A high phytoplankton biomass may directly or indirectly exclude other primary producers (Scheffer et al., 1993) and impoverish the diversity of consumers.

Field studies from temperate regions show that with eutrophication, and with shallow lakes shifting to phytoplankton-turbid regimes, the ratio between primary production and ecosystem respiration can increase and even transform lakes to net CO_2 sinks (Balmer & Downing, 2011; Pacheco et al., 2014; Jeppesen et al., 2016). On the other hand, the major role of decomposition processes and the often anoxic conditions at the water-sediment interface in phytoplankton-turbid lakes have been linked to high total emissions of CH_4 (by both diffusion and ebullition) (Yan et al., 2017; Beaulieu et al., 2019). Sediment-turbid lakes usually support an extremely low primary production due to high sediment resuspension and might be expected to act as net carbon sources; however, data on this type of ecosystems are scarce.

In subtropical regions, the high temperatures over a long period of the year promote higher rates of biological processes than in colder regions (Brown, 2004). A higher primary production than in similar temperate lakes might thus occur in subtropical regions, potentially leading to higher CO_2 sequestration (Natchimuthu et al., 2014). In contrast, higher mineralisation at higher temperatures may also increase CO_2 production (Kosten et al., 2010). The increase in aquatic oxygen consumption, combined with the lower solubility of O_2 in warmer waters, may enhance CH_4 production. Several studies have shown an exponential increase in ebullition with increasing temperature (Natchimuthu et al., 2014; Aben et al., 2017; Beaulieu et al., 2019). Thus, the net balance between emission and uptake of carbon (CO_2 and CH_4) in subtropical shallow lakes remains unclear. Patterns already reported for temperate regions may very well deviate from those in the subtropics as community structure and trophic interactions differ greatly with respect to similar temperate shallow lakes (Meerhoff et al., 2007a; Kosten et al., 2009; Teixeira-De Mello et al., 2009). Particularly, in temperate regions the foraging of fish on benthic fauna has been found to impact CO_2 and CH_4 fluxes by reducing sediment respiration and CO_2 emissions but increasing CH_4 emissions (Colina et al., 2021). In subtropical lakes, with their high diversity in omnivorous fishes and macrofauna, the above-mentioned top-down

effects are weaker (Meerhoff et al., 2007a) with yet unknown consequences for carbon processes.

We hypothesised that carbon fluxes in shallow lakes depend strongly on their regime, mainly represented by the dominant primary producer (i.e., phytoplankton or submerged macrophytes) or by the lack of a well-developed primary producer community (i.e., sediment-turbid lakes). In our comparative study, we expected that: i) in the clear-vegetated lake (dominated by submerged macrophytes), CO_2 uptake and emissions would be balanced due to a combination of high primary production and high respiration at the sediment and in the water column. In addition, we expected that low CH_4 emissions would occur in the clear-vegetated lake due to oxygenation of the sediment through plant roots (Fig. 1A). ii) In the phytoplankton-turbid lake, we expected CO_2 uptake would occur due to a high primary production/respiration ratio. However, high organic matter sedimentation and poor sediment oxygenation is expected to sustain high CH_4 production and emissions under such regime (Fig. 1B). iii) In the sediment-turbid lake, CO_2 fluxes were expected to be dominated by the decomposition of allochthonous material due to resuspension and the lack of primary production, resulting in CO_2 outgassing. Furthermore, we expected low CH_4 production and corresponding low CH_4 emissions in this lake due the near absence of primary production, and therefore low organic matter production and availability (Fig. 1C). iv) Similarly, to the between-lake differences, carbon fluxes were expected to be largely driven by differences in the spatial distribution of the primary producers between the littoral and pelagic zones in shallow lakes. v) Finally, the high temperatures in the subtropical lakes are expected to support higher rates of primary production, respiration, and decomposition than in temperate and boreal regions. Thus, we hypothesized that the general patterns regarding CO_2 and CH_4 fluxes already reported for temperate and cold regions are intensified in subtropical shallow lakes, implying higher CO_2 intake rates and CH_4 emissions due to their comparatively higher biomasses of submerged macrophytes and phytoplankton.

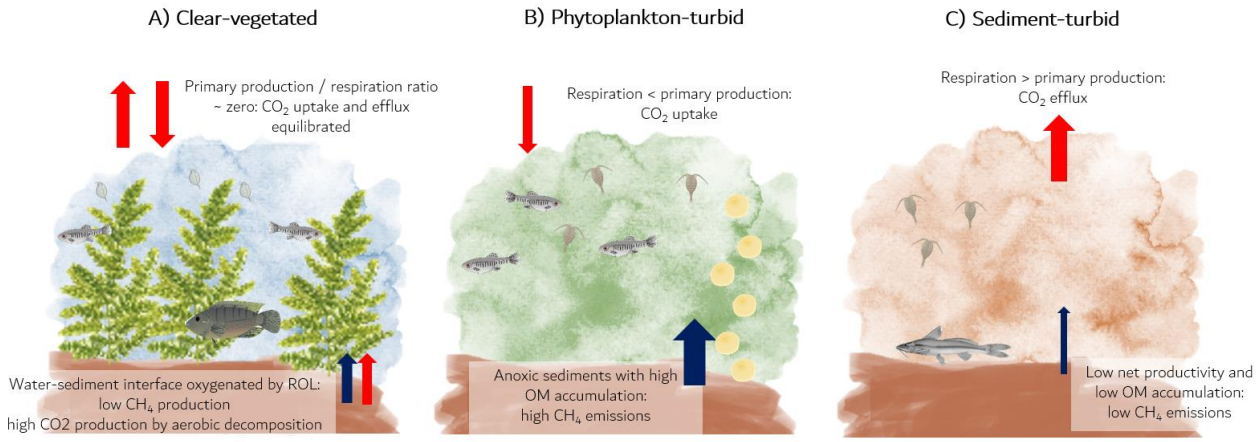

Figure 1. Conceptual image of the hypotheses and predictions related to carbon fluxes in shallow subtropical lakes with contrasting regimes: A) clear-vegetated, B) phytoplankton-turbid, and C) sediment-turbid. Red arrows represent the expected CO_2 fluxes and blue arrows the CH_4 fluxes, the thickness and direction of the arrow shows the expected intensity (in a qualitative way) and direction of the flux.

Materials and Methods

General rationale, sampling strategy and case studies

Summer CO_2 and CH_4 fluxes were assessed in three subtropical shallow lakes with contrasting regimes, i.e., clear-vegetated, phytoplankton-turbid and sediment-turbid. We compared carbon fluxes between the lakes during summer (one sampling campaign conducted during the Austral summer, February 2019) when all biological communities reach maximum productivity. In addition, we focused on the role of submerged macrophytes in regulating carbon fluxes by evaluating the seasonal changes, from winter to summer, in the clear-vegetated lake (one sampling campaign undertaken in each season from August 2018 to February 2019). In all cases, fluxes from the littoral and pelagic zones were evaluated. To obtain insight in the potentially differentiating role of subtropical lakes -as compared to colder lakes- in the global carbon cycle, we compared the measured CO_2 and CH_4 dissolved concentrations in our three subtropical shallow lakes with data from other latitudes obtained from the literature.

The three shallow lakes selected for our study are located along the Atlantic coast of Maldonado, Uruguay (Fig. 2). The lakes are similar as to maximum depth and organic matter (OM) supply from the basin and from underground water but exhibit contrasting conditions as to main primary producers and trophic states. Lake Blanca (location: 34°53'52.8"S-54°50'10.0"W, area: 48ha), now termed 'clear-vegetated lake', is dominated throughout the year by a high biomass of submerged macrophytes (including *Ceratophyllum sp*., *Egeria densa* Planch.) and a permanent clear water regime. The dominant phytoplankton taxonomic groups, in this lake, have changed through the years from cyanobacteria to chlorophytes (Kruk et al., 2006; Pacheco et al., 2010), with one event of a *Ceratium furcoides* bloom in 2012 (Pacheco et al., 2021). The community of consumers in the clear-vegetated lake is diverse; the zooplankton community is dominated by small-bodied cladocerans and copepods, with occasional occurrence of *Daphnia* spp. and other larger-bodied species, the diverse fish community dominated by small-bodied species with a high biomass (Pacheco et al., 2021). Lake Capilla (location: 34°49'18.5"S - 54°37'48.7"W, area: 1ha), hereinafter referred to as 'phytoplankton-turbid', is a small, young (less than 15 years) artificially constructed lake that is in a turbid state due to high phytoplankton biomass. No previous research exists on this lake, but according to personal observation the zooplankton in this lake is dominated by organisms with low to very low grazing capacity and the fish community by small individuals (i.e., less than 5 cm total length) due to the lake's recent creation and because no large fishes have been stocked. Lake Barro (location: 34° 51'01.5"S - 54°42'23.4"W, area: 15ha), hereinafter 'sediment-turbid', is a turbid ecosystem due to sediment resuspension and has a very low biomass of primary producers. Previous research on this lake reported picophytoplankton and flagellates as the main phytoplankton groups. The diversity in consumers is low, the zooplankton is dominated by calanoid copepods and nauplii and fish by omnivorous species with low biomass (Kruk et al., 2006; Meerhoff et al., 2007a, 2007b).

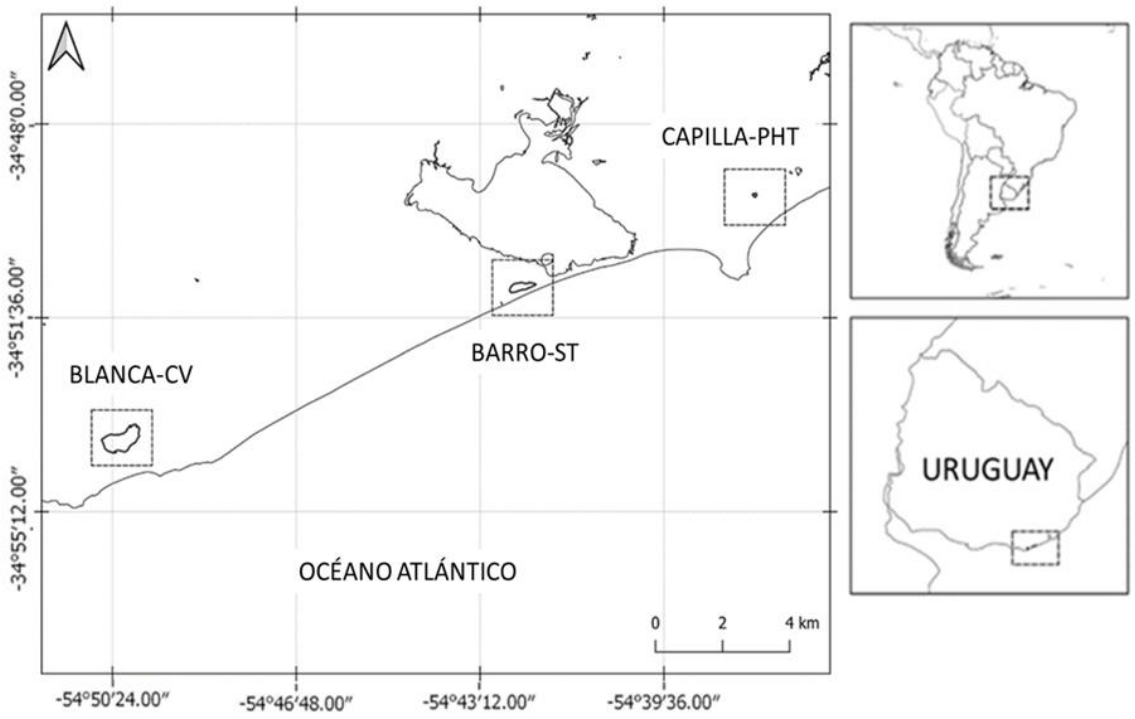

Figure 2. Location of the sampled lakes along the Atlantic coast of Uruguay: the clear-vegetated (CV), Lake Blanca, the phytoplankton-turbid (PHT), Lake Capilla, and the sediment-turbid (ST), Lake Barro.

Physical and chemical variables

In both the littoral and the pelagic, *in situ* measurements were conducted at a single location at the surface and near the bottom with a portable multimeter YSI 6600 (Xylem, Ohio, USA) recording temperature (°C), dissolved oxygen concentration (O_2) and pH. Also, maximum depth and Secchi depth were measured in both lake zones. In the clear-vegetated lake, seasonal measurements were made.

In each lake zone, an integrated water sample (approx. 6L from each of the five sampling spots where also GHG were measured, see GHG sampling) was collected and kept cold and dark during transportation to the laboratory for analysis of alkalinity following a titration method (Bridgewater et al., 2017) and determination of nutrient concentrations, including total nitrogen (TN), total phosphorous (TP), ammonium (NH_4^+), nitrate (NO_3^-) and phosphate (PO_4^{-3}) according to Valderrama, (1981). A sub-sample of the integrated water sample (500 mL or until filter saturation) was filtered through GF/C glass microfibre filters (1.2 µm pore size and 47 mm filter diameter, Munktell, Texas, USA) and total suspended solids (TSS) and OM concentration were determined as the difference in dry (110°C during 24 hr) and burnt (500°C during 15 min) filter weights (Bridgewater et al., 2017).

Primary producers

At each GHG sampling spot, the percentage coverage of macrophytes (% cov.) was estimated based on visual observations and the relative contribution of each macrophytes life form (i.e., submerged, free-floating, and emergent) was assessed. When possible, main species were identified.

Phytoplankton biomass was assessed for each lake zone (for the three lakes and for the three seasons in the clear-vegetated lake) using chlorophyll-a concentrations as a proxy. The chlorophyll-a concentration was assessed from water filtered on GF/C glass microfibre filters (Munktell, Texas, USA) followed by extraction in 95% cold ethanol and spectrophotometric measures of absorbances at 665-750nm (ISO 10260, 1992).

In order to have a general idea about the current phytoplankton composition in each lake zone, 50 µL concentrated samples were retrieved with a plankton net (20 µm pore size), fixed with Lugol´s 4% solution and stored till their observation in an inverted microscope for main taxonomic groups identification.

GHG sampling

In all sampling campaigns, fluxes of CO_2 and CH_4 were measured, always around noon, at the littoral and pelagic zones at five randomly distributed spots (total n=10 samples per lake).

Carbon dioxide air-water gas exchange was measured inside an acrylic floating chamber (0.3 m diameter x 0.4 m height, with 0.05 m of height submerged into the water) connected to an infrared gas analyser EGM-4 (PPSystems, Amesbury, USA), where CO_2 partial pressure (pCO_2, in ppm) was recorded every 30 seconds over 5 minutes. The diffusive fluxes were then calculated based on the slope of pCO_2 versus time, according the equations described in Almeida et al., (2016) (see Supp. Info. for details). When emergent or free-floating macrophytes were present, the acrylic floating chamber was placed in-between the plants in order to focus on water-atmosphere fluxes (excluding direct plant-mediated fluxes). Methane diffusive fluxes were estimated based on the dissolved gas concentration in the surface water following the equations described in Cole & Caraco (1998), and considering wind speed velocity measured at field with an anemometer (see Supp. Info. for details).

Bottom-moored bubble traps, placed at each sampling spot for 24 hours (in order to capture both day and night emissions), were used to sample CH_4 ebullition (IHA, 2010; Almeida et al., 2016; van Bergen et al., 2019). Each trap consisted of an inverted plastic funnel (0.3 m diameter) connected to a glass bottle filled with water. When gas bubbles enter the trap, a water volume equal to the bubble volume is expelled from inside the bottle. After sampling, the total gas volume inside each bottle was recorded and a subsample of gas was extracted through a septum using a syringe with a rubber plunger and transferred to a 3 mL vacuum exetainer (Labco Limited, Lampeter, UK). Samples were stored in dark until analyses. Finally, the ebullitive flux was estimated by multiplying the CH_4 concentration by the total trapped gas

volume in each bottle and dividing it by trap deployment time and funnel area (24 hours and 0.07 m^2) (IHA, 2010).

For all CH_4 samples, 100 µL of gas was injected on a HP 5800 gas chromatograph equipped with a Porapak Q column (80/100 mesh) and a flame ionization detector (GC-FID; Hewlett Packard). The CH_4 concentration was assessed based on a calibration curve created with five different CH_4 standard concentrations (Magen et al., 2014).

Total CH_4 emissions were calculated as the sum of CH_4 diffusion and ebullition and total GHG emissions based on CO_2 equivalents (CO_2-eq) using a global warming potential along a 100-year scale of 34 for CH_4 (Myhre et al., 2013). For each lake – or for each season for the clear-vegetated lake, we estimated a weighted average carbon flux (CO_2-eq in $mg.m^{-2}.day^{-1}$) per zone (littoral and pelagic). To estimate this weighted average system flux, we divided the median value of total carbon emissions in CO_2-eq of each zone by the percent of the lake area occupied by that zone. The percent of the lake area occupied per zone was estimated from satellite images in Google Earth based on the differences in colouring between zones and the estimated area (determined using the polygon area tool in Google Earth). The littoral zone represented around 10% of the total lake surface in the clear-vegetated lake and 7% and 4% in the phytoplankton-turbid and the sediment-turbid lakes, respectively.

The concentration of dissolved CO_2 in surface water was estimated based on pH, alkalinity, and water temperature (Kling et al., 1992; Cole et al., 1994) (see Supp. Info. for details) for a single water sample per lake zone. Dissolved CH_4 was estimated from the headspace created for surface and bottom water samples taken at the 10 measurement spots in each lake (5 at each lake zone). For the surface samples, a 12 mL vacuum exetainer was submerged 0.5 m below the water surface and a needle was inserted in the septum to allow water to fill the exetainer. For the bottom samples, water was gently pumped from the bottom through a hose and a 12 mL exetainer was filled with water and quickly closed (IHA, 2010). In all samples, 0.1 mL of 2.5M H_2SO_4, was injected to halt microbial activity, while – at the same time –an equivalent volume of water was allowed to exit through a second needle. Subsequently, a headspace was created by adding 3 mL of N_2 gas to all exetainers. All vials were vigorously shaken to equilibrate gas concentrations between the water and the headspace, and the samples were preserved upside down and in darkness until analyses (IHA, 2010; Magen et al., 2014). The methane concentration in the headspace of each sample was determined by gas chromatography as described above, and dissolved CH_4 concentrations in the water portion were calculated according to Henry's law (Sander, 2015).

Statistical analyses

Two-way ANOVA tests for the evaluation of carbon fluxes among lakes and between zones (lake, zone, and lake*zone as explanatory variables) were performed for the summer data. In the same way, two-way ANOVA tests for evaluation of carbon fluxes among seasons and between zones (season, zone, and season*zone as explanatory variables) were performed for seasonal data for the clear-vegetated lake. In both cases, response variables were: CO_2 and

CH_4 diffusion, CH_4 ebullition, total CH_4, and total fluxes as CO_2-eq. To evaluate differences among levels in each ANOVA test, Tukey's pairwise comparisons were performed. In addition, the magnitude of effect was estimated from t-values of each pairwise comparison according to Cohen's d statistic, which expresses the distance between the means of two groups in terms of their common standard deviation (Nakagawa & Cuthill, 2007). After that, using Cohen's d statistic and based on McGraw & Wong (1992) equations, magnitudes of effect were translated to a probability between 0.5 and 1 expressed by the common language effect sizes (CLES.d). Effect size statistics are less prone to bias when working with small sample sizes than the commonly used p-values, and allow to express in more intuitive way the weight of the explanatory variables on the observed patterns. As closer to 1 a CLES.d value is, as far from random effect (which will be CLES.d=0.5) can be assumed the observed difference between the means of two paired group (Nakagawa & Cuthill, 2007).

The same statistical approach as for GHG fluxes was applied to analyse differences in dissolved CH_4 gas concentrations (in surface and bottom water) between each lake zone and among lakes or seasons.

To evaluate to which extent subtropical lakes differ from other lakes, we compared CO_2 and CH_4 dissolved gas concentrations in our study lakes, with the gas concentrations of 246 lakes included in the open database of Holgerson & Raymond, (2016) (hereafter 'H&R data'). This database was created based on a metanalysis and contains dissolved CO_2 and CH_4 concentrations in lakes and ponds in Europe and North America which were mainly sampled in open waters. We fit the same regression models as in H&R (2016) between the natural logarithm of CO_2 and CH_4 dissolved concentrations and the CO_2 / CH_4 ratio versus latitude and lake area, using the data of 246 H&R lakes combined with our lakes (i.e., n=258). Regarding the data from our lakes, we considered mean gas concentrations for each lake zone, and for the clear-vegetated lake we also included winter and spring data as H&R also included data from different seasons and from the same system. A quadratic regression with latitude (centered around the mean) was fitted to the data on dissolved CO_2 concentration and CO_2 / CH_4 ratio.

All statistical analyses were performed using the statistical programme Rstudio (RStudio Team, 2018). Prior to analyses, normal distribution was evaluated for all response variables and in the case of CH_4 ebullition log transformation was applied. The final models were validated checking for the normal distribution and homogeneity of variance of the residuals. The function glht from the multcomp package (Hothorn et al., 2016) was used to perform post-hoc analyses in ANOVA tests and to obtain t statistics between groups that were used in the estimations of Cohen's d (McGraw & Wong, 1992).

Results

Characterisation of lakes

The three subtropical shallow lakes considered in our study showed clear differences in general regimes at the time of our sampling campaigns.

In the surface water of the clear-vegetated lake, summer TP concentrations typical of mesotrophic (14.4 µg.L^{-1}, according to (Smith, 1998)) and even oligotrophic (<10.0 µg.L^{-1}) ecosystems were found in the pelagic and littoral zones, respectively. In the surface water of the phytoplankton-turbid and the sediment-turbid lakes, TP concentrations typical for eutrophic lakes (>80 µg.L^{-1}) were recorded in the pelagic, while TP concentrations typical of hypereutrophic (>100 µg.L^{-1}) lakes were observed in the littoral zones. Dissolved O_2 (DO) concentrations, measured around noon, were above 9 mg.L^{-1} at the water surface in all three lakes, except for the littoral zone of the clear-vegetated lake where values around 5 mg.L^{-1} were measured. The highest bottom water O_2 concentration was measured in the pelagic zone of the sediment-turbid lake (around 8 mg.L^{-1}), while the lowest O_2 concentration occurred in the littoral zone of the clear-vegetated lake (below 1 mg.L^{-1}). Zooming in on the clear-vegetated lake comparison among seasons - in the pelagic zone, no differences were found for TP and O_2. In contrast, in the littoral zone, seasonal variations were observed, with TP concentrations typical of eutrophic ecosystems (>30 µg.L^{-1}) occurring in winter and spring and considerably lower TP concentrations in summer. DO concentrations varied seasonally as well with bottom waters being much lower in summer than in winter and spring (see Table 1 for detailed information).

Table 1. Main physical and chemical water variables for the littoral and pelagic zones of each lake. Maximum depth (Zmax, in m); Secchi disk depth (SD., in m); and average concentrations of: total phosphorous, total nitrogen, phosphate, nitrate, and ammonium (TP, TN, PO_4^{-3}, NO_3^-, NH_4^+, in µg. L^{-1}), chlorophyll-a (Chl-a in µg. L^{-1}), organic matter (OM in mg. L^{-1}) and dissolved CO_2 in surface water (in µmol. L^{-1}); for surface and bottom water: temperature (Temp, in °C), pH, dissolved O_2 concentration (DO, in mg. L^{-1}), and dissolved CH_4 (in µmol. L^{-1}). For the clear-vegetated lake data on winter, spring, and summer are presented. For the phytoplankton-turbid and sediment-turbid lakes summer data are presented. Abbreviations: surf.: surface; btm.: bottom; sd: standard deviation; w: winter; sp: spring; s: summer.

	Clear-vegetated						**Phytoplankton-turbid**		**Sediment-turbid**	
	littoral			**pelagic**			**littoral**	**pelagic**	**littoral**	**pelagic**
	w	**sp**	**s**	**w**	**sp**	**s**	**s**	**s**	**s**	**s**
Zmax	3.6	2.0	1.5	3.6	4.0	3.0	1.8	2.0	0.8	2.5
SD	1.2	-	1.0	1.2	-	0.8	0.6	0.6	0.2	0.2

Temp. surf.	15.1	25.8	28.4	15.2	23.7	27.6	25.6	25.8	23.6	22.3
Temp. btm.	12.5	20.6	23.1	12.4	19.8	22.9	23.2	22.8	23.6	22.2
pH surf.	8.4	8.5	6.9	8.3	8.8	8.5	6.8	7.0	7.1	7.5
pH btm.	7.4	7.03	6.9	7.4	7.1	6.5	6.5	6.6	7.4	7.0
TP	37.5	32.1	9.5	22.5	27.2	14.4	99.6	110.8	81.9	118.9
TN	379.2	481.1	303.6	402.9	303.6	392.4	844.2	787.7	715.1	916.8
PO_4^{-3}	35.0	17.5	6.4	21.7	11.1	11.1	20.6	9.6	31.7	17.5
NO_3^-	51.1	284.0	276.5	36.5	-	253.9	464.7	261.4	457.1	366.8
NH_4^+	12.8	-	23.6	11.2	-	-	23.6	4.2	30.9	20.8
Chl-a	3.8	9.8	5.2	12.4	1.5	5.6	47.4	47.3	<0.01	0.01
Surf. DO	11.9	12.4	5.2	11.9	14.6	10.9	9.6	9.8	8.4	8.1
Btm. DO	5.5	2.1	0.8	5.5	2.4	0.8	4.7	3.8	8.2	7.6
OM	161.0	1.9	1.2	29.5	0.9	1.2	1.5	0.7	0.7	0.7
CO_2 surf.	0.7	0.5	18.0	0.7	0.2	0.4	11.9	6.3	50.8	8.7
CH_4 surf.	0.2±0.2	0.6±0.2	9.2±12.0	0.1±0.1	0.2±0.2	0.3±0.2	0.9±0.2	0.5±0.1	0.2±0.1	0.2±0.03
CH_4 btm.	0.6±0.7	3.3±5.5	173.5±329.8	1.2±2.1	0.2±0.1	138.0±186.2	1.4±1.7	1.4±1.1	0.3±0.1	0.4±0.3

A well-developed community of macrophytes was registered in the clear-vegetated lake in all three seasons (winter, spring, and summer) and in both zones (littoral and pelagic) (Fig. ESM1). A submerged macrophyte (mainly *Ceratophyllum demersum*) coverage of 100% was observed in the pelagic zone of the clear-vegetated system, while in the littoral zone, the three different life-forms – free-floating (including, in order of contribution to total coverage, *Eichhornia crassipes* (Mart.) Solms, *Salvinia sp.* and *Azolla sp.*), submerged (including, *Ceratophyllum demersum and Egeria densa* Planch.) and emergent plants (including, *Typha sp.*, among others) were present. The phytoplankton-turbid lake had the highest biomass of phytoplankton of our three study lakes (more than 47 µgChl-a.L^{-1}) and a substantial (~65%) coverage of emergent macrophytes (*Typha sp.*, among others) in the littoral zone (Fig. ESM1A). The sediment-turbid lake had a low biomass of primary producers, i.e., the chlorophyll-a concentration was near zero and no submerged macrophytes were observed. Only emergent macrophytes (*Typha sp.*, among others) were present in the littoral zone of this lake (Fig. ESM1B). The phytoplankton community composition (as of main taxonomic groups) also varied

among lakes, been the clear-vegetated lake mainly dominated by chlorophytes, the phytoplankton-turbid by chlorophytes, dinoflagellates and filamentous algae. The sediment-turbid lake showed the less diverse phytoplankton with mainly filamentous cyanobacteria.

Summer GHG fluxes under contrasting regimes

We found no significant differences in the diffusive CO_2 fluxes between the zones of each lake nor among the lakes in summer (Fig. 3A and Table 2). The three lakes emitted CO_2 to the atmosphere on all occasions and all locations, with the exception of the pelagic zone of the clear-vegetated lake and the littoral zone of the phytoplankton-turbid lake where, respectively, uptake and near zero CO_2 diffusive fluxes were recorded. The pelagic zone of the clear-vegetated lake, was also where we found the lowest CO_2 concentration in the surface water (Table 1-2). The strongest differences in CO_2 diffusion within a lake, according to effect sizes, were registered in the clear-vegetated lake with uptake occurring in the pelagic and emission in the littoral zone (CLES.d=0.74).

Significant differences in CH_4 diffusive fluxes were found among lakes (Fig. 3B and Table 2). The highest emissions were registered in the littoral zone of the clear-vegetated lake where the CH_4 diffusive emission was significantly higher than at the sediment-turbid lake, at both zones, littoral (Tukey's test p=0.01 and CLES.d=0.93) and pelagic (Tukey's test p=0.01 and CLES.d=0.94), where in the last one even CH_4 uptake was found. Compared to the phytoplankton-turbid lake, the CH_4 diffusion in the littoral of the clear-vegetated lake was 13 times higher than the uptake in the pelagic of the phytoplankton turbid lake (Tukey's test p=0.02), and 4 times the emission by the littoral zone, with also high effect sizes for both differences (CLES.d=0.94 and 0.87, respectively). Within the clear-vegetated lake, CH_4 diffusion was significantly higher in the littoral than in the pelagic zone (Tukey's test p=0.02, CLES.d=0.93).

Methane ebullition differed significantly among lakes and for the interaction of zone and lake (Fig. 3C and Table 2), with the highest CH_4 ebullition fluxes occurring in the pelagic zone of the phytoplankton-turbid lake (mean: 57.4±0.4 $mg.m^{-2}.day^{-1}$) and in the littoral zone of the clear-vegetated lake (mean: 79.5±0.4 $mg.m^{-2}.day^{-1}$). The lowest CH_4 ebullition flux was registered in the pelagic zone of the sediment-turbid lake (mean: 0.1±0.4 $mg.m^{-2}.day^{-1}$), corresponding with very low near-bottom CH_4 concentrations (Table 1-2). For near-bottom CH_4 concentrations, also significant differences and strong effect sizes were found for differences between zones within lakes (in all cases Tukey's test $p<0.01$ and CLES.d>0.95).

Both the total CH_4 flux and the total carbon flux based on CO_2 equivalents, significantly differed among lakes (Table 2) following a pattern similar to the diffusive CH_4 fluxes (Fig. ESM2A-B).

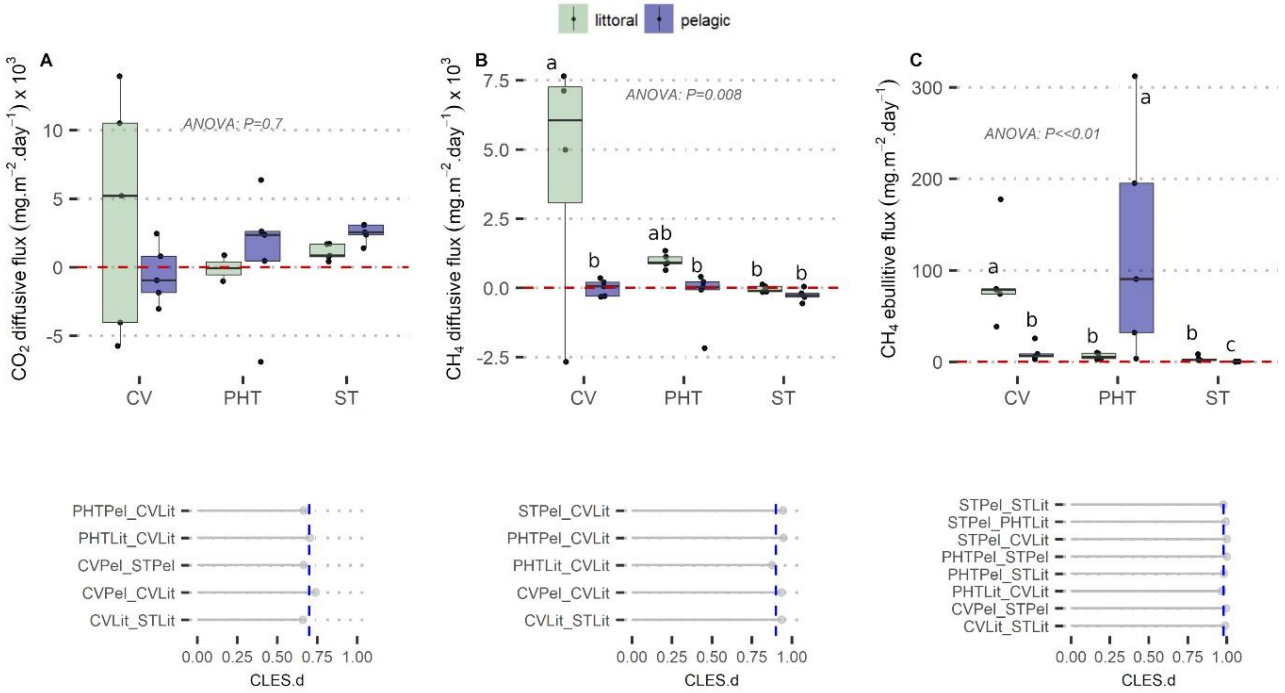

Figure 3. Summer GHG fluxes in shallow lakes of contrasting regimes (CV: clear-vegetated, PHT: phytoplankton-turbid, and ST: sediment-turbid) highlighting two lake zones (Lit: littoral and Pel: pelagic). A-C): above GHG fluxes in $mg.m^{-2}.day^{-1}$: A) CO_2 diffusive flux, B) CH_4 diffusive flux, C) CH_4 ebullitive flux. The dark horizontal lines in the box-plots represent the median, the boxes show the interquartile range with 25% to 75% percentiles, and the vertical lines indicate the distribution range. Black dots show individual data and the horizontal dashed red lines indicate zero fluxes. Letters above the boxes (a, b, and c) summarize the pairwise comparison after ANOVA tests (Tukey´s test). Please note the different scales used for each GHG. A-C) below, indicate common-language effect sizes (CLES.d) enabling comparisons among groups (lake*zone). Only the comparisons where CLES.d was higher than 0.60 are shown, in A) the vertical blue dashed line indicates CLES.d=0.7, in B) indicates CLES.d=0.9 and in C) indicates CLES.d=0.98.

The average system carbon flux, calculated as the weighted mean of the area of each zone, showed that the largest summer emissions occurred in the clear-vegetated lake, with only a minor contribution from its (densely vegetated) pelagic zone and a large contribution from its littoral zone. In contrast, in both the phytoplankton-turbid and the sediment-turbid lakes, total carbon fluxes were mainly driven by fluxes from their pelagic zones (Fig. ESM3A).

Table 2. Main effects of factors: season, zone and their interaction for the clear-vegetated lake, and lake, zone and their interaction for the lakes in summer, on GHG fluxes (all in $mg.m^{-2}.day^{-1}$): CO_2 and CH_4 diffusion (diff.), CH_4 ebullition (eb.), total CH_4 emissions (diffusion + ebullition) and total fluxes as CO_2-eq. (CO_2 +34*total CH_4), and on CH_4 dissolved concentrations at surface and bottom water (in $\mu mol.L^{-1}$). Statistical results of two-way ANOVAs are shown, indicating respective F-values and degrees of freedom (df) and p-values. ns: $p > 0.05$, *: $p \leq 0.05$, **: $p < 0.01$, ***: $p < 0.001$.

For CH_4 dissolved concentrations letters between brackets (a, b, c and d) summarize the pairwise comparison after ANOVA tests (Tukey´s test). Abbreviations: w: winter; sp: spring; s: summer; CV: clear-vegetated; PHT: phytoplankton-turbid; ST: sediment-turbid; Lit: littoral; Pel: pelagic.

	Clear-vegetated lake between seasons									**Between lakes in summer**								
	Season			**Zone**			**Season*Zone**			**Lake**			**Zone**			**Lake*Zone**		
	F	**df**	**p**	**F**	**df**	**p**	**F**	**df**	**p**	**F**	**df**	**p**	**F**	**df**	**p**	**F**	**df**	**p**
Fluxes																		
CO_2 diff.	1.6	2	ns	2.03	1	ns	0.9	2	ns	0.1	2	ns	0.3	1	ns	1.3	2	ns
CH_4 diff.	2.6	2	ns	5.9	1	*	3.8	2	*	3.3	2	*	7.6	1	*	3.2	2	ns
CH_4 eb.	210.5	2	***	23.4	1	***	25.9	2	***	46.8	2	***	8.4	1	**	24.4	2	***
Total CH_4	2.6	2	ns	5.9	1	*	3.9	2	*	3.4	2	*	7.4	1	*	3.3	2	*
CO_2-eq	2.6	2	ns	5.1	1	*	3.6	2	*	2.9	2	ns	5.7	1	*	2.8	2	ns
Diss. conc.																		
CH_4 surf.	14.01	2	***	22.2	1	*	4.3	2	***	15.04	2	***	20.6	1	***	9.9	2	***
	sLit (a)/spLit (b)/spPel, sPel, wLit, wPel (c)									sLit (a)/sPel (ab)/spPel (bc)/spLit, wLit, wPel (c)								
CH_4 btm.	20.6	2	***	2.8	1	ns	0.9	2	ns	23.9	2	***	0.2	1	ns	0.3	2	ns
	CVLit (a)/PHTLit (b)/CVPel, PHTPel (bc)/STLit, STPel (c)									CVLit (ab)/CVPel (bc)/PHTPel (cd)/PHTLit, STLit, STPel (d)								

Seasonal GHG fluxes in the clear-vegetated lake

Even though no significant differences were found in CO_2 diffusion among seasons and zones of the clear-vegetated lake (Table 2), some remarkable patterns with associated strong effect sizes (CLES.d>0.7) emerged (Fig. 4A). In the pelagic zone, median CO_2 diffusive fluxes were negative (i.e., meaning uptake), even in winter. On the other hand, CO_2 diffusion in the littoral zone showed high variability, with uptake in spring but outgassing in winter and summer, when also the highest dissolved CO_2 concentrations were found (Table 1).

Methane diffusion, in contrast, significantly varied among seasons and lake zones (Fig 4B and Table 2), with the highest fluxes occurring in the littoral zone in summer. Methane diffusion in the littoral zone in summer was significantly higher than diffusion in the pelagic zone in winter,

spring and summer (in all cases Tukey's test $p<0.05$ and CLES.d>0.90), as well as in the littoral zone in winter (Tukey's test p=0.02 and CLES.d=0.93). The highest dissolved CH_4 concentrations, in the surface and bottom water, also occurred in the littoral zone in summer (Table 1-2).

Significant differences were also found for methane ebullition among the seasons and between zones (Fig 4C and Table 2). The highest ebullition occurred in the littoral zone in summer, being significantly higher than in all other seasons and locations (in all cases Tukey's test $p<0.05$ and CLES.d>0.95). In winter CH_4 ebullition was almost zero for both lake zones. Total CH_4 emissions and total carbon emissions, based on CO_2 equivalents, followed a similar pattern as CH_4 diffusion (Fig. ESM2C-D and Table 2).

The littoral zone contributed the most to the system-average carbon emission in summer. Furthermore, the system-average carbon emissions in summer, were also approximately 8 times higher than the emissions in winter. Meanwhile, in the (vegetated) pelagic zone carbon uptake took place in spring (Fig. S3B).

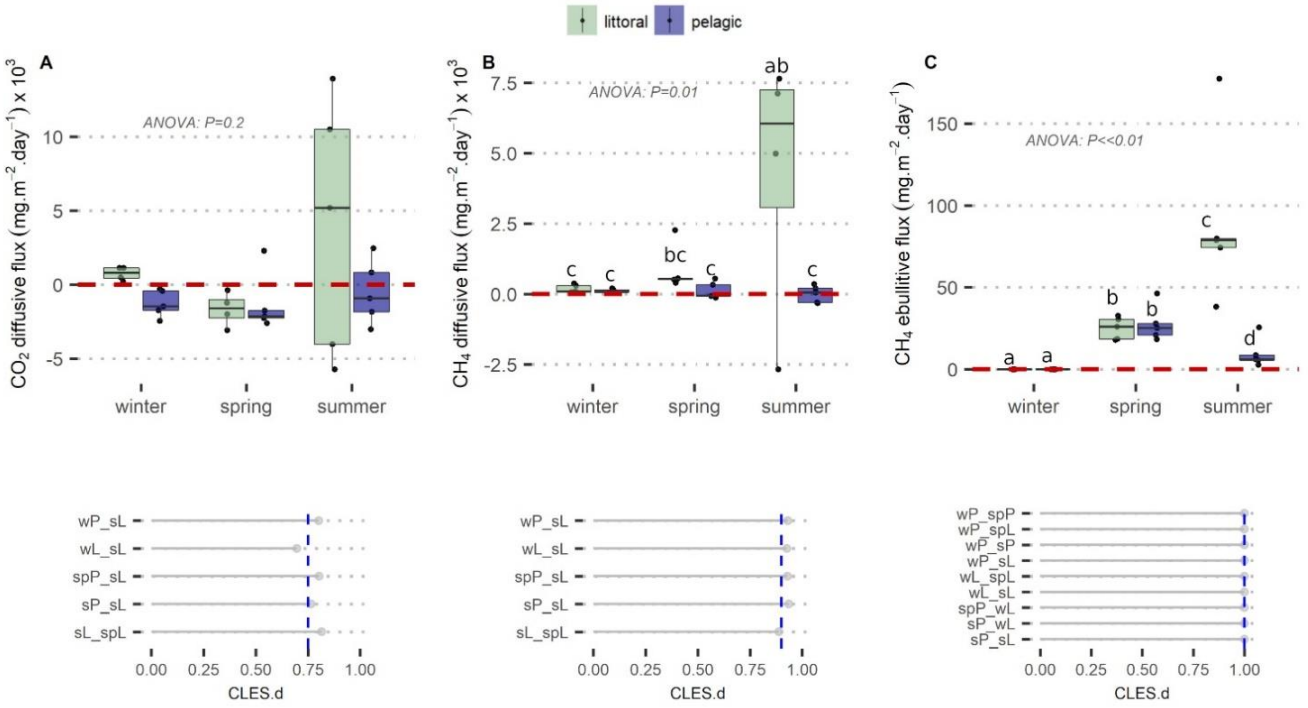

Figure 4. GHG fluxes in the clear-vegetated lake in different seasons (w: winter, sp: spring, and s: summer) and zones (Lit: littoral and Pel: pelagic). A-C) above box-plots of GHG fluxes in $mg.m^{-2}.day^{-1}$: A) CO_2 diffusive flux, B) CH_4 diffusive flux, and C) CH_4 ebullitive flux. The dark horizontal lines represent the median, the boxes show the interquartile range with 25% to 75% percentiles and the vertical lines the distribution range. Black dots show individual data and the horizontal dashed red lines indicate net zero fluxes. Letters above the boxes (a, b, c, and d) summarize the pairwise comparison after ANOVA tests (Tukey´s test). Please note the different scales used for each GHG. A-C) below, common-language effect sizes (CLES.d) enabling comparisons among groups (lake*zone). In A) only comparisons with CLES.d higher than 0.65 are shown and the vertical blue dashed line indicates CLES.d=0.75. In B) only comparisons with CLES.d higher than 0.75 are shown and the vertical blue

dashed line indicates CLES.d=0.9. In C) only comparisons with CLES.d higher than 0.99 are shown and the vertical blue dashed line indicates CLES.d=1.

Plumbing subtropical lakes into carbon latitudinal gradients

Running the regression models developed by Holgerson and Raymond, (2016) to explain the variation in dissolved CO_2 and CH_4 concentrations using the database compiled by H&R combined with our data, resulted in similar parameters than those found in the original study (Table 3). Some of our data points, however, deviated strongly from the concentrations predicted by the model. The dissolved CO_2 concentration in the pelagic zone of our clear-vegetated lake fell far below the quadratic regression line, while data point representing the littoral zone of our sediment-turbid lake was located far above the regression line (Fig 5A). In addition, the dissolved CH_4 concentrations in the Uruguayan lakes were all lower than the predicted by the model, with the exception of the littoral zone of the clear-vegetated lake (Fig 5B). Finally, for both zones of our sediment-turbid lake, the CO_2/CH_4 concentrations ratios were far above the regression line (Fig 5C), which related to the extremely low CH_4 concentrations in that lake.

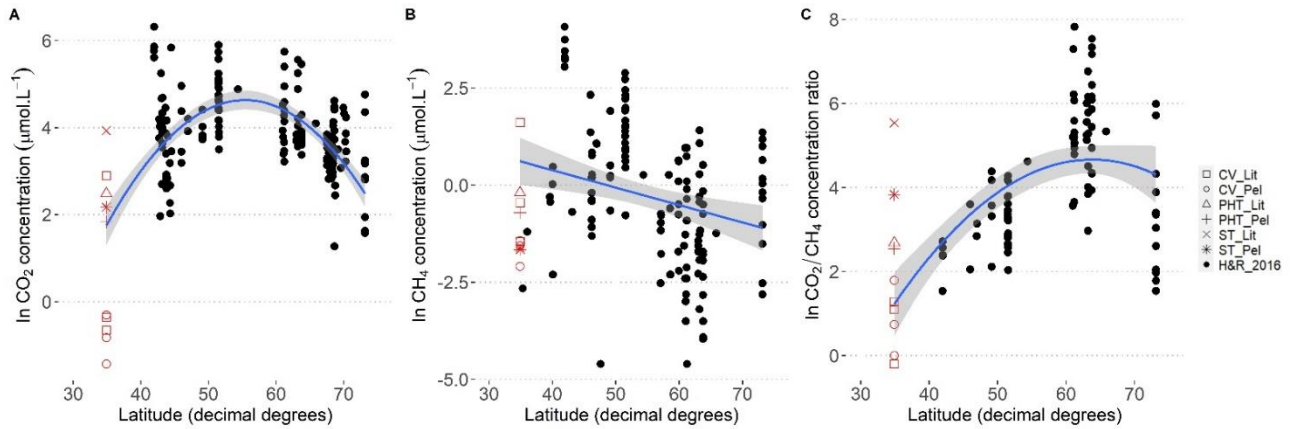

Figure 5. CO_2 and CH_4 gas concentrations in surface waters in relation to latitude according to H&R 2016. A) Natural logarithm of CO_2 concentration (in µmol.L^{-1}) versus latitude, with quadratic regression in blue. B) Natural logarithm of CH_4 concentration (in µmol.L^{-1}) versus latitude, with linear regression in blue. C) Natural logarithm of CO_2/CH_4 versus latitude, with quadratic regression in blue. Black dots correspond to Holgerson & Raymond (2016) data and the red dots to the three Uruguayan lakes. Abbreviations: CV: clear-vegetated, PHT: phytoplankton-turbid and ST: sediment-turbid, Lit: littoral and Pel: pelagic.

Table 3. Relationship between the natural logarithm of dissolved CO_2 and CH_4 concentrations (in µmol. L^{-1}) and the CO_2 / CH_4 ratio versus latitude and lake area, using the same regression models as in Holgerson & Raymond (H&R), (2016). Regressions were fitted adding the mean values of both gases concentrations per zone in the three subtropical lakes from Uruguay to the open database for 246 shallow lakes and ponds considered by H&R. $Latitude_c$ is latitude values centered around the mean. The parameters obtained by H&R for all 427 lakes are shown in italics between brackets.

	Log (CO_2) ~ Log (area)* Latitude$_c$+ Latitude$_c^2$	Log (CH_4) ~ Log (area)* Latitude	Log (CO_2/CH_4) ~ Log (area)* Latitude$_c$+ Latitude$_c^2$
Intercept	4.42 *(4.44)*	3.61 *(4.25)*	4.66 *(5.20)*
Log (area)	-0.113 *(-0.061)*	-0.31 *(-0.278)*	0.19 *(0.19)*
Latitude	-	-0.071 *(-0.080)*	-
Latitude$_c$	-0.038 *(-0.055)*	-	0.080 *(0.063)*
Latitude$_c^2$	-0.0048 *(-0.0042)*	-	-0.0041 *(-0.0081)*
Log (area)*Latitude$_c$	0.0090 *(0.008)*	-	0.0044 *(0.0077)*
F	49.3 *(49.1)*	76.80 *(213.2)*	27.61 *(109.2)*
P	<<0.001 *(<0.001)*	<<0.001 *(<0.001)*	<<0.001 *(<0.001)*
R^2	0.48 *(0.36)*	0.51 *(0.58)*	0.51 *(0.65)*

Discussion

In agreement with our general hypothesis, we found clear differences in CH_4 fluxes (mainly ebullition and CH_4 concentration-derived diffusive fluxes) between our three shallow lakes with contrasting regimes: clear-vegetated, phytoplankton-turbid and sediment-turbid (Fig. 6). As expected, methane ebullition was highest in the phytoplankton-dominated system (Fig. 6B) and lowest in the organic matter-poor sediment-turbid lake (Fig. 6C), where even CH_4 undersaturation was observed, which implies diffusive CH_4 uptake. In the clear-vegetated lake, lower CH_4 emissions (diffusive and ebullitive) occurred in the pelagic zone (with high submerged macrophytes cover) compared to the littoral zone that had fewer submerged plants – but abundant free-floating and emergent plant growth (Fig. 6A).

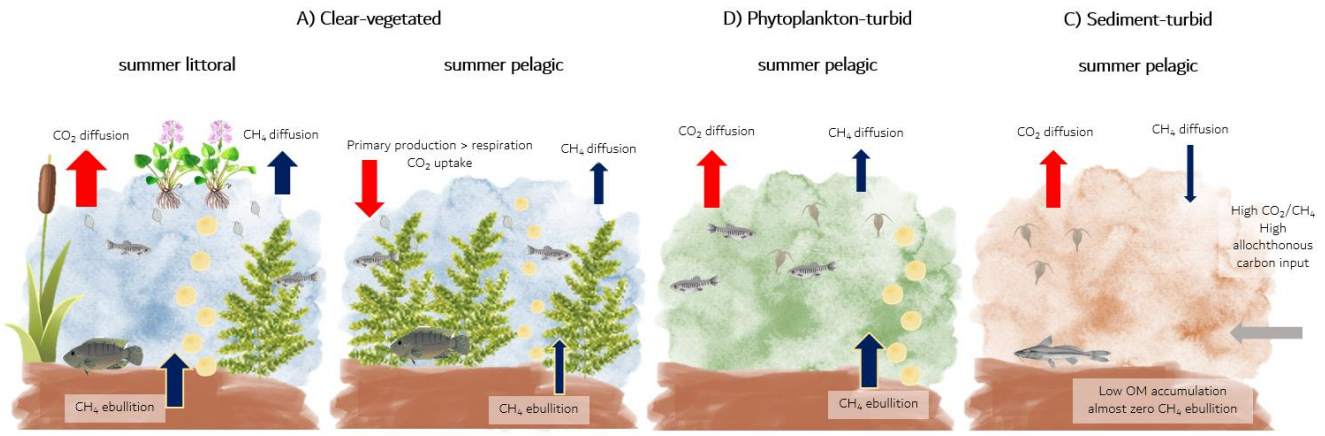

Figure 6. Conceptual summary of the main observed patterns in carbon fluxes for the three shallow subtropical lakes with contrasting regimes: A) clear-vegetated at littoral and pelagic zones, B) phytoplankton-turbid lake, and C) sediment-turbid lake. Red arrows represent the potential CO_2 fluxes and blue arrows the CH_4 fluxes, the thickness and direction of the arrow shows the observed intensity (in a qualitative way) and direction of the flux.

Methane undersaturation in lake surface water is not common (e.g., the overview papers of Bastviken et al., (2011) and Holgerson & Raymond, (2016) do not report CH_4 uptake). Our sediment-turbid lake, where we found CH_4 undersaturation, stands out because of its very low primary producer biomass. This corresponds with low organic carbon accumulation in the sediment: the lake had an organic matter content of ca. 5.1% in the pelagic zone, which is very low compared to, for instance, the clear-vegetated lake, that had an organic matter content of ca. 21.5% (A.F. Lotter, 2008 unpublished data). In addition, the water column was well oxygenated until the sediment surface. A low organic matter availability limits methanogenesis, which would explain the very low CH_4 ebullition rate, while the high O_2 availability likely stimulated CH_4 oxidation, which is in line with the CH_4 undersaturation we observed. The low primary producer biomass in the lake likely also explains the prevailing CO_2 emissions due to ecosystem respiration overruling primary production. The high dissolved CO_2 to CH_4 ratio, compared with predictions based on the latitudinal regression, seems to further reinforce the idea that CO_2 concentrations in the sediment-turbid lake are supported by allochthonous input with low accumulation of organic matter in the system.

The relatively high phytoplankton biomass in the phytoplankton-turbid lake did not result in CO_2 uptake. Although this contradicts our expectations based on reports of eutrophic lakes with low dissolved CO_2 concentrations in their surface waters (e.g., Balmer & Downing, 2011; Pacheco et al., 2014; Jeppesen et al., 2016; Morales-Williams et al., 2021), there are several studies that report CO_2 outgassing in eutrophic lakes as well (Xing et al., 2006; Almeida et al., 2016; Morales-Williams et al., 2021). The underlying causes of these contrasting patterns is likely related to different terrestrial inputs of either organic or inorganic C (Weyhenmeyer et al., 2015; Almeida et al., 2016; Morales-Williams et al., 2021). In contrast, the high CH_4 ebullition rate registered in the pelagic zone of this lake agrees with findings from other studies reporting high CH_4 ebullition from eutrophic shallow lakes (Beaulieu et al., 2019; Yan et al., 2019). The ebullition in the pelagic zone of our phytoplankton-turbid lake was around 100 $mg.m^{-2}.day^{-1}$, with a chlorophyll-a concentration of 47 $\mu g.L^{-1}$, which lies within the range predicted by the chlorophyll-a – CH_4 ebullition relationship published by Beaulieu et al., (2019).

The clear-vegetated lake showed the most pronounced differences between the littoral and pelagic zone, with the highest total CH_4 emissions registered in our study occurring in the littoral zone. The littoral zone had a diverse plant community composed of the three different life forms (submerged, free-floating, and emergent). The decomposition of macrophyte tissues fuelling methane production (Grasset et al., 2019) in a combination with input of terrestrial carbon from the surrounding land might have played a role in the high littoral emissions. Also in temperate and boreal regions, higher CH_4 emissions from the littoral than from the pelagic zones of shallow lakes have been reported (Juutinen et al., 2003; Hofmann et al., 2010). We speculate

that the pronounced difference in CH_4 emissions from the littoral and pelagic zone in our clear-vegetated lake was further enhanced by the presence of a dense vegetation of submerged macrophytes in the pelagic zone, oxygenating the sediment thought radial oxygen loss. While *Ceratophyllum demersum* has a poorly developed root system (Schneider & Carlquist, 1996) and is often even considered submerged free-floating (Xiong et al., 2013), *Egeria densa* – the other abundant species in the pelagic zone - does exhibit a substantial radial oxygen loss (Sorrell et al., 2002; Sorrell & Downes, 2004) which may inhibit methane production and stimulate methane oxidation thereby reducing overall CH_4 emission (Zheng et al., 2018). Low diffusive CH_4 emissions may furthermore be linked to CH_4 oxidation occurring in the water column, particularly on the macrophyte leaves as several submerged plants (and particularly the species reported in this lake) contain high densities of methanotrophic bacteria (Yoshida et al., 2014).

The findings for CO_2 in our clear-vegetated lake, albeit not significant, showed also remarkable differences between lake zones, with lower or even negative (meaning uptake) CO_2 fluxes in the (submerged plant-dominated) pelagic than in the littoral zone. Several studies have already documented a negative correlation between macrophyte biomass and CO_2 emissions (Huss & Wehr, 2004; Xing et al., 2006; Jeppesen et al., 2016), as well as with dissolved CO_2 concentrations (Kosten et al., 2010). The strong capacity of CO_2 uptake by submerged macrophytes in subtropical regions stands results in extremely low concentrations of dissolved CO_2 in the pelagic zone of our clear-vegetated lake (Fig. 5A), particularly when compared to the latitudinal model projections based on the H&R data.

Seasonality in carbon fluxes in the clear-vegetated lake was most pronounced for CH_4, with higher CH_4 emissions occurring at higher temperatures (Fig. 4). This strong temperature effect on CH_4 production and emission has been found before (e.g., Yvon-Durocher et al., 2014; Aben et al., 2017) and has been attributed to the increase in microbial activity with increasing temperature.

Our results furthermore indicate that the contribution of the littoral and pelagic zone to the total greenhouse gas balance (in terms of CO_2-equivalents) varies considerable between lakes and between seasons (Fig. ESM3). While many studies have focused on pelagic emission rates (Trolle et al., 2012; DelSontro et al., 2016; Holgerson & Raymond, 2016), we found high total carbon emissions (in CO_2-eq) from the littoral zones in our lakes. In the clear-vegetated lake in summer, emissions from the littoral zone were even higher than the pelagic zone. This indicates that the littoral area can play an important role contributing to the overall emission of the lake. Although the actual importance of the littoral zone may deviate from our estimations as we did not include plant-mediated CH_4 fluxes of floating and emergent plants – which can be considerable (Bansal et al., 2020; Oliveira Junior et al., 2020)- nor the CO_2 uptake by these plants, it does point out that the littoral area needs more attention in further studies.

Conclusion

Our results support the hypothesis that carbon fluxes in shallow lakes, particularly CH_4, are related to the regime of the lake. The type of the dominant primary producers (i.e., submerged macrophytes or phytoplankton) or near-absence of primary producers (as in our sediment-turbid lake) strongly impacts CH_4 ebullition and diffusion. In the near-absence of autochthonous primary production, our lake acted as a CO_2 source, either due to the decomposition of allochthonous carbon or the inflow of inorganic carbon. In this system, CH_4 emissions were low and at most sites even below atmospheric equilibrium concentrations implying that diffusive CH_4 uptake took place. This is likely linked to the before mentioned low organic carbon availability combined with methanotrophy. This contrasts the behaviour of the highly productive systems, where CH_4 emissions were considerably higher.

Lower CO_2 emissions (or CO_2 uptake) and lower CH_4 emissions occurred when submerged macrophytes were the dominant group (e.g., the pelagic zone in the clear-vegetated lake) than when emergent or free-floating macrophytes dominated (e.g., the littoral zone in the clear-vegetated and phytoplankton-turbid lakes). Thus, our findings support predictions i-iii and the hampering role of submerged macrophytes for carbon emissions already recognised in previous studies (Xing et al., 2006; Jeppesen et al., 2016; Davidson et al., 2018). Indeed, according to patterns observed in our clear-vegetated lake in the subtropical regions, submerged-macrophyte dominance might promote a net CO_2 intake even in the cold season.

We postulate that future work aiming to estimate greenhouse gas emissions from lakes need flux assessments covering different time scales, including seasonal, over longer time periods, explicitly incorporating spatial heterogeneity within lakes. Although, we only studied one shallow lake of each regime, we consider our work an interesting first step in quantifying and understanding carbon fluxes in subtropical shallow lakes and the potential role of regimes.

Acknowledgements

We dedicate this paper in loving memory of our dear late friend Juan M. Clemente, Checho.

We deeply thank the editorial assistance of Anne Mette Poulsen. We would also like to acknowledge Programa para el Desarrollo de las Ciencias Básicas (PEDECIBA-Geociencias, Uruguay) and Agencia Nacional de Investigación e Innovación (ANII, Uruguay) for their support to MC and the Academy Ecology Fund 2018, Royal Netherlands Academy of Arts and Sciences (KNAW, The Netherlands) for supporting our field work. MM is supported by PEDECIBA, ANII (Uruguay).

SUPPLEMENTARY INFORMATION CHAPTER 2

GHGs sampling

Equations for the estimation of CO_2 diffusion (FCO_2, in $mg.m^{-2}.day^{-1}$), (Almeida et al., 2016):

$$FCO_2 = \frac{V}{A} \times slope \times \frac{(P \times F1 \times F2)}{(R \times T)}$$

Where: V is the volume of the floating chamber in m^3, A is the area covered by the floating chamber in m^2, slope is the slope obtained from the regression between pCO_2 and time, P is the atmospheric pressure in atm, F1 is the molecular weight of CO2, 44 $g.mol^{-1}$, F2 is the conversion factor from seconds to days, 86400 $s.d^{-1}$, R is gas constant, 0.082 $l.atm.mol^{-1}.K^{-1}$, T is air temperature in Kelvin.

Equations for the estimation of CH_4 diffusion (FCH_4, in $mg.m^{-2}.day^{-1}$) (Cole & Caraco, 1998; Wanninkhof, 2014):

$$FCH_4 = KL \times ([CH_4]w - [CH_4]a)$$

Where: $[CH_4]w$ and $[CH_4]a$, are the gas concentrations in water and air, respectively in mg. l^{-1}, KL is the gas transfer velocity in $m.h^{-1}$, estimated as:

$$KL = K_{600} \times (Sc/600)^{-x}$$

Where:

$K_{600} = 2.07 + (0.215 \times U10^{1.7})$

$U10 = 1.22 \times v(m.s^{-1})$, where v is wind speed at 1m of heigh.

Sc, is the Schmidt number for CH_4 in freshwater and at the corresponded air temperature, estimated according to Wanninkhof, (2014).

x, is 0.66 if the wind speed is higher than $3m.s^{-1}$ and 0.5 if it is lower.

Equations for dissolved CO_2 concentrations (in µM) in the surface water (Kling et al., 1992; Cole et al., 1994):

$$pK1 = 0.0000009 \times T^3 + 0.0002 \times T^2 - 0.0134 \times T + 6.579$$

$$K1 = 10^{-pK1}$$

$$pK2 = 0.000001 \times T^3 + 0.00006 \times T^2 - 0.014 \times T + 10.625$$

$$K2 = 10^{-pK2}$$

$$[H] = 10^{-pH}$$

$$pKh = 1.12 + 0.014 \times T$$

$$Kh = 10^{-pKh}$$

$$alpha0 = 1 + K1/[H] + K1 \times K2/(H^2)^{-1}$$

$$\text{alpha1} = [\text{H}] \times \text{K1}/([\text{H}]^2 + [\text{H}] \times \text{K1} + \text{K1} \times \text{K2})$$

$$\text{DIC} = [\text{CHO}_3^{-}]/\text{alpha1}$$

$$\text{CO}_2 = \text{DIC} \times \text{alpha0}$$

Where: T is water temperature in °C, pH is water pH measured *in situ,* DIC is dissolved inorganic carbon in µM, [HCO_3^-] is the concentration of bicarbonate in µM, estimated by titillation according to Arocena et al., (1999).

Characterization of lakes

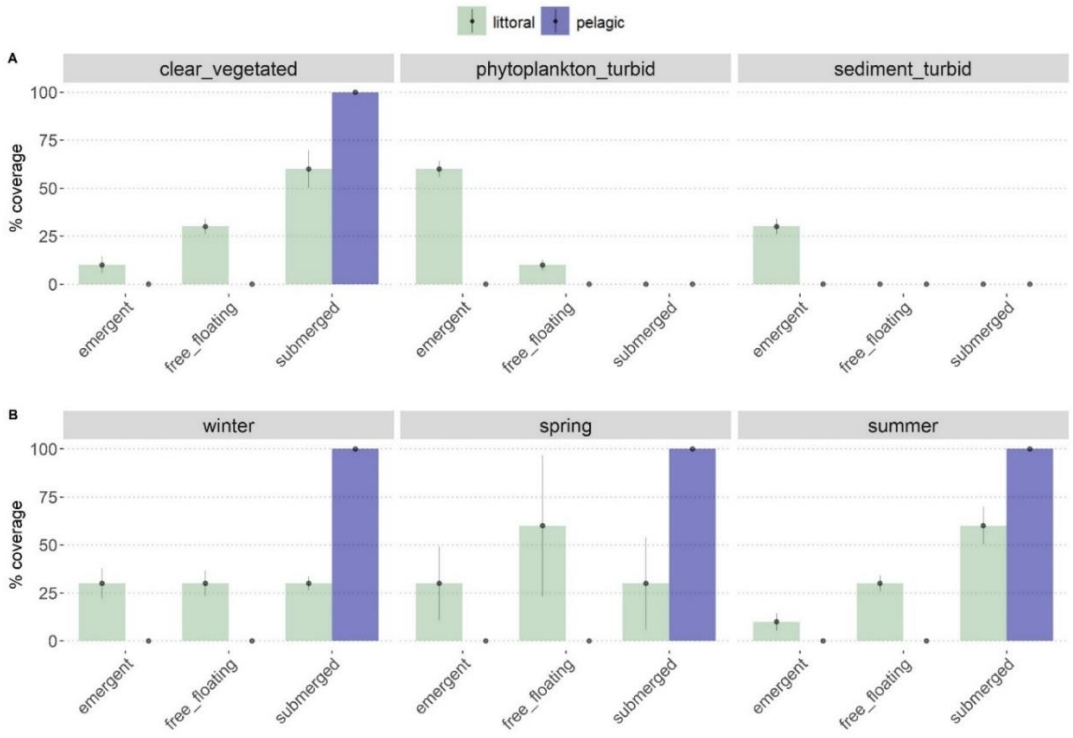

Figure ESM1. Percent of coverage of each macrophytes group, classified according to their life-form as emergent, free floating and submerged. Comparisons between littoral and pelagic lake zones and among: A) among lakes for summer, and B) seasons in the clear vegetated lake. Error bars are presented as black dots and vertical black lines.

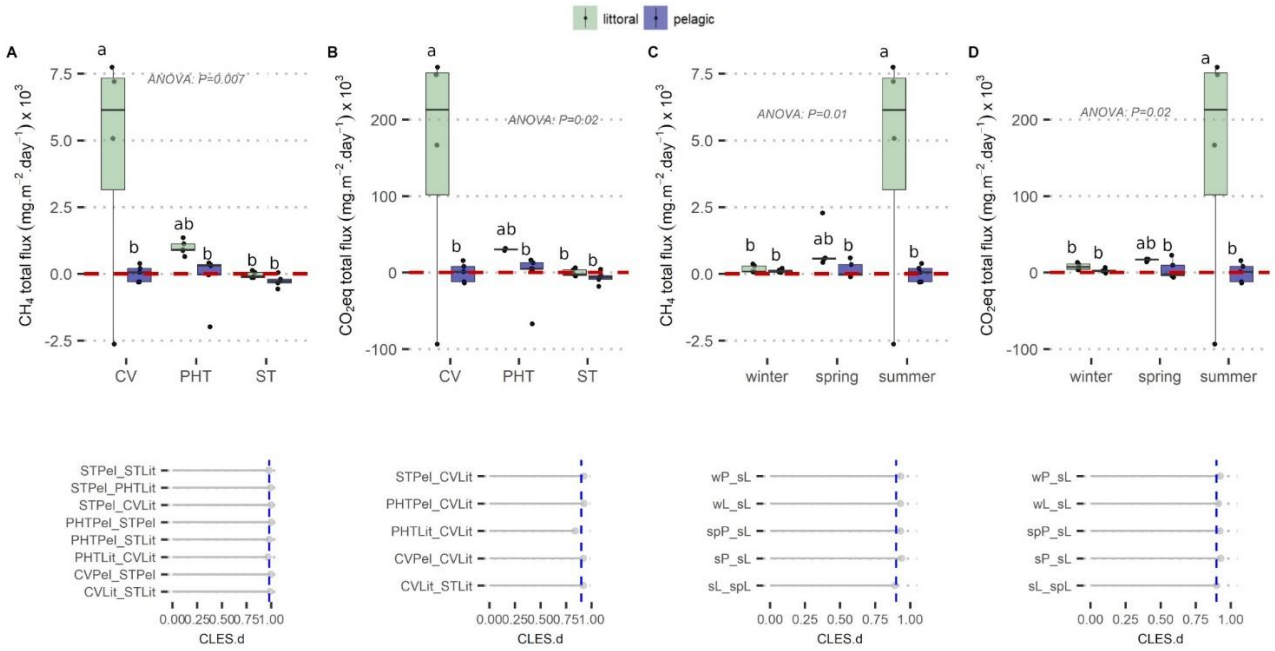

Figure ESM2. Total CH_4 fluxes (diffusion + ebullition) and total carbon fluxes based on CO_2-eq (CO_2 diffusion + 34* total CH_4): in the littoral zone and pelagic zone. A-B) among lakes and between zones in summer; C-D) among seasons and between zones for the clear-vegetated lake. First row with box-plots for GHGs fluxes in $mg.m^{-2}.day^{-1}$, where dark horizontal line represents the median, the boxes the interquartile range with 25% to 75% percentile and the vertical lines the distribution range. Black dots were added to show individual data and the horizontal red dashed line to indicate cero fluxes. Letters on the top of the boxes (a and b), summarize the pairwise comparison after ANOVAs (Tukey´s test). Second row with common-language effect sizes (only CLES.d>0.7 are shown) for comparisons among groups, being the vertical blue dashed line at CLES.d=0.9. w: winter; s: summer; sp: spring; CV: clear-vegetated; PHT: phytoplankton-turbid; ST: sediment-turbid; Lit: littoral; Pel: pelagic.

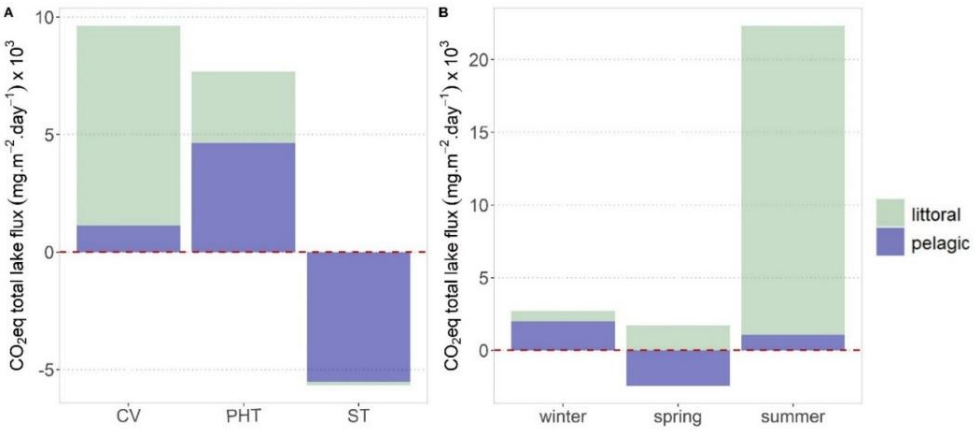

Figure ESM3. Average system flux per lake zone and based on CO_2-eq (in $mg.m^{-2}.day^{-1}$), estimated by dividing the median value of CO_2-eq found for each zone by the percent of the lake area occupied by that zone. In A) comparison between lakes in summer and in B) comparison between seasons for the clear-vegetated lake.

CHAPTER 3

TROPHIC AND NON-TROPHIC EFFECTS OF FISH AND MACROINVERTEBRATES ON CARBON EMISSIONS

Maite Colina[1,2], Mariana Meerhoff[1], Germán Pérez[3], Annelies J. Veraart[2], Paul Bodelier[3], Antoon van der Horst[4], Sarian Kosten[2]

[1] Departamento de Ecología y Gestión Ambiental, Centro Universitario Regional del Este (CURE), Maldonado. Universidad de la República, Uruguay.

[2] Department of Aquatic Ecology and Environmental Biology, Institute for Water and Wetland Research, Radboud University, P.O. Box 9010, 6500 GL Nijmegen, the Netherlands.

[3] Department of Microbial Ecology, Netherlands Institute of Ecology (NIOO-KNAW), Wageningen, The Netherlands, P.O. Box 50, 6708 PB Wageningen, The Netherlands.

[4] Department of Animal Ecology and Physiology, Radboud University, P.O. Box 9010, 6500 GL Nijmegen, the Netherlands.

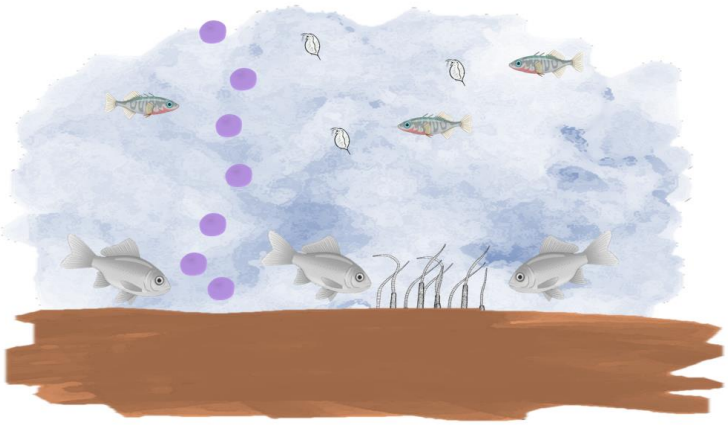

Published:

Colina, M., M. Meerhoff, G. Pérez, A. J. Veraart, P. L. E. Bodelier, & S. Kosten, 2021. Trophic and non-trophic effects of fish and macroinvertebrates on carbon emissions. Freshwater Biology 66: 1831–1845. DOI: 10.1111/fwb.13795.

Abstract

1. Shallow aquatic systems exchange large amounts of carbon dioxide (CO_2) and methane (CH_4) with the atmosphere. The production and consumption of both gases is determined by the interplay between abiotic (such as oxygen availability) and biotic (such as community structure and trophic interactions) factors.

2. Fish communities play a key role in driving carbon fluxes in benthic and pelagic habitats. Previous studies indicate that trophic interactions in the water column, as well as in the benthic zone can strongly affect aquatic CO_2 and CH_4 net emissions. However, the overall effect of fish on both pelagic and benthic processes remains largely unresolved, representing the main focus of our experimental study.

3. We evaluated the effects of benthic and pelagic fish on zooplankton and macroinvertebrates; on CO_2 and CH_4 diffusion and ebullition, as well as on CH_4 production and oxidation, using a full-factorial aquarium experiment. We compared five treatments: absence of fish (control); permanent presence of benthivorous fish (common carps, benthic) or zooplanktivorous fish (sticklebacks, pelagic); and intermittent presence of carps or sticklebacks.

4. We found trophic and non-trophic effects of fish on CO_2 and CH_4 emissions. Intermittent presence of benthivorous fish promoted a short-term increase in CH_4 ebullition, likely due to the physical disturbance of the sediment. As CH_4 ebullition was the major contributor to the total GHG emissions, incidental bioturbation by benthivorous fish was a key factor triggering total carbon emissions from our aquariums.

5. Trophic effects impacted GHG dynamics in different ways in the water column and the sediment. Fish predation on zooplankton led to a top-down trophic cascade effect on methane-oxidizing bacteria. This effect was, however, not strong enough as to substantially alter CH_4 diffusion rates. Top-down trophic effects of zooplanktivorous and benthivorous fish on benthic macroinvertebrates, however, were more pronounced. Continuous fish predation reduced benthic macroinvertebrates biomass decreasing the oxygen penetration depth, which in turn strongly reduced water-atmosphere CO_2 fluxes while it increased CH_4 emission.

6. Our work shows that fish can strongly impact GHG production and consumption processes as well as emission pathways, through trophic and non-trophic effects. Furthermore, our findings suggest their impact on benthic organisms is an important factor regulating carbon (CO_2 and CH_4) emissions.

Keywords: greenhouse gases, benthic processes, pelagic processes, methane production, methane oxidation

Introduction

Shallow freshwaters play a globally important role in carbon transformation and transport. This includes the exchange of the greenhouse gases (GHGs) carbon dioxide (CO_2) and methane (CH_4) with the atmosphere (Tranvik et al., 2009; Holgerson & Raymond, 2016; Aben et al., 2017). Aquatic CO_2 fluxes are strongly influenced by primary production and autotrophic and heterotrophic respiration (Cole et al., 2007; Larsen et al., 2011; Yang et al., 2015; Jeppesen et al., 2016). Methane production and oxidation are conducted by different microorganisms: Archaea mostly produce CH_4 in anoxic and organic matter rich sediments, while aerobic methane-oxidizing bacteria (MOB) oxidize CH_4 at the sediment-water interface and in the water column (Bastviken et al., 2008; Biderre-Petit et al., 2011). Methane produced in the sediments can be released to the atmosphere by diffusion through the water column or by ebullition when bubbles are formed under CH_4 supersaturated conditions (Bastviken et al., 2004). At the ecosystem level, GHG fluxes are therefore determined by the interplay between abiotic factors, such as organic matter and oxygen (O_2) availability, and biotic factors such as community structure and trophic interactions (Bastviken et al., 2008; Palma-Silva et al., 2013; Jeppesen et al., 2016).

Due to the close benthic-pelagic coupling, an intense carbon exchange occurs between these two habitats (Wetzel, 2001). Primary and secondary production occurring in the benthic zone may support consumers typically inhabiting the pelagic zone, and vice-versa; decomposition in pelagic zones supplies organic matter to the benthos, while carbon and nutrient remineralisation in the sediment sustain processes at the water column (Schindler & Scheuerell, 2002; Chumchal & Drenner, 2004; Geurts et al., 2008). However, how the interplay between benthic and pelagic processes affects the emissions of CO_2 and CH_4 remains largely unresolved.

Due to their feeding habits and diel and ontogenic changes in the use of space, fish are an important link between littoral, benthic and pelagic habitats (Schindler & Scheuerell, 2002; Vander Zanden & Vandeboncoeur, 2002; Teixeira-De Mello et al., 2009; Kosten & Meerhoff, 2014). Fish strongly influence lake carbon processes in various ways. Zooplanktivorous fish, for instance, may reduce large-bodied zooplankton densities as to promote phytoplankton growth (Brooks & Dodson, 1965; Hansson et al., 2012), enhancing net primary production and CO_2 fixation (Schindler, 1997; Jeppesen et al., 2016; Grasset et al., 2020). Furthermore, a recent study suggests that zooplanktivores may weaken zooplankton grazing pressure on MOB, resulting in increased MOB biomass (i.e. a trophic cascade) and increased oxidation of CH_4 in the water column (Devlin et al., 2015). This implies that CH_4 produced in lake sediments can represent an important carbon source for pelagic food webs, through the incorporation of CH_4 derived carbon in pelagic MOB and subsequently in zooplankton and even in fish (Bastviken et al., 2003; Jones & Grey, 2011; Sanseverino et al., 2012; Devlin et al., 2015).

In the benthic habitat, bioturbation by benthivorous fish may impact O_2 concentrations at the sediment-water interface in different ways. Bioturbation may increase resuspension of organic

material and its mineralization promoting O_2 consumption (Datta et al., 2009). In addition, resuspension decreases light availability that, jointly with the uprooting of submerged macrophytes, may reduce benthic primary production, resulting in lower O_2 production (Zambrano et al., 2001; Rahman, 2015a). Lower O_2 concentrations may lead to an increase in CH_4 production and a decrease in CH_4 oxidation (Datta et al., 2009). In addition, bioturbation may increase the sediment-water nutrient flux, facilitating phytoplankton blooms and thereby pelagic CO_2 uptake, but also higher deposition of labile organic matter (Havens, 1993; Rahman, 2015a), further fuelling CH_4 production (Rahman, 2015a, 2015b; Oliveira Junior et al., 2019). In turn, the foraging activity of fish may also trigger methane bubble release, where bubbles have already formed. Although not yet causally linked to fish, different studies have shown that occasionally physical disturbance of the sediment triggers the release of gas bubbles from the sediments, thereby increasing CH_4 ebullition (Datta et al., 2009; Bhattacharyya et al., 2013; Ma et al., 2018).

By contrast, resuspension by fish also increases the exposure of organic matter (previously stored anaerobically in the sediment) to O_2, enhancing aerobic decomposition and CO_2 production. Activities of other fauna that increase O_2 exposure are known, for example those of burrowing benthic macroinvertebrates, such as tubifex worms (Leal et al., 2007; Baranov et al., 2016). Tubifex worms are “conveyer-belt” surface deposit feeders that live partially buried in the sediments, head-down, ingesting sediment particles and excreting them at the sediment surface in fecal pellets (Palmer, 1968). Tubifex pump relatively large volumes of oxygenated water through their foraging galleries (also known as bioirrigation) promoting sediment aeration (Lagauzère et al., 2009; Hölker et al., 2015). A similar effect, of enhanced oxygenation of the sediments, may be expected as a result of intense bioturbation by fish.

In this study we aim to unravel the trophic and non-trophic effects of fish on aquatic greenhouse gas emission. To highlight the potential variability of fish impact on water column and sediment processes, we used sticklebacks (mostly zooplanktivorous) and carp (mostly benthivorous) in separate systems. In addition, we compared systems where fish were continuously present with systems with intermittent fish presence, to reveal possible differentiated effects regarding predation pressure and bioturbation intensities. We hypothesized that: 1) intense zooplanktivorous predation on zooplankton leads to higher abundance of methane oxidizers in the water column, reducing CH_4 emissions, and increasing phytoplankton primary production which in turn, reduces CO_2 emissions (Fig. 1.H1); even short-term fish presence is enough to trigger these trophic processes; 2) incidental bioturbation by benthivorous fish triggers CH_4 bubble release, due to physical disturbance of the sediment (Fig. 1.H2); 3) deeper sediment oxygen penetration enhances methane oxidation and decreases its production, thereby decreasing CH_4 emission. Oxygen (O_2) penetration depth is differently affected by direct and indirect fish effects: it increases due to direct bioturbation activity by fish, but decreases when indirect effects of fish, via predation on benthic macroinvertebrates, reduces sediment bioirrigation and oxygenation (Fig. 1.H3).

To test our hypotheses, we evaluated total carbon emission (diffusion and ebullition) in our experimental systems over 86 days, as well as zooplankton, benthic macrofauna, methane oxidizers and methane producers.

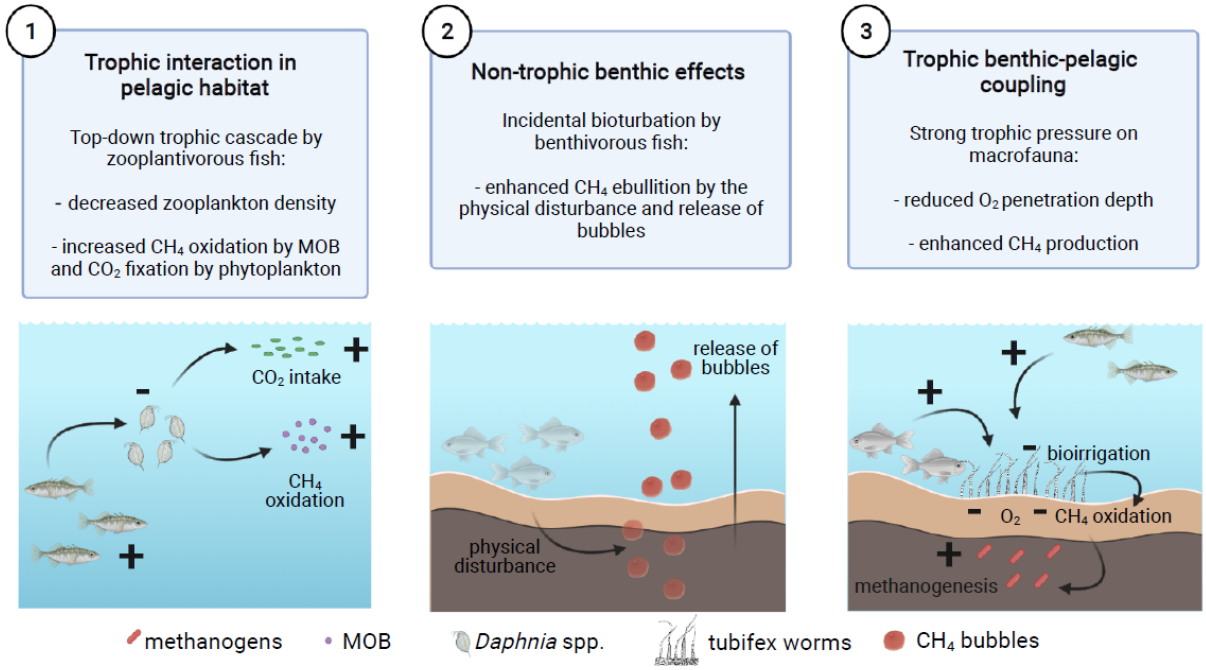

Figure 1. Summary of the main hypothesized effects of benthic and pelagic fish on CO_2 and CH_4 emissions in shallow lakes. Figure created with BioRender.com.

Material and methods

Experimental set up

A full-factorial experiment was conducted over 86 days in a temperature and light controlled climate room. Twenty aquaria (0.48m height, 0.45m width and 0.40m depth, ~86L) were filled with a layer of 0.25m (~22L) of homogenized wet sediments and ~55L of tap filtered water. Sediments were collected from the littoral area of the eutrophic shallow lake Noorderlijke from Langeraar, the Netherlands (52°11'18.5''N 4°42'37.5''E), known for its substantial CH_4 production potential (G. van Dijk personal comm.). From the same lake, a concentrated water inoculum containing the natural phytoplankton, zooplankton and microbial communities was also collected with a plankton net (50µm mesh size). Two litres of well-mixed inoculum were added to each aquarium at the beginning of the experiment. To compensate for evaporation, tap filtered water was added regularly. In order to simulate natural temperature and light changes from late temperate winter to beginning of summer, room temperature was increased

from 12 to 24°C (1-2ºC every 11 days) and hours of light per day from 9 to 13 hours, always after routine measurements.

Experimental fish treatments were created with common carp as benthivorous fish (*Cyprinus carpio*, Linnaeus 1758) and sticklebacks as zooplanktivorous fish (*Gasterosteus aculeatus*, Linnaeus 1758). Five treatments with four replicates were compared: absence of fish (control), permanent presence of carps (CP) or sticklebacks (SP), intermittent presence of carps (CI) or sticklebacks (SI). For intermittent treatments, fish individuals were added for 45-60 minutes every 11 days, simulating conditions of very low fish densities, where foraging pressure on any particular spot could be considered low and sporadic. For CP and CI treatments, four individuals of 10-12cm of total length (TL) -cultured at Wageningen University (Netherlands)- were added per aquarium (~90.56g FW of total fish) and for SP and SI treatments, five individuals of 4-6cm TL– collected in a canal in Groesbeek (51°46'45.8''N 5° 56' 22.0''E) - (~7.10g FW of total fish). Biomass were estimated from allometric relationships according to (Verreycken et al., 2011). Fish densities resembled those commonly found in natural temperate systems (Meerhoff & Jeppesen, 2009; Meerhoff et al., 2012) and were selected based on their social behaviour and to mimic natural processes, but avoiding fish starvation and stress. An ethical review of the experiment by the National Committees for the Protection of Animals Used for Scientific Purposes was not required, according to Article 1 of the EU Directive 2010/63/EU, as fish were neither distressed nor harmed.

GHG measurements

Every 11 days GHG routine measurements were conducted for all aquaria (Fig.S1). Methane and CO_2 diffusive fluxes between the surface water and air, were measured using a rectangular acrylic chamber (0.35m x 0.33m width and 0.11m depth), connected to an Ultra-portable Greenhouse Gas Analyser (UGGA, Los Gatos Research Inc., San Jose, CA, USA). The chamber rested on the edges of each aquarium by handles at two sides and 1cm was submerged into the water creating a headspace of approximately 11L, where changes in gases concentrations were registered over 5 minutes. The diffusive fluxes were calculated based on the slope of the gas concentration versus time, as in (Almeida et al., 2016). For the intermittent treatments, all measurements were conducted at approx. 15min after fish introduction. The fish from the intermittent treatment were kept in aquaria with the same temperature and light conditions, and were fed survival ration of Chironomid larvae (sticklebacks) and commercial fish food (carp), and starved 24 hours before being temporarily added to the experimental aquaria as to secure their feeding activity.

In each aquarium one bubble trap was deployed, consisting of an inverted plastic funnel (0.2m diameter) connected to a glass bottle filled with water and locked at the top by a rubber stopper which could be punctured by a needle. Every 11 days, the total volume of gas trapped inside each bottle was determined and a 3mL subsample was extracted with a syringe and stored in a vacuum Exetainer (Labco Limited, Lampeter, UK) for further CH_4 concentration analyses. CH_4 ebullitive fluxes (11 days-average) were finally determined by multiplying the CH_4

concentration in the trapped gas by their total volume and dividing by the funnel area (0.031m^2) and the period of time (11 days). Bubble traps were temporarily removed to enable acrylic chamber placement every 11 days.

To analyse the effects of low and sporadic bioturbation by carp (intermittent treatment, CI), short-term ebullition was quantified based on the increase in CH_4 concentrations in the head space of the previously described acrylic chamber during approximately 30-40 minutes. Measurements started 15 minutes after fish introduction based on visual observation of fish behaviour. After introduction to a new aquarium, individuals usually gathered for ca. 15 minutes in a corner before starting to forage. The short-term CH_4 ebullition flux was calculated as the difference between the total amount of CH_4 released from the aquarium to the headspace and the diffusive flux (more details in Supp.Info.Fig.S2) (Attermeyer et al., 2016). The same procedure was conducted in the permanent carp (CP) and the control treatments, thus allowing bubble release comparison in the same period.

The total CH_4 ebullition was calculated by summing the 11-day and the short-term ebullitive fluxes and, the total GHG emission based on CO_2 equivalents using a global warming potential in a 100 year scale of 34 for CH_4 (Myhre et al., 2013).

Concentrations of dissolved CO_2 was estimated from total inorganic carbon (TIC), analysed from 1mL water injected into an Infrared Gas Analyser (IRGA, ABB Analytical, Frankfurt, Germany).

Samples for analyses of dissolved CH_4 at surface-water were taken from all aquaria by submerging a 12mL vacuum exetainer 0.5cm below the surface and inserting a needle to fill it with water. For porewater collection, one exetainer was connected to a ceramic moisture sampler (pore size 0.6µm, Rhizosphere, The Netherlands), permanently placed at 3 to 5cm depth into the sediments of each aquarium. All samples were preserved with 0.1mL of 2.5M H_2SO_4 to halt microbial activity and a headspace was created adding 3mL of N_2 gas, at the same time that an equivalent volume of water was allowed to exit through another needle (IHA, 2010). All vials were vigorously shaken to equilibrate gas concentrations between water and the headspace. Dissolved CH_4 concentration was finally calculated according to Henry's law (Sander, 2015).

For all CH_4 samples, concentrations were analysed by injecting 100µL of gas on a HP 5890 gas chromatograph equipped with a Porapak Q column (80/100 mesh) and a flame ionisation detector (GC-FID; Hewlett Packard, USA).

Surface water and porewater analysis

To monitor conditions for fish, dissolved oxygen and pH were checked every 24hrs. Temperature and pH were measured with a portable multimeter (HQ 40d multi, HACH, Loveland, CO, USA) 0.1m below water surface, together with the routine GHG measurements every 11 days. At the same time, 250mL of water were sampled for turbidity (Turb® 550, WTW,

Germany), phytoplankton chlorophyll-a (PHYTO-PAM Phytoplankton Analyzer, Heinz Walz GMBH, Effeltrich, Germany) and bicarbonate (HCO_3^-, estimated from TIC).

At days 1, 46 and 86 of the experiment 500mL of surface-water from each aquarium was filtered using Whatman® glass microfiber filters (GF/C 1.2µm, and 47mm diameter). Total suspended solids (TSS) and organic matter concentration (OM) were determined as the difference in dry (at 110°C during 24hrs) and burnt (at 500° during 15min) weights of the filters (APHA/AWWA/WEF, 2017). 20mL of filtered water was stored at -20°C and later analysed for NH_4^+, NO_3^- and PO_4^{+3} concentrations using an Auto Analyser III (Bran and Luebbe GmbH, Norderstedt, Germany). Porewater was sampled for nutrient analysis with the same frequency by connecting 50mL vacuum vials to the ceramic moisture samplers and storing the samples at -20°C until analysis.

Sediment analysis

At the end of the experiment, sediment samples from the first 5cm depth were taken from each aquarium (1 sample per aquarium, 4 sub-replicates per treatment) using 10mL sterile-syringes and, together with 4 sub-replicates of the initial inoculum were stored at -20°C until analysis. From each sample, 5 grams were dried at 70°C for 48hrs and burnt for 4 hours at 550°C; at each stage samples were re-weighed to determine moisture and organic matter content (%OM) (Heiri et al., 2001). Five mg pre-combusted subsamples were used for carbon (C) and nitrogen (N) content estimations with an elemental analyser (Carlo, Erba NA 1500, Thermo Fisher Scientific, Waltham, MA, USA).

At the end of the experiment, a lighter-coloured layer was clearly differentiable at the top of the sediment column. This coloured layer was measured every 5cm along the width of every aquarium (5 measures per aquarium) as a proxy of oxygen penetration depth (similar to Diaz & Trefry (2006).

Zooplankton and benthic macrofauna

For zooplankton analyses 10L of water were filtered through a 50µm mesh size net and preserved with 1-2mL of Lugol's iodine solution at the start (from the water inoculum) and end of the experiment. The main groups were identified and *Daphnia* spp. abundances (as individuals.mL^{-1}) was estimated according to (Postel et al., 2000).

Benthic macroinvertebrates were sampled by extracting six sediment cores (5.2cm diameter and 15cm depth) from each aquarium at the end of the experiment. Macroinvertebrates were identified up to genus level and counted. Each sample was dried at 70°C for approximately 72 hours to estimate biomass per aquarium (as total dry weight divided by the sampling area ~127cm^2).

Microbiota: MOB and methanogen abundances

We used the abundance of the functional marker genes for methanogenesis (*mrcA*, encoding for methyl coenzyme-M reductase) and aerobic methane oxidation *(pmoA*, particulate methane monooxygenase), obtained by quantitative-PCR (qPCR), as a proxy of the abundance of the respective methanogenic archaea and methane-oxidizing bacteria (MOB). Although DNA-based qPCR data do not reveal activity of the microbiome, these metrics are widely used to reliable compare relative methanogen and MOB abundance between experimental treatments (Hernández et al., 2017; van Kruistum et al., 2018).

For planktonic MOB and methanogens, ~150mL of water retrieved at days 1, 46 and 86, was filtered through 0.2µm cellulose nitrate membrane filters (SartoriusTM, Göttingen, Germany) and stored frozen until DNA extraction. At day 86, from each aquarium 5cm of the top sediment were taken with 10mL sterile syringes from 5 random sites, pooled in a clean 15mL polypropylene tube and immediately flash frozen in liquid N_2. All samples were kept at -80°C until further analyses. The presence of methanogen archaea in the oxic-water column was tested given their capacity to persist under oxic conditions (Angel et al., 2012) or to occur in the core of aggregates of particulate organic matter suspended in the water column.

DNA was extracted using the DNeasy PowerSoil Kit (Qiagen, Venlo, The Netherlands), following manufacturer instructions. Each assay (DNA extract, non-template control and standard curve) was done in duplicates with primer concentrations and PCR protocols as summarized in Table S1. Standard curves were obtained from a 10-fold serial dilution of a known amount of plasmid DNA fragment from pure cultures representing the target gene (107-101 *pmoA* gene copies and 108-101 *mcrA* gene copies). Amplification efficiencies for planktonic and benthic assays ranged between 82 to 95.2%, with R2 values between 0.98-0.99. Amplicon specificity was checked from the melting curve and by running samples on a 1% agarose gel. The qPCR was performed with an iCycler IQ5 (Applied Biosystem, Carlsbad, CA, USA).

Incubations for potential CH_4 production and oxidation

Potential CH_4 production and oxidation rates were determined at the end of the experiment for those treatments where we expected to observe the major differences: permanent fish treatments (CP and SP) and the control. Samples of mixed sediment and water were extracted from each aquarium and incubated in 120mL vials on a gyratory shaker (120rpm) at 24°C and in the dark. To estimate production, ~50mg of sediments plus ~20mL of water were incubated, after flushing the headspace and water with N_2 gas to create anoxic conditions. To estimate oxidation, ~20mg of sediments and ~35mL of water were incubated after 1mL of pure CH_4 was added to each bottle at time zero. CH_4 concentrations were analysed by gas chromatography (GC-FID) every 24hrs for five days to estimate production and every 3hrs for three days to estimate oxidation. Measurement timing and incubation length were determined based on previous knowledge about the kinetics of each process (Steenbergh et al., 2010; Borrel et al.,

2011). Potential production and oxidation rates were estimated from the linear regressions of CH_4 concentration over time and expressed per grams of fresh and dry sediments.

Data analysis

We used two complementary approaches to analyse our data. Firstly, we evaluated the effects of fish type and presence by testing for differences in GHG-emissions among our treatments. Secondly, we evaluated effects of fish by joining data from all treatments and test for significant relations between potential explanatory variables related either to pelagic or benthic processes and the different estimated GHG emission. All statistical analyses were conducted using the software R (RStudio Team, 2018).

To test differences among treatments, we calculated the mean emission during the entire experimental period of each GHG flux for each aquarium (CO_2 and CH_4 diffusion, 11-days average and short-term CH_4 ebullition and CO_2-eq). The mean emission was assessed as the integral - area under the curve estimated by the AUC function from DescTools package (Signorell et al., 2019)- of the flux-intensity versus time (days) graph, divided by the total experimental time (86 days) (Kosten et al., 2018). Differences among treatments in mean emissions were assessed using one-way ANOVAs (3 levels with n=4 for short-term CH_4 ebullition and 5 levels with n=4 for all the other GHG fluxes) and Tukey's HSD function for pairwise comparisons. Effect sizes were estimated by the etaSquared function from the lsr package (Maintainer & Navarro, 2015). Detailed temporal variation in GHG emissions is summarized in the Supp.Info (Table S2 and Fig. S3).

To test for effects on GHG fluxes (CO_2 and CH_4 diffusion, total CH_4 ebullition and total GHG as CO_2-eq) of either pelagic or benthic explanatory variables, we constructed GLM models using just the data at the end of the experiment (day 86). Pelagic explanatory variables were: pH and bicarbonate, *Daphnia* spp. predation index on MOB (ratio of *Daphnia* spp. abundances/*pmoA* gene copy number in surface water), pelagic methanogenic bacteria (*mrcA* gene copy number in surface water) and surface water concentrations of: dissolved O_2, nutrients (as trophic state indicators), chlorophyll-a (as phytoplankton density proxy) and organic matter and transparency (both may relate to phytoplankton growth and resuspension of sediment through bioturbation). Benthic variables were: benthic macroinvertebrate and microbiota in the sediments (MOB and methanogens), O_2 penetration depth and porewater concentrations for dissolved CH_4, NO_3 and NH_4 (as sediment redox potential proxies), OM and C/N ratio (as proxy for decomposition potential). For variables with sub-replicates (microbiota and O_2 penetration depth) median values per aquarium were used. To avoid over-fitting, the models were simplified by removing non-significant variables using the step-AIC function. F values for each explanatory variable were extracted from the ANOVA-table of the simplified models, as a proxy for the relative effect-strength of each single variable to the model, where higher F-values indicate stronger effects.

Next, we zoomed in on the variables directly related to trophic interactions. Differences among treatments were evaluated for *Daphnia* spp. predation index on MOB (5 levels and n=4), benthic macroinvertebrate biomass (5 levels and n=4), O_2 penetration depth (5 levels with n=20) and

methanogens (mrcA gene copy number.mL^{-1}) in sediments (5 levels and n=8) using one-way ANOVA approach as described above. Relationship between MOB in surface water (pmoA gene copy number.mL^{-1}) and *Daphnia* spp. abundance (ind.mL^{-1}) was evaluated with an lm model.

Prior to all analyses we checked for normal distributions and log transformations were applied when necessary. The final GLMs were validated by the evaluation of normal distribution and homogeneity of variance for residuals. In the GLMs with final CO_2 diffusion, one extremely low flux value was removed from the analyses (aquarium 16, CI). Although this value did not affect the general tendency and significance of our models, it affected the accuracy of the models according to residual analyses and was identified as an outlier based on Cook´s distance.

Results

GHG fluxes

The mean CO_2 emissions were significantly higher in the control than in the permanent fish treatments (Fig. 2A; $F_{4,15}$=4.03, p=0.02, Eta.sq: 0.52). The emissions in the control and intermittent-fish treatments (SI and CI) were similar, whereas CO_2 emissions in intermittent treatments were – albeit not significantly so - 1.4 and 1.6 times higher than in the permanent-fish treatments (for carps and sticklebacks, respectively). The mean CH_4 diffusive flux and the 11-day average ebullition did not show a consistent difference among treatments (Fig. 2B & C). The mean CH_4 ebullition assessed based on short-term measurements, however, was significantly higher in the CI treatment than in the control (Fig. 2D; $F_{2,9}$=5.2, p=0.03, Eta.sq: 0.53). The highest short-term ebullition measured in the CI treatment were also considerably higher than those in the CP treatment, but without significant differences in means. The mean CO_2-eq (total GHG) emissions were significantly higher in the treatment with intermittent presence of carp than in treatments with permanent and intermittent presence of sticklebacks (Fig.2E, $F_{4,15}$=5.6, p=0.006, Eta.sq:0.59). Meanwhile non-significant differences in mean CO_2-eq were found between the CI and the control and CP treatment. Ebullition contributed more than 50% to the total GHG emitted in terms of CO_2-eq in all systems. Ebullition contributed significantly more to the overall GHG emission than diffusive emission of CO_2 and CH_4 ($F_{4,15}$= 22.07, p <0.001, Eta.sq: 0.43). The change in emission intensities of all GHG fluxes (CO_2 and CH_4 diffusion, CH_4 11-day average and short-term ebullition and total emissions as CO_2-eq) varied between treatments (Table S2).

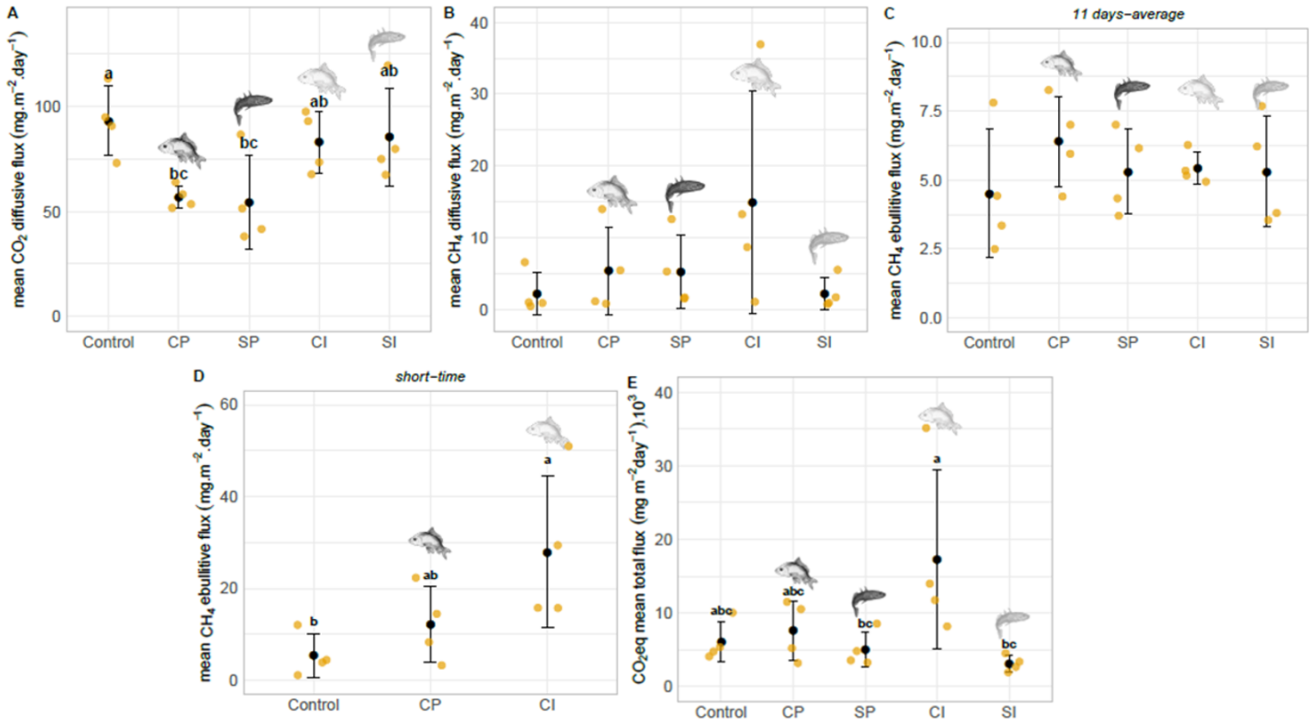

Figure 2. Mean daily fluxes over the course of the experiment among treatments: A) CO_2 diffusive flux; B) CH_4 diffusive flux; C) CH_4 11-day average ebullitive flux quantified based on measurements in permanently installed bubble traps; D) CH_4 short-term ebullitive flux quantified based on measurements with floating chambers deployed during fish introduction in the intermittent treatments and similar periods in the other treatments. E) Total GHG emissions as CO_2-eq (net GHG= diffusive CO_2 +34*(diffusive CH_4 + net ebullitive CH_4). Control (without fish), carp permanently present (CP), sticklebacks permanently present (SP), carp intermittently present (CI) and sticklebacks intermittently present (SI) treatments. Orange dots represents data for each aquarium, black dots the mean values, vertical lines the standard deviation and the letters on the top of the bars (a, b and c) the pairwise comparison after the one-way ANOVA. Black and white images indicate the permanent presence of fish in the respective aquaria and grey images their intermittent presence.

Pelagic processes and their relation with GHG emissions

At the end of the experiment, the different GHG-emission fluxes were explained by different pelagic variables, i.e. different variables were selected in the GLM models (Fig.3A and Table S4). Diffusive CH_4 emissions were related to methanogens (*mcrA* gene copy number) in the surface water ($F_{11,16}$= 4.9, p=0.05), but contrary to our expectations the correlation was negative. Also contrary to what was expected, the relation between CH_4 diffusion and *Daphnia* spp. predation pressure upon MOB (*Daphnia*/MOB ratio) was not statistically significant ($F_{11,16}$= 0.9 and p>0.05). However, high fish predation on daphnids and the release of daphnids grazing on MOB can be inferred as all treatments with fish, except treatments where carps were intermittently present, had a significantly lower *Daphnia*/MOB index than the control treatment ($F_{4,14}$=6.8, p =0.003, Eta.sq:0.66, Tukey test p <0.01) (Fig. 4A); and also, from the significantly negative correlation of the *pmoA* gene copy number (MOB) with *Daphnia* spp. abundance ($F_{16,17}$=6.15, p=0.01) (Fig. 4B). In the same sense, *Daphnia* spp. abundances at the end of the experiment where significantly higher in the control and in the treatment where carps were

intermittently present than in treatments with sticklebacks or permanent carp ($F_{4,\ 15}$=15.5, p<<0.01, Eta.sq: 0.80, Tukey's test p<0.01, Table S3).

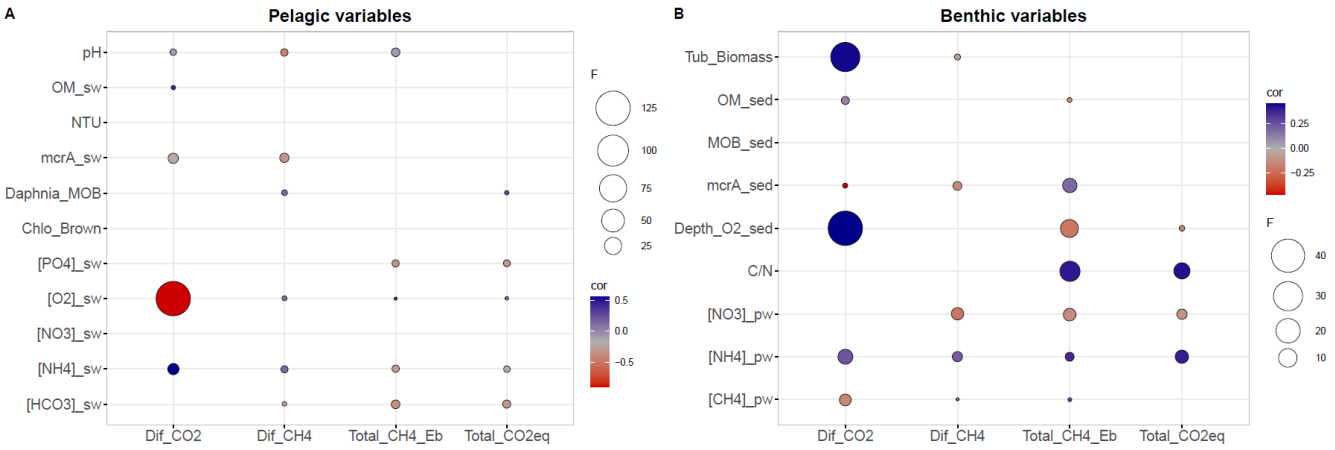

Figure 3. Summary of the GLM models fitted to each GHG emission flux (diffusive CO_2 and CH_4, total CH_4 ebullition and CO_2-eq), versus variables related to pelagic processes (A) or benthic processes (B). Dots represent the selected variables for each GLM model, being dots size according to F values extracted from ANOVA tables. Dot colours are according to Pearson's correlation coefficients. Pelagic explanatory variables: pH, turbidity (NTU), organic matter (OM_sw, in mg.L^{-1}), methanogens (as *mcrA* gene copy.mL^{-1}), zooplankton on MOB trophic predation index (as *Daphnia* spp. (ind.L^{-1})/ *pmoA* gene (copy.mL^{-1})), surface water concentrations of: chlorophyll-a (in µg.L^{-1}), dissolved oxygen ([O_2], in mg.L^{-1}), ammonium, nitrate and phosphate (NH_4_sw, NO_3_sw, and PO_4_sw, respectively and all in mg.L^{-1}), bicarbonate ion (HCO_3^-, in mg.L^{-1}). Benthic explanatory variables: biomass of *Tubifex* sp. worms (Tub_Biomass, in gDW.m^{-2}), O_2 penetration depth (Depth_O_2_sed, in cm), % of organic matter (OM_sed) and carbon/nitrogen ratio ([C/N]) in the sediments; the concentration in porewater of ammonium and nitrate (NH_4_sw and NO_3_sw, respectively and in mg.L^{-1}), dissolved methane (CH_4_sw, in µmol.L^{-1}) and methanogens (as *mcrA* gene copy.mL^{-1}) and MOB (as *pmoA* gene copy.mL^{-1}).

Diffusive CO_2 emissions were strongly negatively related to dissolved O_2, positively to NH_4^+ and negatively to methanogen (*mcrA* gene copy number) (all with statistically significant regressions; $F_{16,18}$=125.7, $F_{14,18}$=8.5 and $F_{13,18}$=6.6; p <0.01). Contrary to our expectations, no significant correlation was found between diffusive CO_2 and chlorophyll-a, being chlorophyll-a, indeed not included in the pruned model. Meanwhile, total CH_4 ebullition and total GHG emissions as CO_2-eq, were not significantly explained by pelagic variables (Table S4). Changes in surface-water variables, zooplankton and the microbiota in the pelagic habitat over time, and in among treatments are summarised in Table S3.

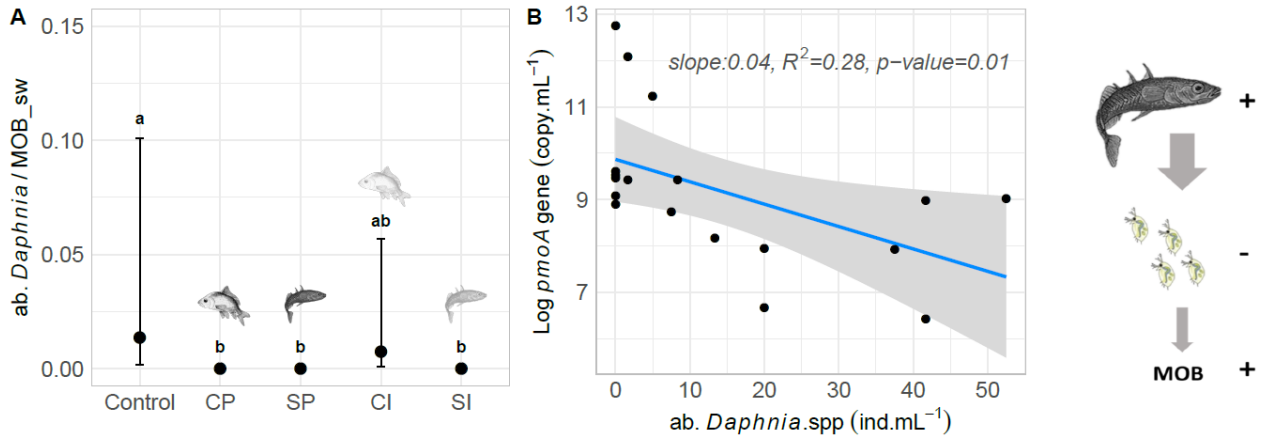

Figure 4. Evidences of top-down cascading effects promoted by zooplanktivorous fish. In A differences among treatments in the *Daphnia* spp. upon MOB predation pressure index (*Daphnia* spp. abundances/MOB as *pmoA* gene copy.mL^{-1}). Black dots represent the mean values, vertical lines the standard deviation and letters on the top of the bars (a, b and c) the results of the pairwise Tukey's test comparison following the one-way ANOVA test. In B graphical output of the linear regression between *pmoA* gen (copy.mL^{-1}, in natural logarithm scale) and *Daphnia* spp. abundance (ind.mL^{-1}). Black and white images indicate the permanent presence of fish in the respective aquaria and grey images their intermittent presence. A scheme of the trophic cascade effects from sticklebacks fish to MOB is also shown.

Benthic processes and their relation with GHG emissions

Although no tubifex worms (*Tubificidae* spp.) were visible at the start of the experiment, during the course of the experiment we observed their appearance in some aquaria. At the end of the experiment, tubifex total biomass significantly differed among treatments ($F_{4,15}$= 8.5, p=0.0008, Eta.sq: 0.69; Fig. 5A and table S3). The permanent presence of fish significantly reduced tubifex biomass compared to the control (Table S3). The intermittent treatments did not differ significantly from the permanent fish treatment and control treatment. Similarly, O_2 did not penetrate as deeply into the sediments in the treatments with permanent fish presence as in the other treatments (Table S3, $F_{4,95}$=23.75, p<<0.001 and Eta.sq:0.50; Fig. 5B).

Methanogens (mrcA copy numbers) also differed among treatments ($F_{4,35}$=9.9, p<<0.01 and Eta.sq:0.53; Fig. 5C and Table S3). The *mcrA* gene copy number in CP treatment were ~2.5 times higher than in the intermittent treatments (SI and CI) and 2.0 times higher than in the control. The SP treatment had twice as many methanogen copies than both intermittent treatments (CI and SI).

At the end of the experiment, for each GHG-emission flux (i.e. CO_2 and CH_4 diffusion, CH_4 total ebullition and total GHG as CO_2-eq) different benthic variables were selected in GLMs (Fig.3B and Table S4). Oxygen penetration depth and tubifex biomass were the benthic variables that best explained CO_2 diffusion, both associated with increasing emissions (Fig.6A & B; $F_{13,16}$=43.1 and $F_{14,16}$=30.03; p<0.0001; respectively). CO_2 diffusion also significantly increased with ammonium in the porewater ($F_{11,16}$=5.9; p=0.01), while CH_4 diffusion significantly decreased with porewater NO_3^- concentration ($F_{13,17}$=3.5; p=0.05). The total CH_4 ebullition was best explained by sediment C/N-ratio (positively, $F_{14,17}$=12.4 and p<0.001). Total ebullition was

also significantly related to O_2-penetration depth, with lower ebullition occurring with deeper O_2-penetration depth ($F_{15,17}$=9.2, p=0.002, Fig. 6C). Higher CH_4 ebullition rates occurred at higher methanogens gene copy numbers in the sediments ($F_{10,17}$=5.4; p<0.05). Total GHG emissions as CO_2-eq were best explained by C/N-ratio and NO_3^- concentration, positively in both cases ($F_{15,17}$=7.3 and p=0.007, $F_{13,17}$=4.5 and p=0.03, respectively).

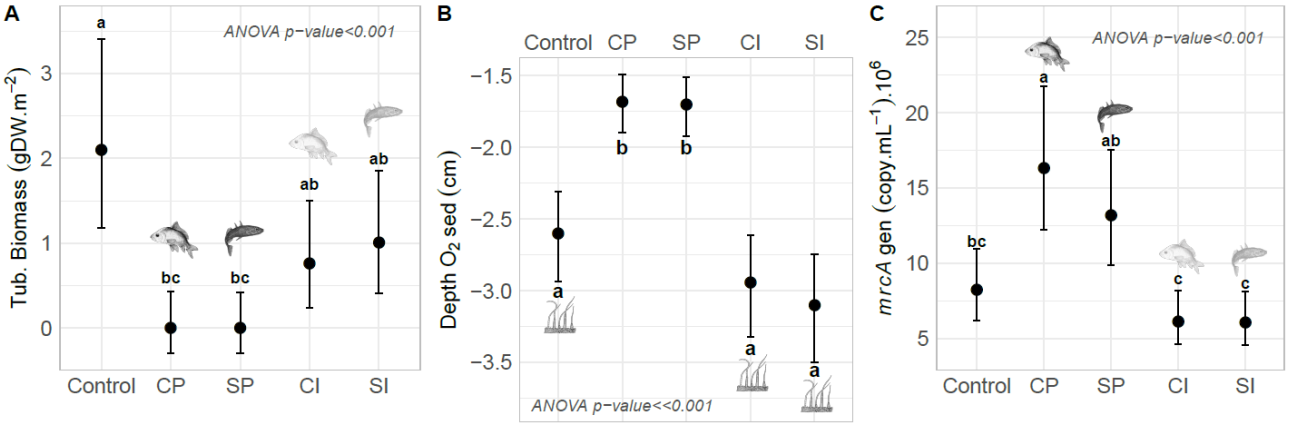

Figure 5. Differences among treatments in main benthic related processes explanatory variables: in A the biomass of Tubifex sp. worms (Tub_Biomass in gDW.m^{-2}, 5 levels with n=4); in B O_2 penetration depth (Depth_O2_sed in cm, 5 levels with n=20) in the sediments column; in C the methanogens as *mrcA* gene (copy.mL^{-1}, 5 levels with n=8) at porewater. Black dots represent the mean values, vertical lines the standard deviation and letters on the top of the bars (a, b and c) the pairwise comparison after the one-way ANOVAs (Tukey's test). ANOVA P-values are presented in grey. Black and white images indicate the permanent presence of fish in the respective aquaria and grey images their intermittent presence.

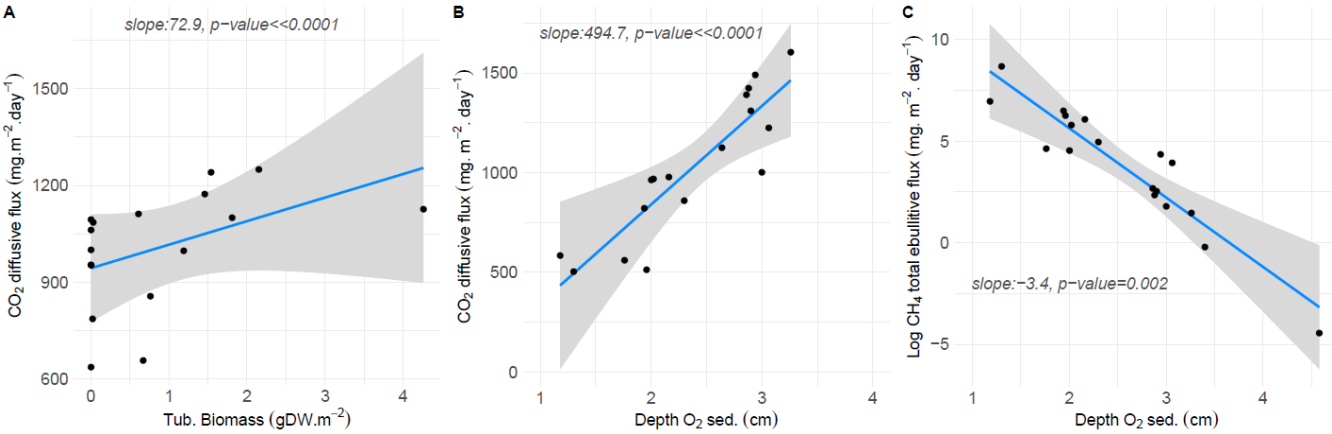

Figure 6. In A and B graphical output of the linear regressions between diffusive CO_2 final flux (in mg.m^{-2}.day^{-1}) and tubifex biomass (in gDW.m^{-2}) and the depth of O_2-penetration in sediments (in cm), respectively. In C graphical output of the linear regression between total CH_4 ebullition estimated as the 11-day average plus short-term (in mg.m^{-2}.day^{-1} and natural logarithm scale), and the depth of O_2 penetration in sediments (in cm). Regression slope (from GLM summary) and P-value (from ANOVA table) are presented in grey letters for each regression. The deviance explained by the GLMs is 89.3% for CO_2 diffusion and 76.5% for total CH_4 ebullition. In all charts the 95% confidence interval is represented by the grey area.

Comparing the explanatory power of pelagic and benthic variables (F-values in Figure 2 and Table S3), we found that benthic processes tended to have a stronger role in driving GHG emissions than pelagic processes. This was particularly observed for CH_4 ebullition and total emissions in terms of CO_2-eq.

Potential CH_4 production and oxidation rates and GHG emissions

Potential production and aerobic oxidation rates of CH_4 were similar among treatments ($F_{2.4}$=1.3 and p=0.35 for production rates and $F_{2,9}$=0.7 and p=0.49 for oxidation rates, Fig.S4). None of the final CH_4 fluxes (i.e. diffusion, 11-day average, short-term and total ebullition) were related to potential production or oxidation rates (p for all regressions >0.1). Contrary to our expectations, we found no significant correlations between O_2-penetration depth, MOB or methanogen copy numbers in sediments (p>0.1 for all regressions).

Discussion

Our results show that fish can substantially alter GHG emission intensities and pathways through trophic and non-trophic processes. We found indications for pelagic trophic cascading effects from zooplanktivorous fish to MOB, but trophic effects did not translate into differences in diffusive CH_4 emissions (in contrast to our H1). We observed non-trophic effects of benthivorous fish on CH_4 ebullition, as CH_4 ebullition significantly increased shortly after fish introduction in the intermittent carp treatments (supporting our H2). Indirect trophic effects of both benthic and pelagic fish on carbon emissions were confirmed (as expected in H3), mainly as differences in CO_2 emissions among treatments. Control aquariums emitted significantly more CO_2 than those with the permanent presence of fish. Our results indicate that the main driver of the differences in CO_2 emission was the density of tubifex worms in the sediments. Tubifex strongly impacted sediment oxygenation and GHG dynamics resulting in a relatively strong role of benthic processes compared to pelagic ones in our experimental setup.

Fish led to the almost complete absence of *Daphnia* spp., indicating strong trophic pressure exerted upon zooplankton by both sticklebacks and carp, as found elsewhere (Jakobsen et al., 2003, 2004). We did not find, in contrast to what we hypothesized (H1), a relation between zooplankton and phytoplankton (chl-*a*) and CO_2 diffusion. Zooplanktivorous predation pressure however did translate into the release of trophic pressure by *Daphnia* spp. on pelagic MOB, clearly evidenced by the lower *Daphnia*/MOB ratio in the fish treatments and the negative correlation between MOB and *Daphnia* spp. Despite the clear evidence of cascading trophic effects of zooplanktivores, we did not observe changes in CH_4 diffusion (Fig 7B), as we had predicted based on the findings of (Devlin et al., 2015). We speculate that this discrepancy may be caused by the shallow water column in our experiment (0.25m depth), as shallow systems typically have a shorter “gas residence time” (Cole et al., 2010). In our experiment, the

residence time of CH_4 was likely not enough for oxidation to substantially alter CH_4 concentration and the related diffusive emission.

At the benthic habitat, the short-term increase in CH_4 ebullition observed after carp introduction is in line with several field studies (Frei et al., 2007; Bhattacharyya et al., 2013; Ma et al., 2018), supporting the hypothesis of a direct physical impact of bioturbation on bubbles release (Fig 7D). We did not, however, observe a clear effect of continuous fish bioturbation on GHG emission (Fig 7C). This contradicts other studies where intense bioturbation was found to affect GHG production and consumption (Rahman, 2015a; Oliveira Junior et al., 2019), likely largely caused by changes in O_2 availability. The difference in the effect of fish between the study of (Oliveira Junior et al., 2019) and ours may be related to the lower carp biomass used in our permanent treatments (~400g FW.m^{-2} versus ~280g fresh fish.m^{-2} in (Oliveira Junior et al., 2019)) but may also be related to differences in sediment characteristics. The biomass in our intermittent carp treatments was comparable to the biomass reported by (Bhattacharyya et al., 2013) (~0.0015g FW.m^{-2}), who also found a significant increase in CH_4 emissions related to carp presence .

We found a clear effect of our O_2-penetration depth proxy on GHG dynamics (i.e., it was positively related with diffusive CO_2 emissions and negatively with CH_4 ebullition). The O_2-penetration depth proxy, however, was not directly related to the presence of fish, but instead to the density of tubifex worms in the systems (Fig. 7A). Tubifex strongly impacted the O_2-penetration depth, through the bioirrigation of sediments developed in their foraging galleries (Lagauzère et al., 2009; Hölker et al., 2015). Both carp and sticklebacks effectively controlled the development of tubifex biomass in the sediments, lowering their biomass 1.6-1.8 times in the permanent fish treatments compared to the control and intermittent treatments. The benthic foraging of sticklebacks – in combination with the above-described pelagic foraging of carp – likely underlie the strong benthic-pelagic coupling of GHG dynamics in our aquariums.

In our setup, tubifex density was strongly and positively related to O_2-penetration depth and to CO_2 emissions. Sediment oxygenation likely explains the observed CO_2 diffusion patterns, as aerobic decomposition and respiration are enhanced in oxygenated sediments (Leal et al., 2007; Baranov et al., 2016). In addition, the O_2-penetration depth, promoted by tubifex activity, was negatively related to CH_4 ebullition which, in turn, was positively related to methanogen gene copy numbers. Deeper O_2-penetration may have very well limited CH_4 production by hampering methanogen activity or by enhancing MOB activity, as has been suggested by other studies (Hölker et al., 2015). We found, however, no evidence of an O_2-penetration depth effect on potential CH_4 production and oxidation rates. Also, CH_4 emissions and concentrations (in both surface and porewater) and microbiota gene copy numbers were not significantly related to potential CH_4 production and oxidation rates. While some studies have found a good agreement between potential rates and methanotroph/ methanogen gene abundance (Kajan & Frenzel, 1999; Figueiredo-Barros et al., 2009), others have also found no relationship between MOB and methanogen gene abundance and activity (Cadillo-Quiroz et al., 2006; Kim et al., 2015). This discrepancy can be explained by, on the one hand, not all DNA present reflects living, active bacteria, and on the other hand, sometimes minorities in the microbiome are

responsible for the majority of process rates (Bodelier et al., 2013). In our case, lack of a relationship between potential process rates and gene copy numbers may also have been caused by the *ex situ* quantification of the CH_4 production and oxidation potential (i.e. in flasks with standardized conditions) (Cadillo-Quiroz et al., 2006; Kim et al., 2015). *In situ* methane production and oxidation and gene abundance are likely largely driven by varying O_2 presence and CH_4 availability. The standardized conditions in our *ex-situ* essays may thus have masked potential differences occurring between the systems. Moreover, part of the methane oxidation may have been anaerobic, and therefore not picked up by our *pmoA*-based quantification assay.

Depending on regional and local conditions, shallow temperate lakes can have different food-web structures, in which, most frequently, primary production can be either macrophyte driven or phytoplankton driven (Scheffer et al., 1993). Important feedbacks between the dominant vegetation type and the dominant zooplankton, macroinvertebrates and fish communities occur in a lake, which, will impact GHG-emissions. Various studies have shown the impact of macrophytes and phytoplankton on GHG production, consumption and emission (Hilt et al., 2017). We suggest that the impact of the main primary producers can be reduced or increased by bioturbation of both macroinvertebrates and fish. In submerged macrophyte-dominated lakes with a well-developed bioirrigating macroinvertebrates community, such conditions would lead to low CH_4 production and, at least at some periods of the year, sediment respiration could be compensated by CO_2 fixation by the macrophytes. On the other hand, in phytoplankton-dominated systems with high biomasses of bioturbating fish, positive feedbacks would reinforce carbon emissions, mainly of CH_4. Bioturbation by fish would facilitate the exclusion of submerged macrophytes, by uprooting and by creating turbid conditions, as well as facilitating the exclusion of macroinvertebrates due to direct predation.

Conclusions and outlook

In the last decade various studies have highlighted the effect of lake internal factors, such as primary producers (Ger et al., 2014; Davidson et al., 2015; Almeida et al., 2016; Audet et al., 2017), and of external drivers, such as eutrophication (Yvon-Durocher et al., 2011; Hansson et al., 2012; Davidson et al., 2015; Jeppesen et al., 2016), hydrological input (Weyhenmeyer et al., 2015; Kosten et al., 2018; Keller et al., 2020) and temperature (Kosten et al., 2010; Gudasz et al., 2015; Aben et al., 2017) on aquatic GHG dynamics. The effect of fish has, however, been largely overlooked. Our results demonstrate that fish affect CO_2 and CH_4 emissions by trophic and non-trophic mechanisms (Fig. 7). We found that benthic fish can trigger CH_4 ebullition when disturbing sediments in which bubbles have had enough time to be formed. In addition, through trophic-cascade effects, fish predation on *Daphnia* spp. can release trophic pressure on methane oxidizing bacteria. Also, fish predation on benthic macroinvertebrates can strongly reduce O_2 availability in the sediment, decreasing water-atmosphere CO_2 fluxes. We found that in our setup benthic processes played a stronger role in regulating GHG dynamics than pelagic

processes. In particular, benthic macrofauna was a key driver of GHG dynamics through their oxygenation of sediments. Our findings shed light on the functioning of shallow aquatic ecosystems, contributing to understanding of the way that changes in fish communities are translated into changes in carbon emissions, and of the strong coupling between benthic and pelagic carbon related processes.

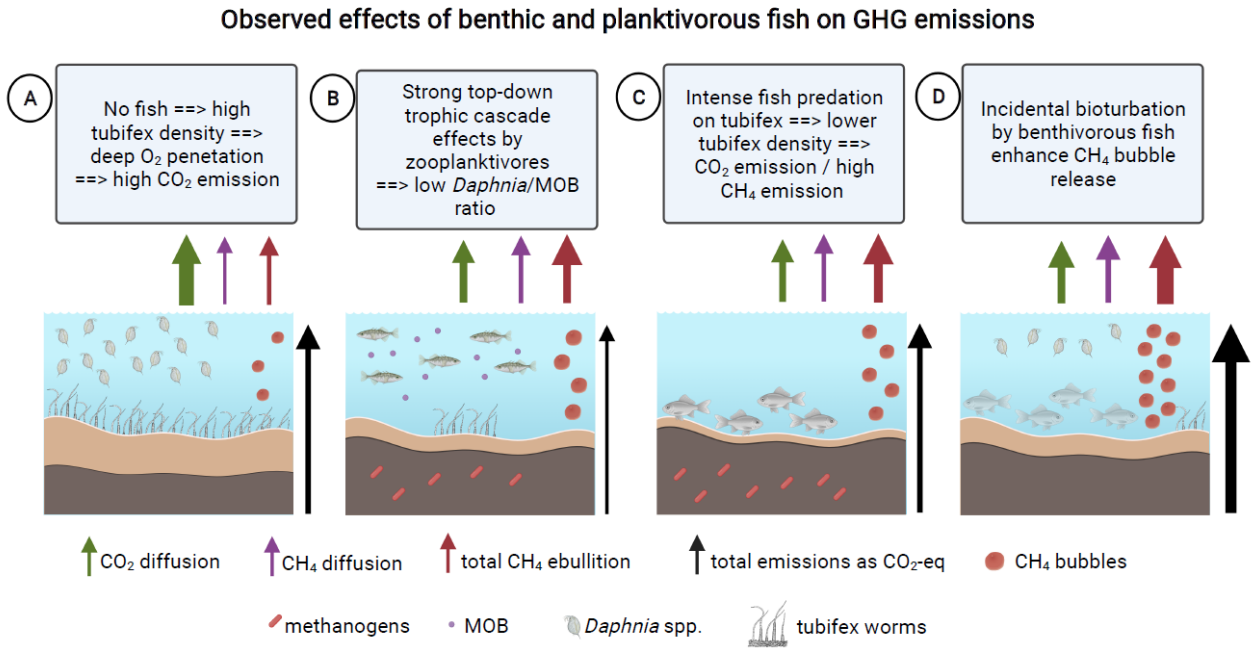

Figure 7. Summary of the main observed effects of benthic and planktivorous fish in our experimental treatments. A) Control treatments, without fish predation or bioturbation effects. B) Permanent and intermittent sticklebacks treatments (SP and SI), with pelagic trophic cascading effects. C) Permanent carp treatments (CP), with intense bioturbation pressure on sediments and intense predation on benthic macroinvertebrates. D) Intermittent carp treatments (CI), with low bioturbation pressure due to low benthivorous fish and moderate predation on benthic macroinvertebrates. Arrows of different colours represent the different GHG fluxes: green for CO_2 diffusive flux, violet for CH_4 diffusive flux, red for CH_4 ebullitive flux and black for total GHG emissions as CO_2-eq (diffusive CO_2 + 34*(diffusive CH_4 + ebullitive CH_4)). The thickness of arrows are proportional to the relative importance of the emission flux compared to the control and the light coloured sediment layer represents the oxygenated layer. Figure created with BioRender.com.

Acknowledgements

The authors would like to thank Janneke Roelofs and Gijs van Dijk for their help during the set-up of the experiment. Also, to Sebastian Krosse, Paul van der Ven, Germa Verheggen and Roy Peters for their help in the laboratory. This work was supported by ANII (Agencia Nacional de Investigación e Innovación –Uruguay) and PEDECIBA (Uruguay).

SUPPLEMENTARY INFORMATION CHAPTER 3

2. Methods

2.1 Experimental set up

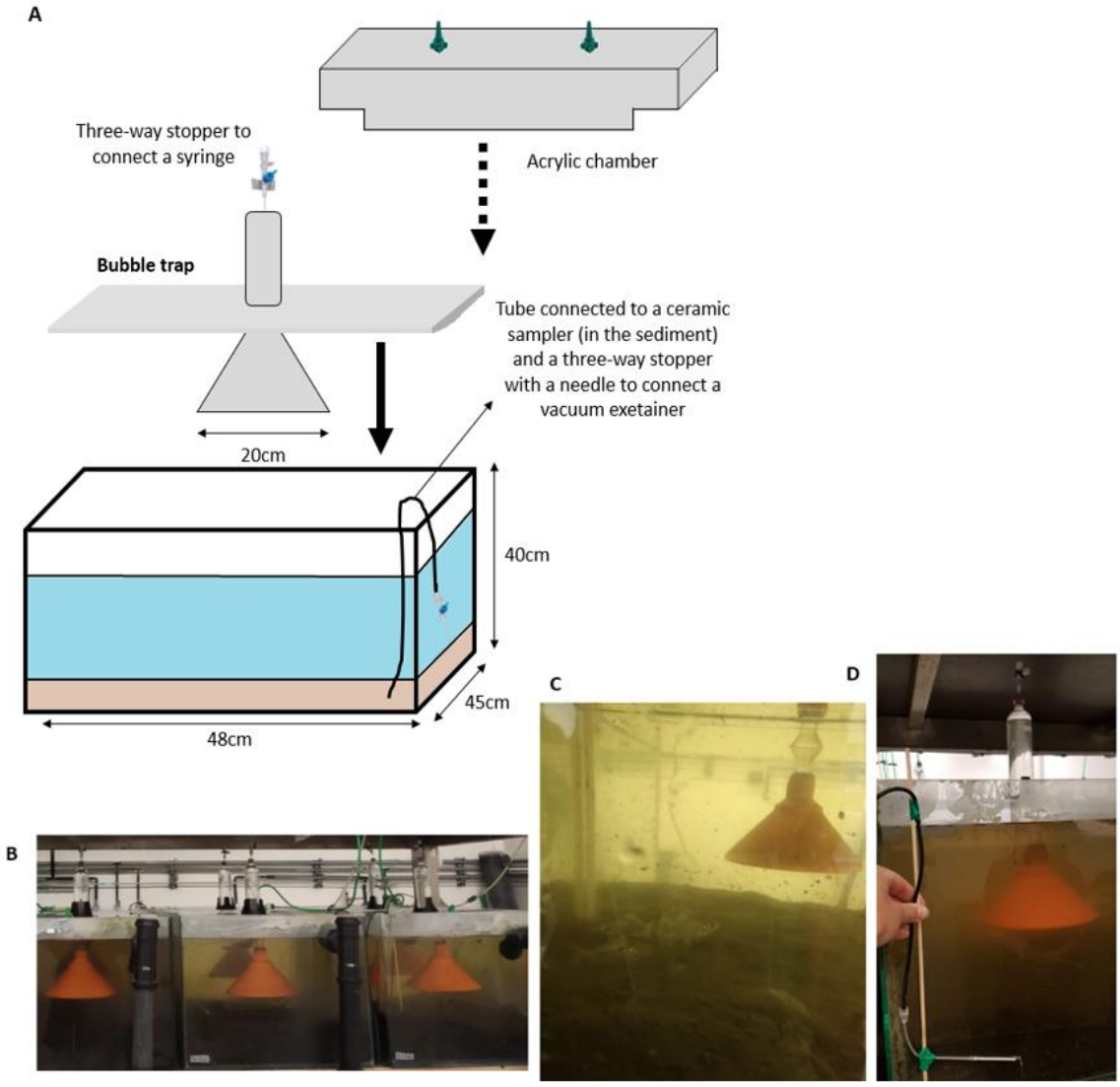

Figure S1. In A) an schematic diagram of an aquarium with a ceramic sampler, bubble traps and the acrylic chamber used for GHG sampling. In B) picture of aquariums with bubble traps. In C) picture of carp fish inside the aquarium and in D) ceramic sampler before colocation inside the sediment.

2.2 GHG measurements

Example of CH_4 ebullition estimations from chromatograms obtained with the greenhouse gas analyser, following the same methodology than in (Attermeyer et al., 2016) .

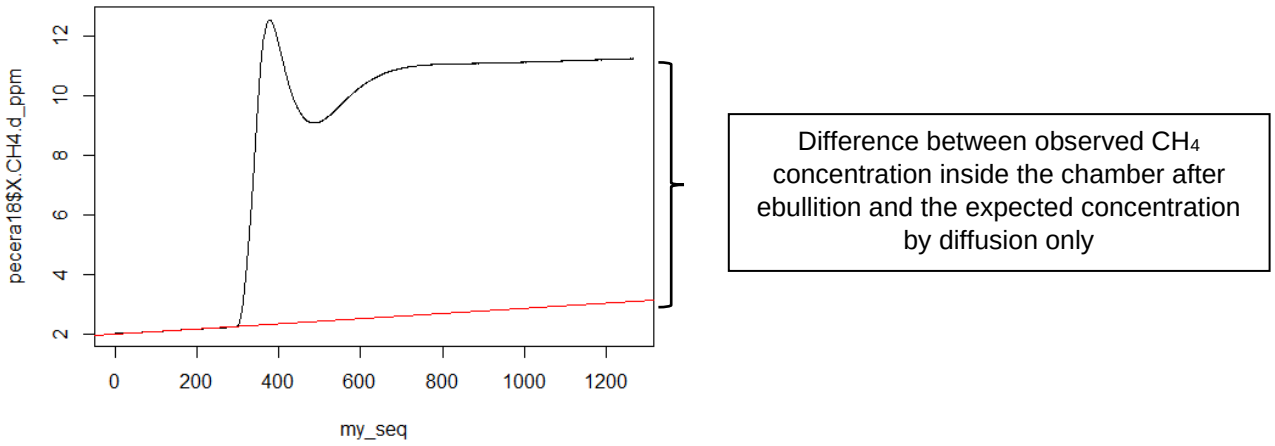

Figure S2. Chromatogram obtained with the greenhouse gas analyzer for the change in CH_4 gas concentration inside the floating chamber. In black the change in CH_4 obtained when ebullition occurs and the peak correspond to the release of a gas bubble. In red the predicted change by diffusion only (without ebullition).

The predicted change in CH_4 (red line) was obtained by fitting a linear model to the first 200 second of measurement, before the release of the gas bubble, according to the formula:

$$(\mathrm{CH_4 ppm}) = \mathrm{a.x} + \mathrm{b}$$

Where: x is the time in seconds, a the slope and b the intercept.

The difference in CH_4 concentration, at final time (1200 seconds and after gas mixing inside the chamber), between the observed in the chromatogram and the predicted by the lineal model represents the amount of CH_4 released by ebullition.

CH_4 ppm were transformed to mg.m-3 using the general law of gases:

$$\mathrm{mg.m^{-3}} = \mathrm{ppmCH_4} \times \mathrm{Mweight\ (g.mol^{-1})} \times \mathrm{Patm\ (atm)} \Big/ \mathrm{R(L.atm.mol^{-1}.K^{-1})} \times \mathrm{time(sec.)}$$

Where: $ppmCH_4$ correspond to the difference in ppm between observed and predicted lines in chromatogram, Mweight is the molecular weight of CH_4, Patm the atmospheric pressure in atmospheres, R the gas constant (0.082L.atm.mol^{-1}.K^{-1}) and time is the sampling time in seconds.

And ebullitive flux as follows:

$$\mathrm{CH_4 ebullition.\ (mg.\,m^{-2}.\,day^{-1})} = [\mathrm{CH_4}](\mathrm{mg.\,m^{-3}}) \times \mathrm{chamber\ volume\ (m^3)} \times \mathrm{F2\ (s.\,day^{-1})} \Big/ \mathrm{chamber\ area\ (m^2)} \times \mathrm{time(sec.)}$$

Where: [CH_4] correspond gas concentrations in mg.m^{-3} previously estimated, chamber volume the total gas volume inside the floating chamber in m^3, chamber area the surface covered by the chamber in m^2, F2 the transforming factor from seconds to days and time the sampling time in seconds.

2.6 Microbiota: MOB and methanogen abundances

Table S1. Primers and PCR conditions used to amplify fragments of functional marker genes *pmoA* and *mrcA* by qPCR. Each qPCR reaction (20µL final volume) for both genes consisted of 10µL 2X SensiFAST SYBR (BIOLENE, Alphen aan den Rijn, The Netherlands), 1µL of forward and reverse primers (targeting *pmoA*) and 3.5µL (targeting *mrcA*), 1µL bovine serum albumin (5µg/µL, Invitrogen, Breda, The Netherlands) and 1-2µL DNA template. For the non-template controls, a 1-2µL volume of DNase-and-RNase-free water was used. For benthonic DNA samples, PCR reactions were done in 1:100 diluted DNA extracts.

Gene	Bacterial group	Primer sets	PCR conditions	PCR product length (bp)	References
mcrA	Methanogens	mlas/ mcrA-rev	95 °C/3min, 40 cycles (95°C/10sec, 60°C/10sec, 72°C/25sec), 65 to 95°C (+1°C/sec) for denaturation curve.	645	(Steinberg & Regan, 2008)
pmoA	MOB	A189/ Mb661-rev	95 °C/3min, 45 cycles (95°C/10sec, 60°C/15sec, 72°C/25sec, 82°C/10sec), 70 to 99°C (+1°C/sec) for denaturation curve.	472	(Costello & Lidstrom, 1999)

3. Results

3.1 GHG fluxes

Table S2. Summary of GLM models explaining GHG fluxes over time (days since start of the measurements) in the different treatments (factor with 5 levels or 3 for short-term ebullition). The significance of explanatory variables (evaluated with ANOVA test), main differences in slopes (rate of change in the amount of GHG flux over the 86 days) among treatments, the percent of deviance explained (%Dev.ex), degrees of freedom (df) and the family of each model are listed. The Tukey p-values from pairwise comparisons (assessed with glht function from the multcomp package) are listed when applicable. (* for P-value≥0.01 and <0.05, ** for P-value<0.01).

All the final GLMs were validated by the evaluation of normal distribution and homogeneity of variance for residuals.

GHG	Emission ($mg.m^{-2}.day^{-1}$)	Significant variables (p-value ANOVA, Chi^2 test)	Slope	% Dev.exp	df	Family	Tukey p-values
CH_4	**diffusion**	Time** Treatment Time × Treatment*	SI> Ctr.>SP>CP>0 CI<0	17.5	183	LogNormal	-
	ebullition 11-days average	Time** Treatment Time × Treatment*	CP>SP>SI>CI>0 Ctr.<0	19.2	161	Normal	-
	ebullition short-term	Time* Treatment** Time × Treatment	Ctr.>SI>CP>SP>CI>0	15.4	119	Neg.binomial	CI-Ctr**
CO_2	**diffusion**	Time* Treatment** Time × Treatment**	Ctr.>SI>CP>SP>CI>0	31.6	192	LogNormal	CI-SI**
CO_2 eq.	**total GHG**	Time** Treatment** Time × Treatment	CP>Ctr. >CI>0	37.2	128	LogNormal	CI-Ctr* CI-CP* CI-SP** CI-SI**

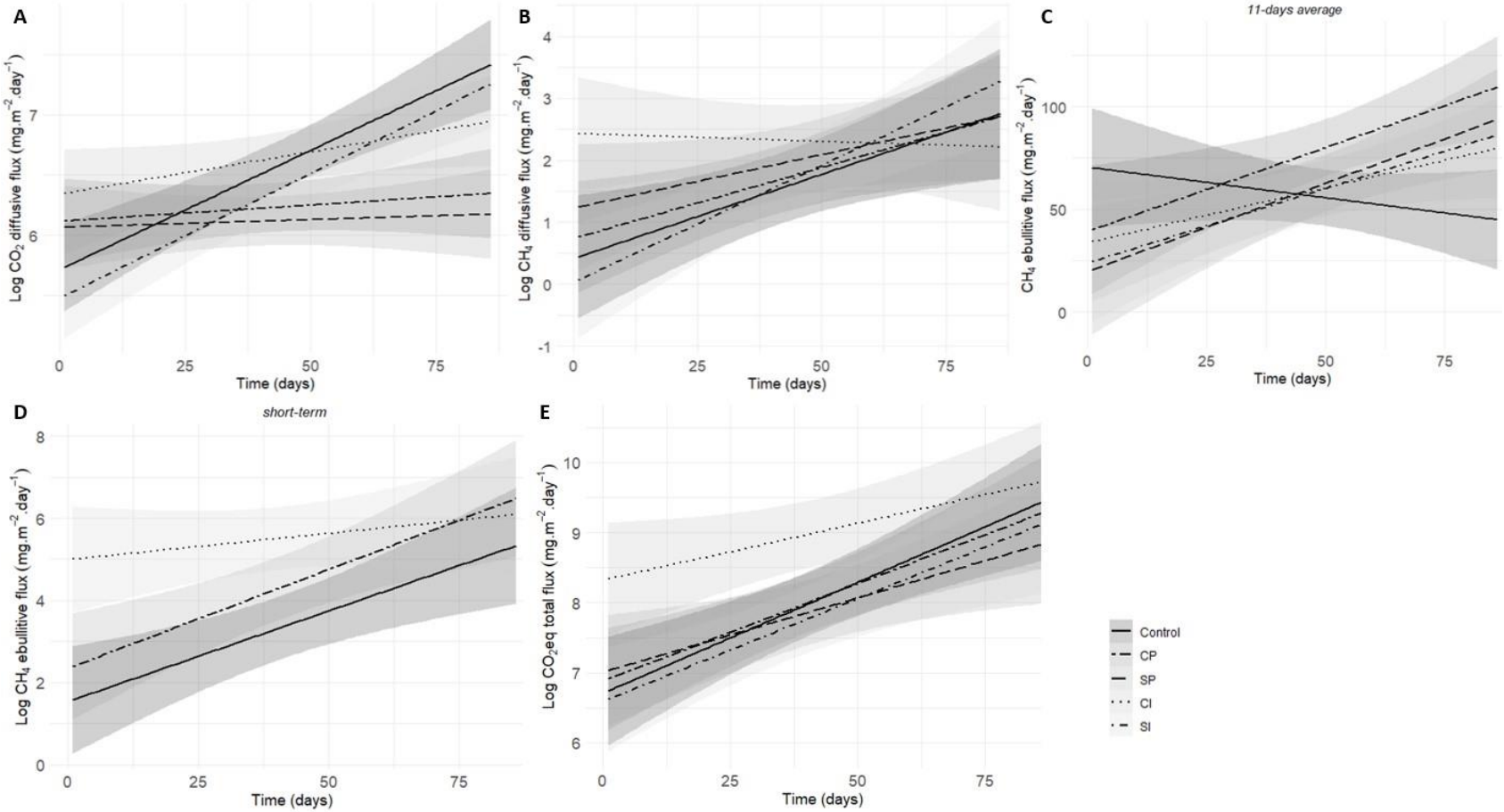
A
Log CO_2 diffusive flux (mg.m^{-2}.day^{-1})
Time (days)
B
Log CH_4 diffusive flux (mg.m^{-2}.day^{-1})
Time (days)
C
11-days average
CH_4 ebullitive flux (mg.m^{-2}.day^{-1})
Time (days)
D
short-term
Log CH_4 ebullitive flux (mg.m^{-2}.day^{-1})
Time (days)
E
Log CO_2-eq total flux (mg.m^{-2}.day^{-1})
Time (days)
Control
CP
SP
CI
SI

Figure S3. Graphical outputs of the GLM models explaining GHG fluxes over time (days since start of the measurements) in the different treatments (factor with 5 levels or 3 for short-term ebullition). CO_2 diffusion in A, CH_4 diffusion in B, 11-days average CH_4 ebullition in C, short-term CH_4 ebullition in D and total emissions as CO_2-eq in E. In all charts, different line types represent the different treatments and the 95% confidence interval is represented by grey areas.

3.2 -3.3 Pelagic and benthic processes and their relation with GHG emissions

Table S3. Summary of the main pelagic and benthic variables related to GHG emissions. For variables measured every 11 days or at days 1, 46 and 86 GLMs with treatment and time (days) as explanatory variables were used and for variables just measured at the end of the experiment one-way ANOVA tests.

Pelagic variables are: water temperature, dissolved oxygen concentration in the surface water (O_2), pH, turbidity (NTU), chlorophyll-a, bicarbonate concentration (HCO_3^-); dissolved CH_4 and CO_2 concentrations, total suspended solids (TSS), organic matter (OM), ammonium, nitrate and phosphate concentrations (NH_4^+, NO_3^-, and PO_4^{+3}), the abundances in surface water (sw) of methanogens as *mcrA* gene, MOB as *pmoA* gene and *Daphnia* spp.

Benthic variables are: the porewater concentrations of ammonium and nitrate (NH_4^+ and NO_3^-), dissolved CH_4, the % of organic matter in the sediment (OM %), sediment carbon/nitrogen ratio (C/N), the biomass of *Tubifex* sp. worms (Tub_Biomass), the O_2 penetration depth (Depth.O_2.sed), and the abundances of methanogens as *mcrA* gene and MOB as *pmoA* gene.

Explained variables with significant effects, according to ANOVA test, are presented: P-value<0.0001***, P-value<0.01** and P-value<0.05*. The family for GLM models or data transformation in ANOVA test is also summarized.

	Average ± SD					**Sampling frequency** **n**	**Applied model and significant explained variables** **(ANOVA, Chi^2 test: p-value<0.05)**	**Family** **(GLM) –data transformation**
	Control	**CP**	**SP**	**CI**	**SI**			
Pelagic variables								
Temp (°C)	17.7 ± 2.0	17.7 ± 2.0	17.6 ± 2.0	17.7 ± 2.0	17.7 ± 2.0	every 11 days n=9	GLM: time***	Normal
O_2 (mg.L^{-1})	6.2 ± 1.7	6.9 ± 1.2	7.7 ± 0.6	6.7 ± 1.5	6.7 ± 1.7	every 11 days n=9	GLM: time***, treatment***time × treatment***	Normal
pH	7.5 ± 0.2	7.5 ± 0.2	7.6 ± 0.1	7.5 ± 0.2	7.5 ± 0.2	every 11 days n=9	GLM: time**	Normal
NTU	3.2 ± 5.6	8.7 ± 5.2	3.0 ± 2.0	6.4 ± 10.9	3.6 ± 5.6	every 11 days	GLM: time***, treatment***, time × treatment***	Lognormal

						n=9		
Chl (µg.L^{-1})	4.7 ± 1.6	6.9 ± 1.7	4.1 ± 0.5	5.1 ± 2.0	4.7 ± 1.3	every 11 days n=9	GLM: time***, treatment***, time × treatment***	Lognormal
[CH_4] surface water (mg.L^{-1})	0.08 ± 0.04	0.06 ± 0.04	0.08 ± 0.05	0.09 ± 0.06	0.07 ± 0.04	Every 11 days n=9	GLM: time***	Lognormal
[CO_2] surface water (mg.L^{-1})	8.8 ± 3.2	9.1 ± 4.1	8.1 ± 3.05	9.1 ± 3.9	9.4 ± 3.4	Every 11 days n=9	GLM: time***	Lognormal
[HCO_3^-] (mg.L^{-1})	161.7 ± 11.5	145.5 ± 15.5	156.6 ± 10.3 -	153.6 ± 13.2	158.8 ± 11.71	every 11 days n=9	GLM: time**, treatment***	Normal
TSS (mg.L^{-1})	7.4 ± 8.6	8.9 ± 16.2	4.5 ± 3.9	13.8 ± 18.6	4.2 ± 3.6	days 1-46-86 n=3	GLM: time**, treatment**, time × treatment**	Lognormal
OM (mg.L^{-1})	5.8 ± 6.7	3.3 ± 1.6	3.3 ± 1.9	8.2 ± 9.7	3.2 ± 2.0	days 1-46-86 n=3	GLM: time**	Lognormal
[NH_4^+] (mg.L^{-1})	0.7 ± 1.3	0.02 ± 0.05	0.03 ± 0.03	0.5 ± 0.8	0.3 ± 0.4	days 1-46-86 n=3	GLM: time***, treatment***, time × treatment***	Lognormal
[NO_3^-] (mg.L^{-1})	8.8 ± 4.5	10.9 ± 3.1	8.8 ± 4.4	10.2 ± 4.4	10.6 ± 4.4	days 1-46-86 n=3	GLM: time**	Normal
[PO_4^{+3}] (mg.L^{-1})	0.1 ± 0.08	0.09 ± 0.06	1.5 ± 0.1	0.2 ± 0.1	0.2 ± 0.1	days 1-46-86 n=3	GLM: time***, treatment*	Lognormal
MOB sw (*pmoA* gene copy.mL^{-1})	$4.3x10^4$ ± $6.2x10^4$	$9.7x10^4$ ± $1.6x10^5$	$5.0x10^4$ ± $6.7x10^4$	$7.7x10^4$ ± $1.4x10^5$	$6.9x10^4$ ± $1.2x10^5$	days 1-46-86 n=6	-	Lognormal
Methanogens sw (*mcrA* gene copy.mL^{-1})	35.18 ± 45.9	187.8 ± 251.2	81.6 ± 119.2	81.4 ± 127.2	50.9 ± 35.2	days 1-46-86 n=6	GLM: treatment**, time × treatment**	Lognormal
***Daphnia* spp. (ind.L^{-1})**	43.3 ± 13.3	0 ± 0	2.7 ± 1.2	42.1 ± 19.3	5.8 ± 2.3	day 86 n=4	One-way ANOVA: treatment**	Lognormal
Benthic variables								

$[NH_4^+]$ ($mg.L^{-1}$)	9.1 ± 3.3	11.2 ± 4.7	8.2 ± 3.5	10.05 ± 5.4	9.6 ± 3.3	days 1-46-86 n=3	GLM: time***	Normal
$[NO_3^-]$ ($mg.L^{-1}$)	0.0 ± 1.7	0.0 ± 1.9	0.0 ± 0.02	0.0 ± 2.4	0.0 ± 0.9	days 1-46-86 n=3	GLM: time**	Lognormal
$[CH_4]$ porewater ($mg.L^{-1}$)	4.4 ± 4.4	4.9 ± 5.3	5.6 ± 6.4	4.4 ± 6.3	4.9 ± 4.5	every 11 days n=9	GLM: time***	Lognormal
OM (%)	79.9 ± 26.8	66.1 ± 20.4	91.7 ± 29.6	99.6 ± 31.6	103.6 ± 31.9	day 86 n=4	-	Normal
C/N	14.5 ± 4.4	14.1 ± 4.3	14.2 ± 4.3	15.2 ± 4.6	14.7 ± 4.5	day 86 n=4	-	Lognormal
Tub_Biomass ($gDW.m^{-2}$)	2.3 ± 0.8	0.005 ± 0.003	0 ± 0	0.8 ± 0.3	1.2 ± 0.5	day 86 n=4	One-way ANOVA: treatment**	Lognormal
Depth O_2 sed. (cm)	2.7 ± 0.7	1.7 ± 0.4	1.7 ± 0.5	3.1 ± 1.05	3.1 ± 0.5	day 86 n=8	One-way ANOVA: treatment**	Lognormal
MOB sed. (*pmoA* gene $copy.mL^{-1}$)	$9.9x10^8$ ± $6.3x10^7$	$9.0x10^8$ ± $4.1x10^8$	$7.3x10^8$ ± $1.7x10^9$	$5.6x10^8$ ± $1.5x10^8$	$1.2x10^9$ ± $4.0x10^8$	day 86 n=8	One-way ANOVA: treatment**	Lognormal
Methanogens sed. (*mcrA* gene $copy.mL^{-1}$)	$8.6x10^7$ ± $2.5x10^6$	$1.7x10^7$ ± $5.9x10^5$	13305461.2 ± 2177814.3	$7.2x10^6$ ± $4.7x10^6$	$6.7x10^6$ ± $3.2x10^6$	day 85 n=8	One-way ANOVA: Treatment***	Lognormal

Table S4. GLMs best explaining the variation in flux intensities of the different GHG emission parameter (CO_2 and CH_4 diffusion, CH_4 total ebullition and total GHG emissions as CO_2-eq) at the end of the experiment. The explanatory variables were categorized as related to pelagic or benthic processes.

Included variables related to pelagic processes are: the dissolved oxygen concentration ($[O_2]$, in $mg.L^{-1}$ in surface water of), pH, turbidity (NTU), organic matter (OM_sw, in $mg.L^{-1}$), ammonium, nitrate and phosphate ($[NH_4]$_sw, $[NO_3]$_sw, and $[PO_4]$_sw, respectively all in $mg.L^{-1}$), bicarbonate ($[HCO_3^-]$, in $mg.L^{-1}$) and dissolved methane ($[CH_4]$_sw, in $\mu mol.L^{-1}$); the abundance of methanogens as *mcrA* gene ($copy.mL^{-1}$) and the *Daphnia*/MOB ratio as a trophic predation index estimated as *Daphnia* spp. ($ind.L^{-1}$) /(*pmoA* gene ($copy.mL^{-1}$).

Included variables related to benthic processes are: the biomass of *Tubifex* sp. worms (Tub_Biomass, in $gDW.m^{-2}$), the O_2 penetration depth (Depth_O_2_sed, in cm), % of organic matter (OM_sed) and carbon/nitrogen ratio (C/N) in the sediments; the concentration in porewater of ammonium and nitrate ($[NH_4]$_sw and $[NO_3]$_sw, respectively

and in mg.L^{-1}), dissolved methane ([CH_4]_sw, in µmol.L^{-1}) and the abundance of methanogens as *mcrA* gene (copy.mL^{-1}).

Emission parameter	Selected variables	F-value (ANOVA, test F)	Significant p-values (ANOVA, test Chi^2)	% deviance explained (GLM)	Family (GLM)	Pearson´s cor. coefficient
			Pelagic processes			
CO_2 final diffusion (mg.m^{-2}.day^{-1})	[O_2]_sw	125.7	<2.2e-16	91.6	Lognormal	-0.9
	[NH_4]_sw	8.5	0.003			0.5
	*mcrA*_sw	6.6	0.009			-0.2
	pH	1.5	-			-0.1
	OM_sw	0.24	-			0.4
CH_4 final diffusion (mg.m^{-2}.day^{-1})	*mcrA*_sw	4.9	0.02	52.81	Lognormal	-0.3
	pH	2.4	-			0.4
	NH_4_sw	2.2	-			-0.1
	*Daphnia*_MOB	0.9	-			0.1
	[O_2]_sw	0.4	-			0.1
	[HCO_3]_sw	0.3	-			-0.2
CH_4 total ebullition (mg.m^{-2}.day^{-1})	[HCO_3]_sw	3.9	0.05	45.91	Lognormal	-0.4
	pH	3.8	0.05			-0.07
	[NH_4]_pw	2.3	-			-0.2
	[PO_4]_pw	2.1	-			-0.3
	[O_2]_sw	0.01	-			-0.07
11 days-average + short term						
Total GHGs as CO_2 equivalents (mg.m^{-2}.day^{-1})	[HCO_3]_sw	3.2	-	45.91	Lognormal	-0.3
	[PO_4]_pw	1.8	-			-0.3
	[NH_4]_pw	1.5	-			-0.2
	*Daphnia*_MOB	0.2	-			0.2
	[O_2]_sw	0.05	-			0.1
			Benthic processes			
CO_2 final diffusion (mg.m^{-2}.day^{-1})	Depth_O_2_sed	43.1	5.2e-11	89.31	Lognormal	0.4
	Tub_Biomass	30.03	4.2e-8			0.4
	[NH_4]_pw	5.9	0.01			0.2
	[CH_4]_pw	3.2	-			-0.5
	OM_sed	1.06	-			-0.1
	mcrA_sed	0.1	-			0.1

CH_4 final diffusion (mg.m^{-2}.day^{-1})	$[NO_3]$_pw	3.7	0.05	39.05	Lognormal	-0.2
	$[NH_4]$_pw	2.2	-			0.2
	mcrA_sed	1.4	-			-0.1
	Tub_Biomass	0.4	-			-0.06
	$[CH_4]$_pw	0.003	-			0.02
CH_4 total ebullition (mg.m^{-2}.day^{-1})	C/N	12.4	0.0004	76.5	Lognormal	0.4
	Depth_O_2_sed	9.2	0.002			-0.2
	mcrA_sed	5.4	0.02			0.2
	$[NO_3]$_pw	3.9	0.04			-0.1
	$[NH_4]$_pw	1.5	-			0.3
11 days-average + short term	OM_sed	0.1	-			-0.1
	$[CH_4]$_pw	0.03	-			0.2
Total GHGs as CO_2 equivalents (mg.m^{-2}.day^{-1})	C/N	7.3	0.007	52.3	Lognormal	0.4
	$[NH_4]$_pw	4.5	0.03			0.4
	$[NO_3]$_pw	2.2	-			-0.1
	Depth_O_2_sed	0.3	-			-0.2

3.4 Potential CH_4 production and oxidation rates and GHG emissions

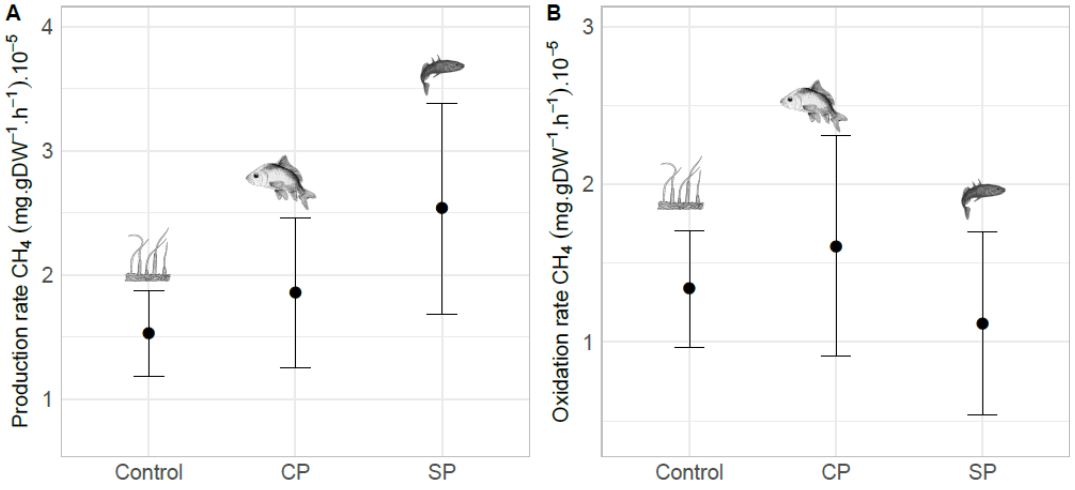

Figure.S4. Sediment CH_4 production (A) and oxidation (B) rates in the experimental treatments. Black dots represent the mean values and the vertical lines the standard deviation. The pictograms above each treatment show *Tubifex* sp., carp and sticklebacks as the dominant group in each treatment.

CHAPTER 4

EXPERIMENTAL WARMER CONDITIONS PROMOTE STRONGEST CARBON DIOXIDE UPTAKE BY FRESHWATER PELAGIC COMMUNITIES DOMINATED BY CYANOBACTERIA WITH POOR INCORPORATION OF CARBON INTO THE CLASSIC TROPHIC WEB

Maite Colina[1], Mariana Meerhoff[1,3], Sarian Kosten[2]

[1] Departamento de Ecología y Gestión Ambiental, Centro Universitario Regional del Este, Universidad de la República, Tacuarembó s/n CP 20000, Maldonado, Uruguay.

[2] Department of Aquatic Ecology and Environmental Biology, Institute of Water and Wetland Research, Radboud University, P.O. Box 9010, 6500 GL Nijmegen, the Netherlands.

[3] Department of Bioscience, Aarhus University, Silkeborg, Denmark.

In.prep.

Abstract

Shallow freshwaters can exchange large amounts of carbon dioxide (CO_2) with the atmosphere as well as store significant quantities of carbon in their sediments. Current climatic and anthropogenic pressures, such as warming and changes in species composition are expected to alter the metabolic balance in planktonic communities of shallow freshwaters, as well as facilitate the increase in total phytoplankton biomass when cyanobacteria are dominating. However, it is still poorly understood how the combined effects of warming and changes in planktonic community composition affect ecosystem metabolism and, ultimately, the role of shallow freshwater ecosystems in the carbon cycle. To contribute to unravel this, a microcosm scale experiment was conducted where changes in CO_2 fluxes and carbon sedimentation were evaluated for two contrasting plankton communities: palatable chlorophytes-dominated versus unpalatable cyanobacteria-dominated, both with a similar zooplankton community with a potentially high grazing capacity (i.e., presence of large-bodied cladocerans), at two different temperatures (control and +4^{o}C). In our simple plankton communities, that were not limited by light and nutrients, we found a clear increase in CO_2 uptake with warming. This increase in CO_2 uptake was significantly stronger for the cyanobacteria-dominated in comparison to chlorophyte-dominated regime. However, a low amount of the fixed carbon seemed to translate into increased phytoplankton (chl-*a*) or zooplankton biomass, but instead into increased dissolved inorganic carbon and sedimented organic matter.

Keywords: phytoplankton, zooplankton, eutrophication, climate warming, CO_2 diffusion

Introduction

Ponds and shallow lakes are active compartments in the carbon cycle. In the last decade, several lines of evidence have pointed out their relevant role in transporting, transforming, emitting, and burying carbon (Cole et al., 2007; Battin et al., 2009; Tranvik et al., 2009, 2018). Particularly, the contribution of shallow lakes to the global emissions of carbon dioxide (CO_2) matches the uptake by the oceans on an annual basis (Tranvik et al., 2009). On the other hand, estimated organic carbon burial by inland waters exceeds the organic carbon sedimentation in the oceans (Downing et al., 2008; Battin et al., 2009; Sobek et al., 2009). Current climatic (e.g., warming) and more local anthropogenic (e.g., eutrophication) pressures might alter the role of shallow lakes and ponds in the carbon cycle, and a better understanding of the individual and potentially synergistic effects of these pressures is crucial to predict future scenarios and to develop appropriate mitigation measures (Battin et al., 2009; Moss, 2010, 2011; Meerhoff et al., 2022).

Warmer conditions predicted for the coming decades (IPCC, 2021) are expected to impact the metabolic balance (CO_2 uptake: CO_2 efflux ratio) in aquatic and terrestrial ecosystems. Respiration rates tend to increase faster with temperature than photosynthesis, and a consequent reduction in the ratio between gross primary production (GPP) and ecosystem respiration (ER) is expected under warmer conditions (Allen et al., 2005; Acuña et al., 2008; Yvon-Durocher et al., 2011; IPCC, 2021). Indeed, this changes in GPP and ER ratios may hamper the capacity of aquatic ecosystems to sequester CO_2, while increasing CO_2 emission (Kosten et al., 2010) as the proportion of the stored carbon respired and released as CO_2 increases (Moss, 2010; Yvon-Durocher et al., 2010, 2011; Pacheco et al., 2014). This effect can be most pronounced in systems with well mixed water columns where sediments are well oxygenated (Carey et al., 2018).

The processes of eutrophication, through the high supply of nutrients from the watersheds, has become one of the major anthropogenic impacts on inland and coastal waters all around the world (Smith, 1998; Moss, 2011; Paerl et al., 2011; Paerl & Paul, 2012). Ongoing eutrophication may cause plankton communities in shallow freshwaters to shift from moderate biomass of phytoplankton and diverse groups compositions, to turbid conditions with extremely high biomass of phytoplankton, often dominated by cyanobacteria (Scheffer et al., 1993; Paerl et al., 2011; Glibert, 2017). Thus, impacting the entire structure of biological communities (i.e., pauperizing the communities of fish and macroinvertebrates) and promoting the loss of biodiversity and valuable ecosystem services (Scheffer et al., 1993; Hilt et al., 2017; Janssen et al., 2020).

Synergistic effects of climate warming and eutrophication might occur through different processes. When climate warming leads to an increase in the frequency and intensity of precipitation and storms, nutrient supply from the watersheds will also increase (Jeppesen et al., 2009). In areas where a decrease in precipitation promoting more frequent and longer water

column stratification this may lead to more nutrients release from anoxic sediments (Søndergaard et al., 2013). In summary, warmer and eutrophic conditions can facilitate cyanobacteria-dominated regimes worldwide (Paerl & Huisman, 2008; Moss, 2010, 2011; Kosten et al., 2012; Paerl & Paul, 2012; Yan et al., 2017; Lürling et al., 2018).

Cyanobacteria, despite being a taxonomically highly diverse group, have several competitive advantages that allow them to exclude other phytoplankton groups (such as chlorophytes). These advantages include a high assimilation and stocking capacity of P, atmospheric N_2 fixation capabilities, presence of resting stages, efficient light capturing at low intensities and the capacity to control their buoyancy (Nõges et al., 2008; Litchman et al., 2010; Carey et al., 2012; Lürling et al., 2013; Visser et al., 2016). Moreover, zooplankton grazing pressure on cyanobacteria is expected to be lower than on more palatable groups, such as chlorophytes. The potential production of toxins, their deficiency in sterols and polyunsaturated fatty acids (PUFAs) and the aggregation in large and inedible colonies or filamentous that may clog the filtration apparatus in cladocerans, make cyanobacteria a poor-quality food for zooplankton (Ahlgren et al., 1990; DeMott, 1999; DeMott et al., 2001; Colina et al., 2016). Besides, the share of cyanobacteria in phytoplankton communities tends to increase with temperature (Mooij et al., 2005; Paerl & Huisman, 2008; Kosten et al., 2012; Paerl & Paul, 2012). This likely due to a strong tolerance to high temperatures for cyanobacteria in comparison with other phytoplankton groups (Carey et al., 2012; Visser et al., 2016), and to a decrease in grazing pressure with warming as a consequence of the low proportion or absence of large-bodied grazers in zooplankton communities (e.g., large cladocerans such as *Daphnia* spp.) (Meerhoff et al., 2007, 2012; Sarmento, 2012). The combined effect of shift in plankton community composition and warming may therefore induce a weakening of the coupling between primary producers and zooplankton, which – in turn - may promote a poor energy and carbon transfer to higher trophic levels, and the disruption of the classic food web (Ger et al., 2014).

While the development of a high cyanobacteria biomass enhances CO_2 uptake, a major proportion of this organic carbon may be decomposed either in the water column or after sedimentation (Sobek et al., 2009; Tranvik et al., 2009; Bastviken et al., 2011). Decomposition rates are strongly temperature dependent (Gudasz et al., 2010, 2015) with higher rates occurring at higher temperature. Decomposition rates also differ depending on the organic matter quality (Fallon & Brock, 1980; Gudasz et al., 2012; Yan et al., 2019), and may therefore also differ between cyanobacteria and chlorophytes. Combined effects of changes in phytoplankton communities and warming on metabolic processes and ultimately on carbon budgets in shallow freshwaters are still unclear (Yan et al., 2017, 2019).

We aimed to contribute to the understanding of how the metabolic balance (in particular the net CO_2 flux over the water-atmosphere interface) of aquatic ecosystems, changes under warmer conditions with a likely higher frequency of cyanobacterial dominance, which is expected to

occur in freshwaters world-wide. On a microcosm scale, we subjected two contrasting plankton communities - one dominated by palatable chlorophytes versus one dominated by unpalatable cyanobacteria, both with a similar zooplankton community with a potentially high grazing capacity (i.e., presence of large-bodied cladocerans) – to a control and a warm (+4ºC) temperature. The changes in CO_2 fluxes and carbon sedimentation were evaluated for these experimental microcosms. We hypothesize that the difference in growth rates under warmer conditions between the two phytoplankton groups, as well as the differences in potential grazing pressure of zooplankton communities on the different phytoplankton communities (chlorophyte-dominated versus cyanobacteria-dominated), will translate into differentiated metabolic balances (i.e., net CO_2 flux) in simple microcosm systems without carbon inputs other than atmospheric CO_2, and in which nutrients and light do no limit phytoplankton growth. We expect higher CO_2 uptake in the cyanobacterial dominated systems compared to the chlorophyte dominated systems. In addition, we expect higher carbon sedimentation in cyanobacteria than in chlorophytes dominated systems, given the lower zooplankton grazing on cyanobacteria. For both phytoplankton communities, we expect higher relative CO_2 uptake and carbon sedimentation under warming (Fig.1A-B).

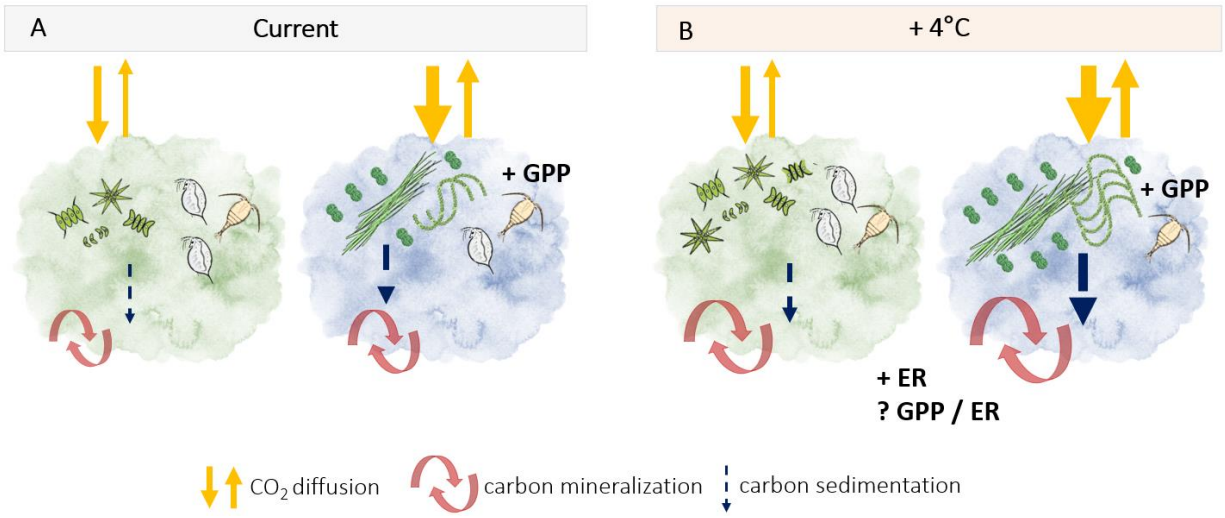

Figure 1. Hypotheses for chlorophyte- dominated communities (in green background) versus cyanobacteria-dominated (in blue background). In A current temperature (control) and in B + 4°C warming scenario. The size of the arrows is proportional to the expected amount of associated carbon, and unfilled arrows indicate highly uncertain predictions, and their direction indicates either influx or efflux of CO_2.

Materials and Methods

We ran a full-factorial microcosm experiment, where phytoplankton communities with either cyanobacteria dominance or chlorophyte dominance (refer as Cya and Chlo, respectively) were subjected to 19.5°C, as the mean temperature expected for spring in subtropical regions, and 23.5°C as the expected under the 4°C increase in global surface temperature by the end of the

XXI century (IPCC, 2021). We used 40 cylindrical aquaria (4.5L total volume, 23.5cm of diameter and 10cm of height) with 10 replicates per combination of phytoplankton regime and temperature conditions. Both temperatures (refer from now as control-C and warm-W) were recreated in two contiguous independent climatized rooms (IDPlus Eliwell, Schneider Electric, France) and the experiment was run over 19 days. Both rooms started at 19.5°C to avoid a temperature shock to the plankton communities, and for the warm treatment the temperature was gradually increased up to 23.5°C within the following 10 days.

Experimental setup

The initial spring phytoplankton assemblages (from now onwards, Chlo and Cya) were collected with a 20µm mesh size net from natural shallow lakes with a known phytoplankton contrasting compositions (i.e., mainly chlorophytes species versus mainly cyanobacteria species, personal observation). Initial assemblages were maintained over 15 days in the laboratory at 19°C and 15:9 hours light: dark photoperiod for their acclimatization. Two homogenized water media were prepared in 70L containers with dechlorinated tap water and 440mL of a nutrient-enriched medium (prepared following Redfield nitrogen: phosphorus ratio of 16:1), to achieve eutrophic conditions with concentrations of total phosphorus (TP) of approximately 80µg.L^{-1} and total nitrogen (TN) of approximately 500µg.L^{-1}. The phytoplankton inocula were added to each media in enough volume to reach an initial chlorophyll-a concentration similar to the expected in natural eutrophic subtropical shallow lakes (approx. 30µg.L^{-1}, Kruk et al., 2009; Meerhoff et al., 2012). For the Cya, a 5L sample (initial conc.~ 300µg Chl-a.L^{-1}), and for the Chlo, an inoculum of 9L (initial conc.~ 190µg Chl-a.L^{-1}) were added. In the resulting inocula (water with media plus phytoplankton) Chlo was dominated by *Monoraphidium* sp., *Scenedesmus* sp. and *Ankistrodesmus* sp., and Cya by *Synechococcus nidulans* and *Planktothrix* sp. (Table 1); both with mean biomasses of 23.2 ± 7.4 and 46.6 ± 2.3 µgChl-a.L^{-1}, respectively.

An equal number of 3.5L microcosms for Cya and Chlo were randomly distributed between the two temperature rooms (Fig. S1). All microcosms were exposed to the same light intensity of around 20-21µmol photon. m^{-2}. s^{-1}, similarly to the expected in the water column of eutrophic lakes (Kosten et al., 2009; Li et al., 2019). The photoperiod over the experiment was the same as during the acclimatation period.

Immediately before starting the experiment, a zooplankton mix composed of 10 individuals of *Daphnia magna* and 10 of *Daphnia pulex* were added to each microcosm, covering similar body size ranges. This *Daphnia* spp. abundance was chosen to establish a potentially high grazing pressure while avoiding phytoplankton to be fully grazed down. According to the median clearance rate reported for cladocerans (~20mL.ind^{-1}.day^{-1}, considering the most palatable morphology-based functional group- MBFG, Colina et al., 2016), the experimental addition would be able to filter around 10% of the microcosm phytoplankton volume. *D. magna* and *D. pulex* individuals were obtained from laboratory cultures. Other smaller-bodied zooplankton groups, such as rotifers and copepods, as well as small body-sized species of cladocerans and

natural microbiota, were also added together with the phytoplankton inocula collected from the shallow lakes.

The water surface was manually and carefully mixed every 24-48 hours with a stick, to prevent bacterial aggregation on the water surface and minimize phytoplankton sedimentation. Regularly, the level of the water at each aquarium was checked and extra dechlorinated water was added to maintain a fixed water lever when necessary. Once a week (after routine measurements), nutrients were added to maintain eutrophic conditions all over the experiment (~10mL of the initial mix with TP concentration ~80µg.L^{-1}).

Microcosm general characterization

Every 3 days, double routine measurements were conducted for each microcosm, at the middle of the light hours and at the middle of dark hours, respectively. *In situ* measurements were conducted for dissolved oxygen concentration (DO in mg.L^{-1}) and saturation (%) using an OxyGuard Handy Polaris probe (OxyGuard International, Denmark), and pH and water temperature (°C) with a portable sensor (HNNA Instruments, USA).

At the start (day 0), middle (day 7), and final dates (days 16 and 19) of the experiment, total nitrogen (TN) and total phosphorous (TP) concentrations were measured from 20mL of water collected from each microcosm. At initial and final times (days 0 and 19), also nitrate ($N\text{-}NO_3^-$), ammonium ($N\text{-}NH_4^+$) and orthophosphate ($P\text{-}PO_4^{3-}$) were determined from water samples previously filtrated through GF/C glass microfiber filters (1.2µm pore size and 47mm diameter, Munktell, Texas, USA). For the initial time, the nutrient analyses were performed for 10 replicates retrieved from each water with media plus phytoplankton inocula (Cya and Chlo).

CO_2 diffusive flux estimations

Starting four days after the inoculation and subsequently every 3 days, and for each microcosm, the CO_2 diffusion (in mg.m^{-2}.day^{-1}) between the water and the atmosphere was estimated for light and dark periods. The difference between the concentration of dissolved CO_2 in the water and the saturation concentration (assumed equal to the concentration in the air) was used for CO_2 diffusive flux estimation according to Cole & Caraco, (1998):

$$\mathrm{F} = \mathrm{KL} \cdot ß \cdot (\mathrm{pCO_2w} - \mathrm{pCO_2a})$$

The partial pressure of CO_2 in the ambient air (*pCO_2a*), inside each climatized room was assumed to be constant during the experimental time, according to the registered values by automatic CO_2 loggers (K33 ELG, SenseAir, Sweden), with 550ppm and 750ppm for the 19.5°C and 23.5°C temperature conditions, respectively. The concentration of dissolved CO_2 in the water (*pCO_2w*) was estimated from the dissolved inorganic carbon (DIC) concentrations measured in samples taken at the end of the experiment, combined with the water temperature and pH at the different sampling days, and measured during light and dark periods (the calculations were done following Kling et al. 1992 and Cole et al. 1994, see supplementary

methods for details). For DIC analyses 3mL of water were extracted from each microcosm and stored in 3mL exetainers with 0.1mL of ZnCl (final concentration of 0.03%vol/vol) to half microbial activity. Samples were stored dark and cool until analysis. The concentration of DIC was analyzed by injecting 1mL of sample into an Infrared Gas Analyzer (IRGA, ABB Analytical). The gas transfer velocity (*KL*, in $m.d^{-1}$) for O_2 was empirically estimated for both experimental temperatures, from the dissolved O_2 concentration increase in deoxygenated water (same experimental volume that for the microcosms), according to Tribe et al. (1995). Then, *KL* for CO_2 was derived based on the ratio between the Schmidt numbers for O_2 (*ScO_2*) and CO_2 (*ScCO_2*), both corrected by temperature and assuming low wind action (*n*=0.66) (Cole & Caraco, 1998), according to:

$$\mathrm{KL_{CO_2}/KL_{O_2}} = (\mathrm{Sc_{CO_2}/Sc_{O_2}})^{\mathrm{n}}$$

The high pH in our aquaria as a result of the high primary production chemically enhances CO_2 uptake – particularly at a pH> 9 as CO_2 diffusing into the water reacts with OH^- maintaining a strong CO_2 concentration gradient over the atmosphere-water interface (Bade & Cole, 2006). To account for this potential effect on the CO_2 diffusive flux, for each sampling day with pH>9 we estimated the chemical enhancement factor (ß, dimensionless) based on water temperature and pH using equations described in Bade & Cole (2006) (see Supp.Info for all equations).

Independent estimations for light and dark periods were conducted to capture the differences in CO_2 diffusion, that might occur between day and night according to the changes in GPP and ER. Next, the diel CO_2 diffusion from each microcosm was estimated as: CO_2 diffusion during the light period (in $mg.m^{-2}.hrs^{-1}$) multiplied by the total amount of light hours per day (15 hours), plus CO_2 diffusion during the dark period (in $mg.m^{-2}.hrs^{-1}$) multiplied by the dark hours per day (9 hours).

Suspended organic matter and particulate matter sedimentation

For 10 replicates of the two initial water and media plus phytoplankton inocula (Cya and Chlo) and for each microcosm at final experimental time, 0.2-0.3L of water were filtered through GF/C glass microfiber filters (1.2µm pore size and 47mm diameter, Munktell, Texas, USA) and the total suspended solids (SST) and the suspended organic matter (SOM, in $mg.L^{-1}$) were determined as the difference between dried (110°C during 24 h) and burnt (500°C during 15 min) filter weights (Rice et al., 2017).

To quantify the amount of sedimented particulate matter (Sed. PM, in $g.m^{-2}$) two glass vials (base: $9.6cm^2$ and height: 6cm) were placed on the bottom of each microcosm at the beginning of the experiment. From each aquarium, at the end of the experiment and before any other manipulation, glass vials were carefully removed from the aquaria. The difference between empty (time 0) and dry (110°C during 48 h, at final time) weights was used to roughly estimate the amount of Sed. PM accumulated at the bottom during the experimental period.

Plankton biomass and composition: phytoplankton and zooplankton

Phytoplankton biomass quantification was assessed using chlorophyll-a concentration as a proxy. We took 10 replicates of the two initial water with media plus phytoplankton inocula (Cya and Chlo) and for each microcosm at the final experimental time, 0.2-0.3L of water were filtered through GF/C glass microfiber filters (1.2µm pore size and 47mm diameter, Munktell, Texas, USA), followed by pigment extraction from the filters in 95% cold ethanol and spectrophotometric measurements of the absorbances at 665-750nm (ISO 10260, 1992). Also, from each water plus phytoplankton inocula and from each microcosm at final time (day 19), 50mL of water were collected and fixed with Lugol´s 4% solution, for the identification of the main taxonomic groups in an inverted microscope (Nikon Y-TV55, Japan).

At final experimental time, and after retrieved all other samples, the entire remaining water volume of each microcosm was filtered through a 50µm mesh size net and the concentrated fraction preserved with Lugol´s 4% solution. The main taxonomic groups (calanoids, copepods and rotifers) were identified under a binocular microscope (Olympus CX31, Tokyo, Japan) and abundances (as individuals. L^{-1}) determined, with relevant species or genera identified to the finest resolution possible. The presence of cladocerans resting eggs was also checked as a potential indicator of stress conditions for zooplankton. Biomass for each genera or taxonomic group were estimated by multiplying their abundances per the mean dry weight (DW in $\mu gDW.L^{-1}$) of adult individuals reported in the literature (Dumont et al., 1975; Burns & Hegarty, 1994; Masundire, 1994). The ratio between the biomass of cladocerans (in $\mu gDW.L^{-1}$) and biomass of phytoplankton (in $\mu gChl\text{-}a.L^{-1}$) was estimated as a proxy for zooplankton potential grazing pressure over the phytoplankton. We only included cladocerans as they are the zooplankton group with the higher grazing potential and able to exert a significant effect on the biomass of the phytoplankton.

Allocation of total carbon stock among the different biotic and abiotic components

The amount of carbon gained by the microcosms systems, and the total carbon allocation among phytoplankton, zooplankton, suspended organic matter and sedimented particulate matter at the end of the experiment was estimated.

For phytoplankton, carbon content was estimated from chlorophyll-a concentration, assuming the ratio C:Chl-a ~ 30 (Cloern, 1995; Reynolds, 2006). For the carbon content in the zooplankton, it was assumed that carbon accounts for 45% of the dry weight of all the taxonomic groups (Hessen, 1992). DIC was quantified as described above, and 80% of the Sed. PM was assumed to be carbon.

The delta carbon (final-initial carbon concentration, ΔC) was estimated from the diel CO_2 diffusion for the total experimental period (according to molecular weight). Diel CO_2 diffusion for the total experimental period was assessed as the integral -area under the curve- of the flux intensity (CO_2 diffusion per each individual sampling date) versus time (days) graph, for each

aquarium. For further details on all the equations used to estimate the carbon budget, please refer to the Supp.Info.

Statistical analyses

All statistical analyses were performed using the software R (RStudio Team, 2018), and prior to defining the statistical analyses to apply, normal distributions were checked, and log transformations were applied when corresponded.

For the final experimental time, significant differences in the biomass of phytoplankton, biomass of cladocerans potential grazing pressure (using cladocerans biomass/ phytoplankton biomass as a proxy), suspended organic matter and the sedimentation of particulate matter were addressed using two-way ANOVA tests with phytoplankton and temperature (both as categorical variables: Chlo and Cya, and control and warm, respectively) and their interaction as the explanatory variables. Differences within groups were analyzed with pairwise comparisons, using the function glht from the multcomp package. In all cases, the response variables were log transformed prior to ANOVA tests, and a constant equal to 1 was added to the biomass of cladocerans and potential grazing pressure, to manage zeros before log transformation.

The mean CO_2 diffusive flux, for the total experimental time, and independently for light, dark and diel periods, was estimated for each microcosm. Mean fluxes were assessed as the integral -area under the curve- of the flux intensity versus time (days) graph, divided by the total experimental time (19 days). The function AUC from DescTools package was used to estimate the integral values in flux intensity versus time graphs. To evaluate differences in mean CO_2 diffusion between phytoplankton and temperature conditions two-way ANOVAS were used in addition to pairwise comparisons to test differences between groups, as described above. In addition, for each period (i.e., light, dark and diel), the diffusion intensity of CO_2 estimated per sampling day was evaluated versus time, temperature (control-C or warm-W) and phytoplankton composition (Chlo or Cya) as the explanatory variables, with a GLM with gaussian distribution. The significance of the explanatory variables was evaluated based on p-values extracted from the ANOVA-table. Statistical analyses for the direct estimations of CO_2 diffusion are summarized in the Supp.Info.

Differences in carbon allocation between the different biotic and abiotic components of the microcosms, for chlorophyte-dominated and cyanobacteria-dominated systems and temperature conditions, independently, were assessed with one-way ANOVAS in addition to pairwise comparisons to test differences between groups.

The water chemical characteristics over the experiment, including water temperature, pH and dissolved oxygen concentration were evaluated versus time (in days), the cross combination of phytoplankton and temperature conditions (Cya-Control, Cya-Warm, Chlo-Control and Chlo-Warm) and the period (light or dark hours) using generalized lineal models (GLM). A similar approach was applied to evaluate nutrient dynamics over the experiment, with phytoplankton and temperature as explanatory variables.

In all cases, models (ANOVAs and GLMs) were validated by the evaluation of normal distribution and homogeneity of variance in the residuals.

Results

Microcosms general characterization

Water temperature in all microcosms located at the control temperature room (19°C), started around 19.5°C and stabilize at 19°C by day 4. Meanwhile, for the microcosms located at the warm temperature room (23.5°C), water temperature started around 20°C and stabilized around 23.5°C by the day 10 (Fig. 2a). For each temperature condition, no temperature differences were found between light and dark periods (Table S1).

pH did not show a significant trend over the course of the experiment for any of the treatments (Table S1). However, differences between light and dark periods were observed for the chlorophyte-dominated treatments, with higher pH values during light hours in both control and warm temperature conditions. For the cyanobacteria-dominated treatments, pH was remarkably higher at the warm temperature condition in comparison to the control temperature, during both light and dark periods (Fig. 2b).

DO concentration did not vary significantly over the experimental time for any of the treatments (Table S1). However, we observed a trend for higher DO values during light hours in comparison to dark hours, particularly at the warm temperature condition for both phytoplankton communities (Fig. 2c).

For all treatments (Chlo-Control, Chlo-Warm, Cya-Control and Cya-Warm), and despite P additions, TP concentration in the water decreased during the experiment, with the decrease rate being slightly stronger at the control temperature (Fig. 2d and Table S1). TN concentrations slightly decreased over time for the microcosms kept at the control temperature, but clearly increased in microcosms kept at the warm temperature, with the strongest increase in the cyanobacteria-dominated systems (Fig. 2e and Table S1). At the end of the experiment, dissolved nutrient concentrations ($P\text{-}PO4_3^-$, $N\text{-}NO_3^-$ and $N\text{-}NH_4^+$) in the cyanobacteria-dominated systems were significantly higher at the warm temperature than at the control temperature. The same was true for $N\text{-}NO_3^-$ in the chlorophytes-dominated systems, where instead, no differences in the concentrations of $PO4_3^-$ and NH_4^+ were observed between control and warm temperatures (Table S1 and Fig. S2b-d).

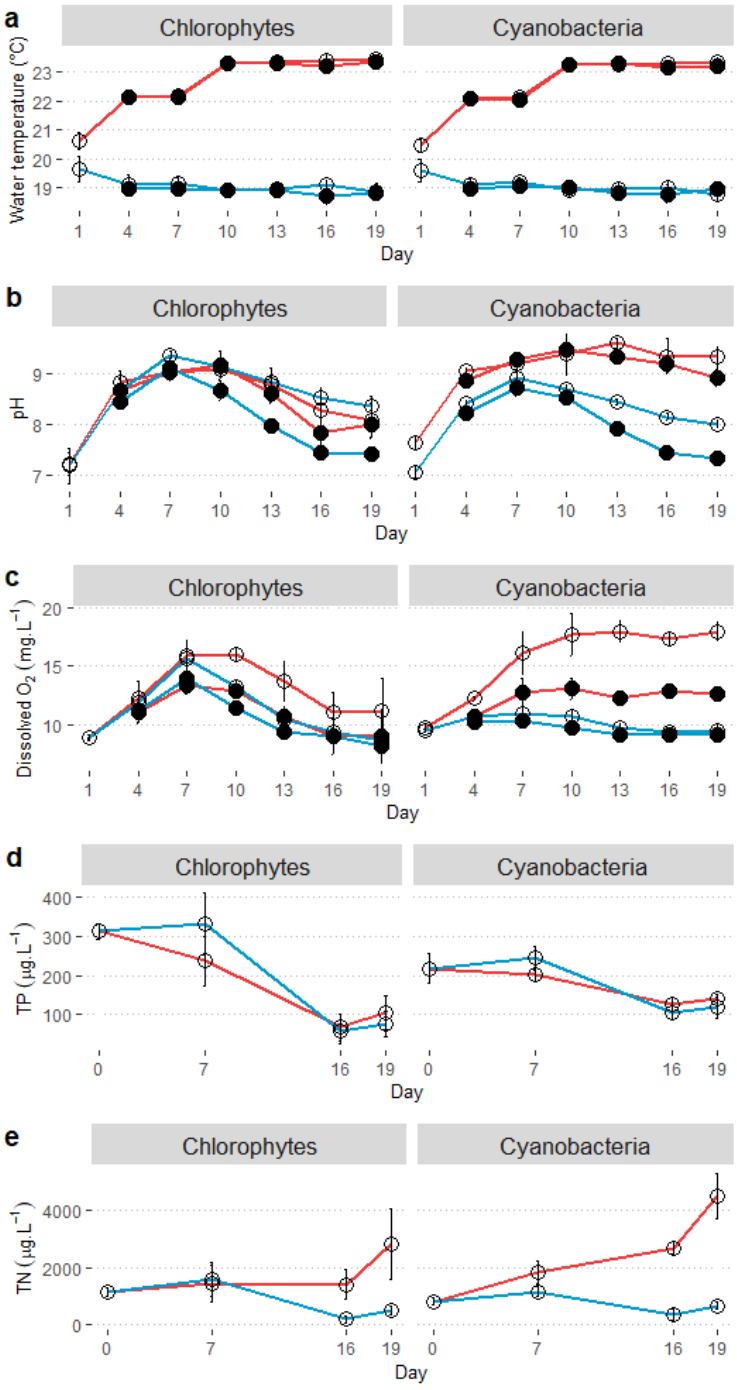

Figure 2. Comparison between phytoplankton communities (chlorophytes versus cyanobacteria) and between temperature conditions (control in sky-blue and warm in red) for the change over time of variables: a) water temperature, b) pH, c) dissolved O_2, d) total phosphorous (TP), and e) total nitrogen (TN). Unfilled dots correspond to measurements conducted during light hours and black dots to dark hours measurements, except for TP and TN (d and e) where no differences between light and dark periods are shown. Each dot represents the mean value for the 10 replicates and vertical lines the standard deviation.

Plankton communities: phytoplankton and zooplankton

Even when for both phytoplankton communities the composition of taxonomic groups did not significantly change from the inocula to the final experimental time (Table 1), for the cyanobacteria-dominated systems a particular increase in the relative representation of *Synechococcus* sp. was observed, mainly in the warm treatment. For the phytoplankton biomass at the end of the experiment, we found a clear effect of temperature ($p << 0.001$, $F_{5,54}=62.2$ and $R^2 = 0.8$, Fig 3a and Table 2). As expected, warmer conditions led to higher phytoplankton biomass compared to the control temperature, and at cyanobacteria-dominated systems total biomass was always higher than at chlorophytes-dominated systems (post-hoc $p <0.02$ in all cases). Because the cyanobacteria grew faster than chlorophytes in the stock solutions used to inoculate the microcosms, the start chlorophyll- a concentration in the cyanobacteria-dominated was twice as high as in the chlorophytes-dominated systems. At the end of the experiment in the control temperature the chlorophyll-a concentration (which decreased in time) was still twice as high in the Cya systems compared to the Chlo dominated systems. In the warm temperature chlorophyll-a (that increased during the experiment) was four times higher in Cya systems than in Chlo systems. The lowest phytoplankton biomass was observed for the Chlo-control treatment and the highest for the Cy-warm treatment.

At the end of the experiment, the highest number of zooplankton taxonomic groups was found for the Chlo-warm treatment and the lowest for the Cya-warm treatment. In addition, in the Cya-warm treatment no individuals of *D.magna* were found and it was the only treatment where cladocerans resting eggs were found (Table 1). The dry weight of cladocerans was significantly different according to the interaction between phytoplankton community and temperature condition ($p << 0.001$, $F_{3,36}=9.7$ and $R^2 = 0.4$, Fig 3b and Table 2). Cladoceran DW in the Chlo-warm treatment was significantly higher than in the Cya-warm and Chlo-control treatments (post-hoc $p <0.001$). At the control temperature condition, cladocerans DW was the highest at the Cya treatment (post-hoc $p <0.05$). No differences were found between Cya-control and Cya-warm treatments, neither between Cya-warm and Chlo-control treatments.

The zooplankton potential grazing pressure on the phytoplankton, estimated as the ratio Clad. DW / Chl-a, significantly differed according to the phytoplankton community and to the interaction between phytoplankton community and temperature conditions ($p << 0.001$, $F_{3,36}=13.4$ and $R^2 = 0.5$, Fig 3c and Table 2), with the Cya-warm treatment having a lower grazing pressure than the Chlo-warm and Cya-control treatments (post-hoc $p< 0.001$).

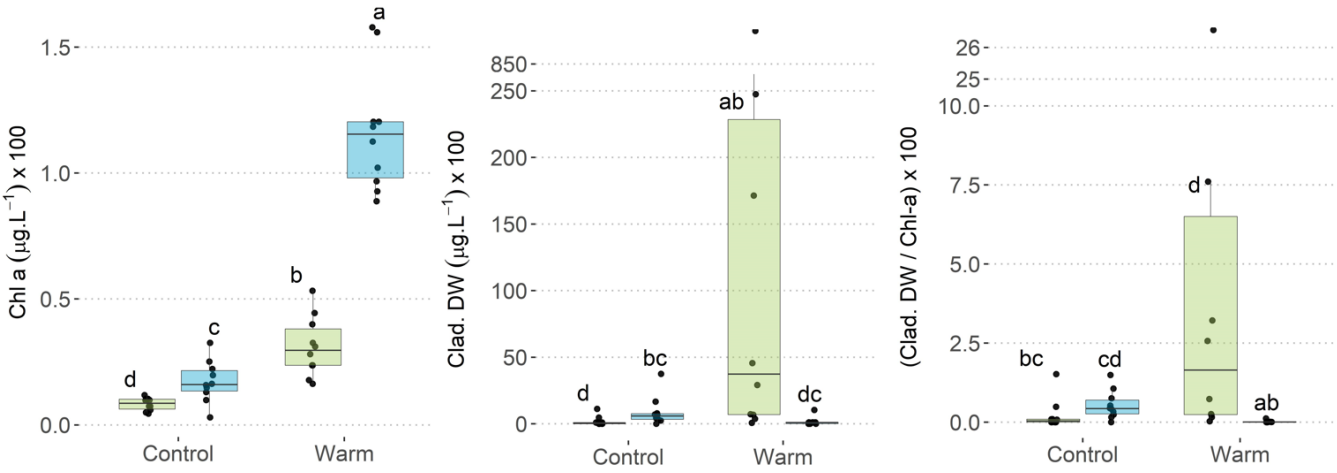

Figure 3. Comparison, at the end of the experiment, between phytoplankton communities (Chlo in green and Cya in blue) and temperature condition (control and warm), for variables: a) chlorophyll-a concentration (Chl-a, in µg.L^{-1}), b) cladocerans dry weigh (Clad. DW, in µgDW.L^{-1}), and c) zooplankton potential grazing pressure over phytoplankton assessed as the ratio between cladocerans DW and chlorophyll-a concentration (Clad. DW /Chl-a, dimensionless). The horizontal dark lines in the box-plots represent the median value, the boxes show the interquartile range with 25% and 75% percentiles, and the vertical lines indicate the distribution range. Black dots show individual data and letters on the top of the boxes (a, b, c and d) indicate the results of the pairwise comparison after the two-way ANOVAs (Tukey's test). In all cases, units are *100, and for b) and c) breaks on the y axis were added.

Table 1. Taxonomic groups of phytoplankton and zooplankton found for samples at the initial (day 0) and final (day 19) times samples are summarized according to chlorophytes-dominated (Chlo) versus cyanobacteria-dominated (Cya) and at control or warm temperature conditions. Individual species are summarized when their identifications was possible.

	Phytoplankton		**Zooplankton**	
	Chlo	**Cya**	**Chlo**	**Cya**
Inoculum	*Monoraphidium* sp.	*Synechococcus nidulans*	Naupli	
	Scenedesmus sp.	*Planktothrix* sp.	Rotifers	
	Ankistrodesmus sp.	*Scenedesmus* sp.	*Daphnia magna*	
	Nitzschia sp.	*Ankistrodesmus sp.*	*Daphnia pulex*	
		Nitzschia sp.	*Chydorus* sp.	
		Trachelomonas sp.		
CONTROL	*Monoraphidium* sp.	*Synechococcus nidulans*	Nauplii	Nauplii
	Nitzschia sp.	*Monoraphidium* sp.	Copepodites	Copepodites
	Trachelomonas sp.	Planktothrix sp.	Calanoida	Calanoida
		Trachelomonas sp.	Cyclopoida	Cyclopoida
		Nitzschia sp.	*Daphnia pulex*	Harpacticoida
			Rotifers	*Daphnia pulex*

			Simocephalus sp.	*Daphnia magna* Rotifers *Ceriodaphnia* sp.
warm	*Monoraphidium* sp. *Nitzschia* sp. *Trachelomonas* sp.	*Synechococcus nidulans* *Planktothrix* sp. *Monoraphidium* sp. *Ankistrodesmus* sp.	Nauplii Copepodites Cyclopoida Harpacticoida *Daphnia pulex* *Daphnia magna* Rotifers *Ceriodaphnia* sp. *Chydorus* sp. *Bosmina* sp. *Simocephalus* sp.	Nauplii Copepodites Rotifers *Daphnia pulex* Cyclopoida Cladocerans resting eggs

Suspended organic matter and sedimentation of particulate matter at the end of the experiment

The SOM significantly differed between phytoplankton communities and temperature conditions ($p << 0.001$, $F_{3,35}=14.3$ and $R^2 = 0.5$, Table 2 and Fig. 4a), with the highest values at the Cya-warm treatment (mean: 37.0 ± 16.1 $mg.L^{-1}$). The SOM at Cya-warm was 2.5 times higher than at Cya-control (mean: 14.4 ± 7.1 $mg.L^{-1}$), 3 times higher than at Chlo-control (mean: 12.4 ± 3.1 $mg.L^{-1}$) and 3.5 times higher than at Chlo-warm (mean: 10.4 ± 3.8 $mg.L^{-1}$). The amount of Sed.PM also differed significantly between treatments ($p << 0.001$, $F_{3, 35}=42.1$ and $R^2=0.7$, Table 2 and Fig. 4b), with the lowest sedimentation at the Cya-control treatment (mean: 3900 ± 700 $mg.m^{-2}$). Also, the Sed.PM for Chlo-control treatment (mean: 13600 ± 2700 $mg.m^{-2}$) was significantly higher than at the Cya-warm treatment (mean: 9700 ± 3000 $mg.m^{-2}$).

CO_2 diffusion

We find a clear effect of the experimental warming and the phytoplankton community composition on the mean CO_2 diffusion (Fig.5) and CO_2 diffusive flux intensity (Table 3, and Fig. S3), all along the experimental time and across light conditions. The mean CO_2 diffusive flux significantly differed between temperature conditions and between phytoplankton communities, at light hours ($p << 0.001$, $F_{3, 36}=60$ and $R^2=0.8$), dark hours ($p << 0.001$, $F_{3, 36}=39.3$ and $R^2=0.7$) and for the diel flux ($p << 0.001$, $F_{3, 36}=50.4$ and $R^2=0.8$). Across light conditions, the strongest mean CO_2 uptake always occurred at the warm temperature condition for the cyanobacteria-dominated systems (all post-hoc values $p <0.001$). Calculated diel fluxes indicate a net CO_2 efflux under control temperature conditions for both phytoplankton communities.

Table 2. Main effects of factors: temperature (temp., as control or warm), phytoplankton regime (phyto., as Chlo and Cya) and their interaction, on chlorophyll-a concentration (Chl-a, in µgChl-a.L^{-1}), dry weight of cladocerans (Clad. DW, in µgDW-a.L^{-1}), zooplankton potential grazing pressure over phytoplankton (Grazing pressure, as Clad. DW/ Chl-a), the suspended organic matter (SOM, in mg.L^{-1}) and the sedimented particulate matter (Sed. PM, in mg.m^{-2}).

	temp.			phyto.			temp. * phyto.		
	F	**d.f.**	**P**	**F**	**d.f.**	**P**	**F**	**d.f.**	**P**
Chl-a	151.8	1	***	54.4	1	***	7.2	1	*
Clad. DW	3.7	1		0.8	1		24.7	1	***
Grazing pressure	0.1	1		4.8	1	*	35.3	1	***
SOM	5.8	1	*	19.9	1	***	17.3	1	***
Sed.PM	18.4	1	***	73.6	1	***	34.4	1	***

Statistical results of two-way ANOVAs are shown, indicating respective F-values, degrees of freedom (d.f.) and P-values: * P < 0.05; ** P < 0.01; *** P < 0.001.

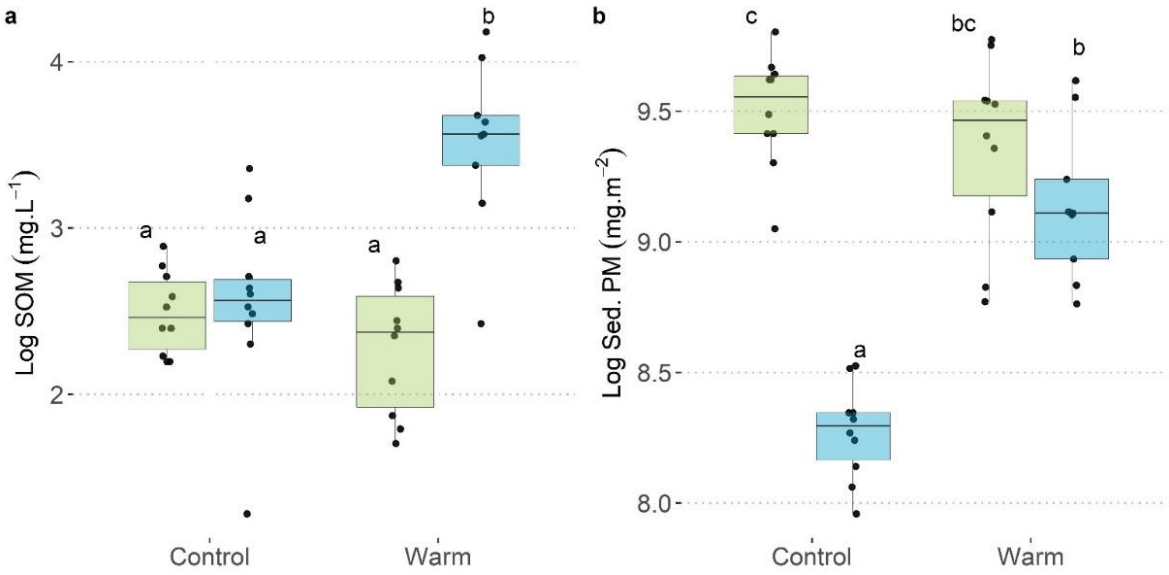

Figure 4. Box-plot for the comparison, at the end of the experiment, between phytoplankton (Chlorophytes (Chlo) in green and Cyanobacteria (Cya) in blue) and temperature (Cool and Warm) conditions, for: a) suspended organic matter (SOM, in mg.L^{-1}), b) sedimented particulate matter (Sed. PM, in mg.m^{-2}). The horizontal dark lines in the box-plots represent the median value, the boxes show the interquartile range with 25% and 75% percentiles, and vertical lines indicate the distribution range. Black dots show individual data and letters on the top of the boxes (a, b and c) the pairwise comparison after the two-way ANOVAs (Tukey's test).

Table 3. Main effects of factors: time (in days), temperature (temp., as cool or warm) and phytoplankton (phyto., as Ch and Cy), on the CO_2 diffusive flux intensity (in $mg.m^{-2}.day^{-1}$) for light, dark and diel estimations.

	light			dark			diel		
	time	**temp.**	**phyto.**	**time**	**temp.**	**phyto.**	**time**	**temp.**	**phyto.**
F	31.6	60.9	12.6	122.5	84.5	6.6	93.8	91.4	11.2
d.f.	238	237	236	238	237	236	238	237	236
P	***	***	***	***	***	*	***	***	***

Statistical results of ANOVA table for GLMs, indicating respective F-values, degrees of freedom (d.f.) and P-values: * P < 0.05; ** P < 0.01; *** P < 0.001

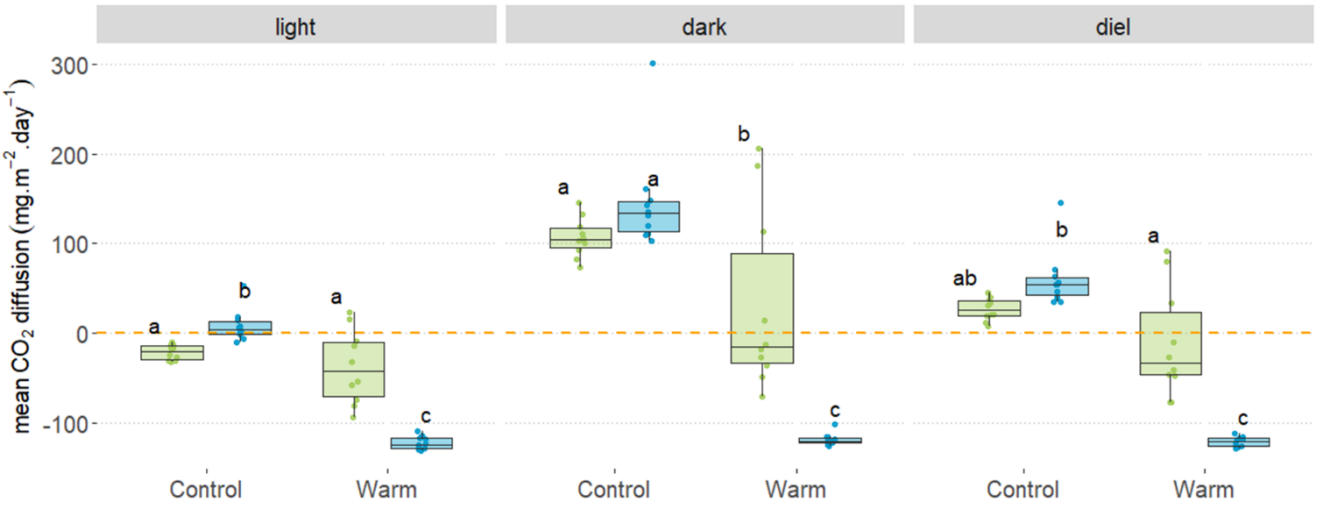

Figure 5. Mean CO_2 diffusive fluxes over the entire experimental time (in $mg.m^{-2}.day^{-1}$), between phytoplankton communities (Chlo in green and Cya in blue) and temperature conditions (control and warm). In: a) mean flux for light periods, b) mean flux for dark periods, and c) diel mean flux. The horizontal dark lines in the box-plots represent the median value, the boxes show the interquartile range with 25% and 75% percentiles, and the vertical lines indicate the distribution range. Colored dots show individual data and the letters on the top of the boxes (a, b and c) indicate the results of the pairwise comparisons after ANOVA tests.

Allocation of total carbon stock among the different biotic and abiotic components

At the end of the experiment total dissolved and sedimented carbon made up the largest carbon stocks, for chlorophytes-dominated systems at control ($p << 0.001$, $F_{4, 95}=14.01$ and $R^2=0.3$) and warm temperatures ($p << 0.001$, $F_{4, 95}=8.7$ and $R^2=0.3$), and for cyanobacteria-dominated systems also at control ($p << 0.001$, $F_{4, 95}=15.1$ and $R^2=0.4$) and warm ($p << 0.001$, $F_{4, 95}=5.8$ and $R^2=0.2$) temperatures with a negligible contribution by phytoplankton and zooplankton (Fig. 6a-b, all post-hoc values $p < 0.001$). For the cyanobacteria-dominated systems at the control temperature, carbon allocation at the dissolved inorganic portion was significantly higher than

the sedimented carbon (post-hoc value p <0.001), but even when the opposite pattern was true at the warm temperature the differences were not significant. From general patterns comparison between both phytoplankton compositions at the warm temperature condition, carbon allocation at sedimented carbon was higher for cyanobacteria than for chlorophytes systems. Meanwhile, carbon allocation in zooplankton was higher for chlorophytes than for cyanobacteria, with the opposite pattern for carbon allocation in phytoplankton.

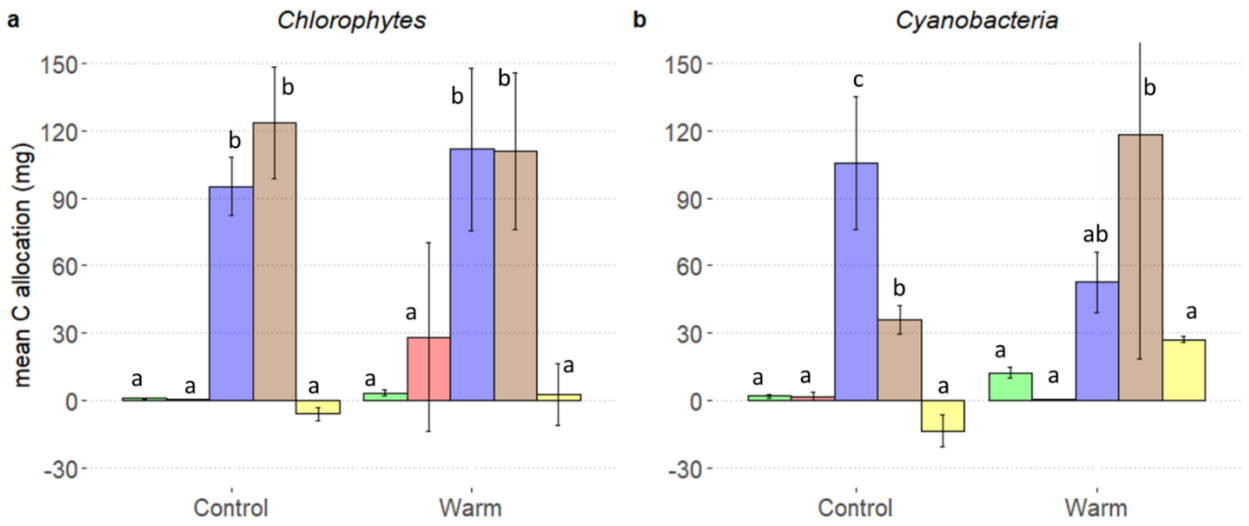

Figure 6. Mean value per treatment for the carbon allocated at each biotic and abiotic component in the mesocosms: phytoplankton in green, zooplankton in red, dissolved inorganic carbon in blue, sedimented carbon in brown and carbon gained over the experiment (here negative values mean efflux) in yellow. In a) chlorophytes-dominated and in b) cyanobacteria-dominated systems. Vertical lines represent the standard deviation and letters (a, b and c) the results of the pairwise comparisons after ANOVA tests.

Discussion

In our microcosm systems, without allochthonous carbon inputs, a clear increase in CO_2 uptake occurred under warm temperature conditions with the strongest CO_2 uptake in cyanobacteria-dominated systems. This finding supports our hypotheses that warming alters the metabolic balance in freshwater aquatic ecosystems. Warming also affected phytoplankton development, with higher biomass (as chl-a concentration) occurring under warm conditions particularly in the cyanobacteria dominated systems. Also, the strong increase in cyanobacteria biomass in the warm temperature condition, affected the zooplankton community composition resulting in a lower potential grazing capacity when cyanobacteria dominate than when chlorophytes dominate.

The changes in total biomass and phytoplankton species observed under warming for our microcosms, are in line with previous research. The increase in the relative representation of *Synechococcus* sp. observed for the cyanobacteria-dominated systems at the warm scenario, concurs with the already existing evidence that increased temperatures benefit smaller cells, as they might grow, reproduce, and utilize resources faster than organisms with larger cells (Brasil & Huszar, 2011; Callieri, 2017). In addition, the observed pattern of higher total phytoplankton biomass at the warmer temperature condition, agrees with results found at similar experimental scales (Borges Machado et al., 2019; Moresco et al., in.prep.), as well as with documented latitudinal patterns where phytoplankton total biomass showed a negative correlation with latitude (Meerhoff et al., 2012). This higher total phytoplankton biomass (assessed according to chlorophyll-a concentration) at the +4ºC compared to control temperature condition, was particularly strong in the cyanobacteria-dominated systems, suggesting a stronger effect of warming on cyanobacteria growth than on chlorophytes growth. Thereby, our results support the already documented hypothesis that cyanobacteria would profit more than chlorophytes from warmer conditions and therefore dominate in mixed phytoplankton assemblages under warmer conditions (De Senerpont Domis et al., 2007; Carey et al., 2012; Kosten et al., 2012; Lürling et al., 2018; Borges Machado et al., 2019; Moresco et al., in.prep.).

The observed difference in the zooplankton community composition and in the total biomass of Cladocera (assessed according to calculated dry weight) between the phytoplankton treatments, may be explained based on the palatability of each phytoplankton community (Ahlgren et al., 1990; DeMott, 1999; Colina et al., 2016; Li et al., 2019). A lack of palatable food could readily explain the low total biomass and low potential grazing pressure found in the cyanobacteria dominated systems. Furthermore, the presence of resting stage eggs of Cladocera, clearly evidenced the unfavourable conditions for Cladocera in the cyanobacteria-dominated systems. This also hints at a weak coupling between phytoplankton and zooplankton and a weak transfer of the assimilated carbon by the phytoplankton to the classic trophic web (Ger et al., 2014). The low biomass of Cladocera found in the chlorophyte-dominated systems at the control temperature was an unexpected result. We speculate that the high grazing pressure on the palatable phytoplankton have caused a food-limitation and induced the collapse of the zooplankton. Indeed, observations over experimental time allowed to register a much higher Cladocera abundance a few days before the end of the experiment, and chl-a in the Chlo-control treatment strongly decreased over the experiment. In addition, the high total biomass of Cladocera found in the chlorophytes-dominated systems at 23.5ºC (warm temperature condition), with an important presence of large-body size species like *D.magna*, was also in contrast to the expected pattern. We hypothesized that, even with palatable phytoplankton, this temperature would be too high for *D. magna* to grow well as a low tolerance to warm temperatures has been widely documented for large-body size Cladocera (Gillooly, 2000; Gillooly & Dodson, 2000; Mckee et al., 2002; Gyllström et al., 2005). However, evidence

of adaptation to warm conditions, and in quite short number of generations, has been also found for *Daphnia sp.* (Geerts et al., 2015).

The highest phytoplankton biomass – occurring in the cyanobacteria-dominated systems exposed to warm temperatures - translated into the strongest CO_2 uptake, confirming that the effects of warming on total phytoplankton biomass and composition affect the metabolic balance of freshwater ecosystems. Our finding regarding CO_2 uptake increases with warming, is in contrast to findings in larger scale experiments and field observations where sediments are included and a decrease in CO_2 uptake or an increase in CO_2 emissions had been linked to warming (Yvon-Durocher et al., 2010, 2011, 2017). We argue that this can be explained by the strong impact of sediment respiration -and allochthonous C sources, in the case of natural ecosystems or experimental systems with sediments- on the net CO_2 flux. Particularly, sediment respiration has been reported to account for the major proportion of respiration in freshwater shallow ecosystems (Bachmann et al., 2000; Kortelainen et al., 2006), and to also increase with warming (Gudasz et al., 2010, 2015), which might likely overrule a potential increase in CO_2 uptake due to increases in phytoplankton primary production. The calculated diel emission in the control treatments is puzzling. As, at the end of the experiment, the phytoplankton biomass in the cyanobacteria-dominated systems was significantly higher than in the chlorophytes-dominates systems, we would expect CO_2 uptake or at least less efflux in the former (similarly than at the warm temperature condition). Although we cannot rule out that methodological issues impacted the calculated diel flux, as the flux calculations are, for instance, very sensitive for pH where small discrepancies in pH measurements can already strongly impact calculated fluxes. Still, the pattern remains intriguing and merits further study looking closer into the DIC pool and directly measuring the fluxes. However, we can hypothesize that given that the phytoplankton biomass decreased during the study in the control systems, the relatively low pH – due to the relatively low phytoplankton biomass and related primary production - sustained above atmosphere CO_2 partial pressures in the water leading to an overall CO_2 efflux likely fuelled by the large inorganic carbon pool (which is the largest C-stock in the systems, see below).

The analyses of the carbon stocks contained in the different biotic and abiotic components at the end of the experiment indicated that the great majority of the carbon was allocated between dissolved inorganic carbon and, mainly for cyanobacteria at warm temperatures, in sedimented carbon. Carbon allocated into the biomasses of phytoplankton of zooplankton represented a minor proportion. The suspended and sedimented organic carbon, may - in time - be mineralized into CO_2. Alternatively, it may accumulate on the bottom and if not decomposed to CO_2, or CH_4– due to the reducing conditions that often occur in sediments – may be buried and translated into a carbon sink. However, more processes than the tested in our experiment can play a relevant role in the final net carbon fluxes and net role (as a sink or source of carbon) in natural shallow freshwaters. For example, at highly productive ecosystems, where high carbon sedimentation occurs, a large amount of the fixed carbon may be ultimately mineralized under anaerobic conditions and released as CH_4 (Yan et al., 2017, 2019; Beaulieu et al., 2019;

Grasset et al., 2019, 2020), which would be enhanced under warmer temperatures (Yvon-Durocher et al., 2011, 2017; Aben et al., 2017). In addition, recently CH_4 oxic production by cyanobacteria was also postulated as a relevant potential source of CH_4 (Bižić et al., 2020).

Small scale micro and mesocosm experiments always represent a compromise between the capability of control and replicable conditions and an oversimplification of complex real ecosystems (Stewart et al., 2013). The results obtained from small scale microcosm, should indeed been considered with caution when conclusions tempt to be extrapolated to natural ecosystems. Despite such limitations, we consider that our experiment contributes to stress out that the synergistic effects of shifts in plankton community composition and warming might promote clear shifts in the metabolic balance in shallow freshwater ecosystems. In our experimental microcosms, purely pelagic and without external carbon inputs neither nutrients and light limitation, warming boosted phytoplankton growth with resulting net CO_2 uptake. Likely due to better adaptation to eutrophic and warming, and/or because a lower palatability for zooplankton, total biomass increased more in cyanobacteria-dominated than in chlorophytes-dominated systems, with also strongest CO_2 uptake (Fig.7). However, the fixed carbon was greatly sedimented and thereby likely at least in part unavailable for the classic food web (Fig. 7), representing a potential source for mineralization into CO_2 and CH_4. In the context of natural ecosystems, our results support that planktonic communities in warmer scenarios will be dominated by cyanobacteria, and stress that even under high primary production a high organic matter availability might boost CO_2 and CH_4 emissions, when pelagic and benthic processes been considered altogether.

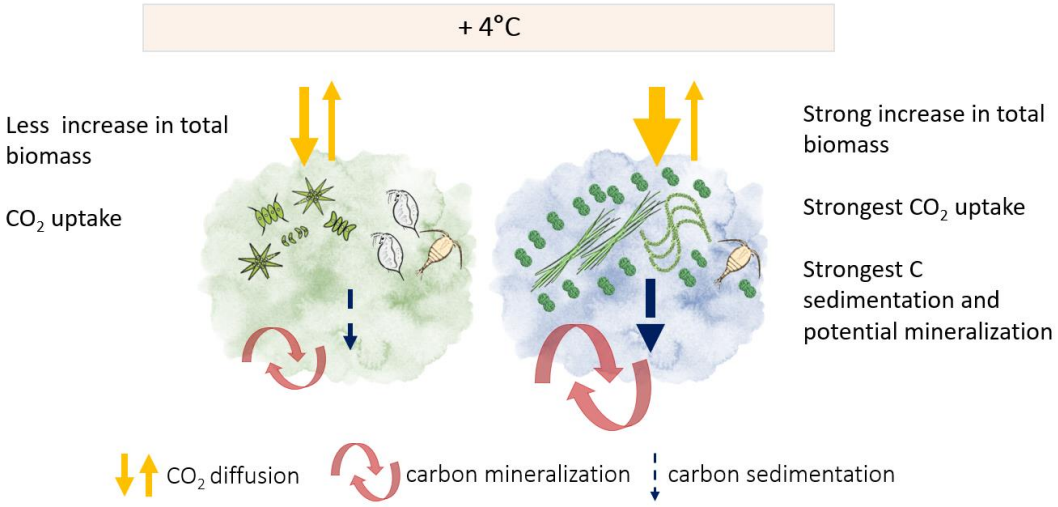

Figure 7. Summary of the main results for chlorophytes-dominated communities (in green background) versus cyanobacteria-dominated communities (in blue background) under eutrophic and warmer scenarios. The size of the arrows is proportional to the expected amount of associated carbon. And their direction indicates either influx or efflux of CO_2

Acknowledgements

We would like to acknowledge Programa para el Desarrollo de las Ciencias Básicas (PEDECIBA Geociencias, Uruguay) and Agencia Nacional de Investigación e Innovación (ANII, Uruguay) for their support to MC. To the International Society of Limnology (SIL) for providing the funds to cover this experiment through the Tonolli Award programme. MM is supported by PEDECIBA and ANII (Uruguay). We would also like to include a special thanks to everyone who contributed in some way with this experiment: Lucía Cabrera how analyzed TIC samples, Margeny Barros and Clementina Calvo for helping with the experimental set up, to Geovanni Moresco for helping with phytoplankton identification and to Alberto Perez for setting up the CO_2 sensors.

SUPPLEMENTARY INFORMATION CHAPTER 4

Materials and Methods

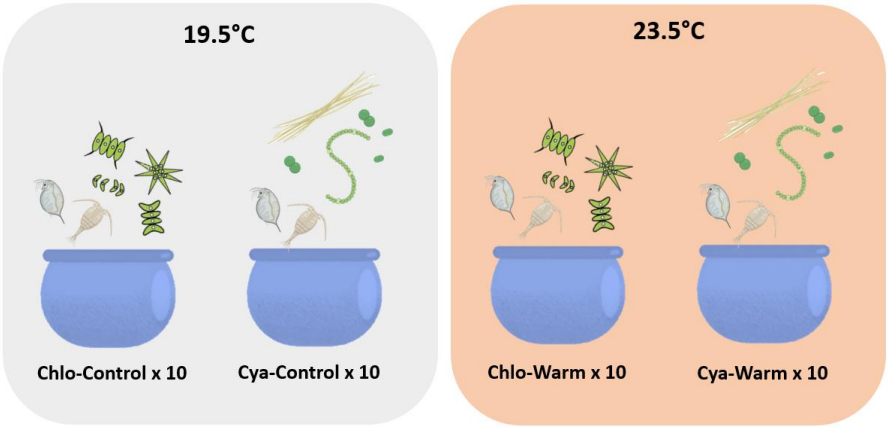

Figure S1. Scheme of the experimental treatments with the two phytoplankton community compositions, chlorophyte dominance versus cyanobacteria dominance (Chlo and Cya, respectively), and the two temperature scenarios, 19.5°C and 23.5°C (Control-C and Warm-W, respectively).

Equations for CO_2 diffusive flux estimations based on pH and water temperature

Diffusive flux of CO_2 estimated based on the difference between water and air gas concentrations (Cole & Caraco, 1998):

$$F = KL \cdot ß \cdot ((pCO_2w - pCO_2a) \times 44)$$

Where:

pCO_2a: is the CO_2 partial pressure in the air inside each climatized room. Assumed constant during the experimental time and extracted from the registered values by automatic CO_2 loggers (K33 ELG, SenseAir, Sweden), with 550ppm and 750ppm for 19.5°C and 23.5°C temperature conditions, respectively. According to ideal gas law (PV=nRT), with constant temperature and atmospheric pressure equal to 1atm, CO_2 concentration inside the climatized room were estimated as 20.8 µmol.L^{-1} and 26.4 µmol.L^{-1}.

pCO_2w: is the concentration of dissolved CO_2 in the water in µmol.L^{-1} and extrapolated from the expected carbonic balance according to the equations presented below (Cole J. J. et al., 1994; Kling et al., 1992).

$\mathrm{pK1} = 0.0000009 \times \mathrm{T}^3 + 0.0002 \times \mathrm{T}^2 - 0.0134 \times \mathrm{T} + 6.579$	with water temperature (T) in Celsius
$\mathrm{K1} = 10^{-\mathrm{pK1}}$	Cte.
$\mathrm{pK2} = 0.000001 \times \mathrm{T}^3 + 0.00006 \times \mathrm{T}^2 - 0.014 \times \mathrm{T} + 10.625$	with water temperature (T) in Celsius
$\mathrm{K2} = 10^{-\mathrm{pK2}}$	Cte.
$[\mathrm{H}^+] = 10^{-\mathrm{pH}}$	concentration of H+ in µmol.L^{-1} according to water pH
$\mathrm{pKh} = 1.12 + 0.014 \times \mathrm{T}$	with water temperature (T) in Celsius
$\mathrm{Kh} = 10^{-\mathrm{pKh}}$	Cte.
$\mathrm{alpha0} = 1 + \mathrm{K1}/[\mathrm{H}^+] + \mathrm{K1} \times \mathrm{K2}/([\mathrm{H}^+]^2)^{-1}$	Cte.
$\mathrm{CO_2aq} = \mathrm{DIC} \times \mathrm{alpha0}$	concentration of dissolved carbon dioxide (CO_2aq) directly measured for initial and final times and extrapolated according to pH and water temperature for in between dates, in µmol.L^{-1}

The pCO_2 was multiplied: by 10^{-6} to convert from µmol.L^{-1} to mol.L^{-1}, by the molecular weight of CO_2 (44gr.mol^{-1}) to convert from mol to gr, by 1000 to convert gr to mg and by 1/0.001 to convert L^{-1} to m^{-3}.

KL: is the gas transfer velocity, in m.d^{-1}. Was empirically estimated, at same aquarium volume that for the experimental microcosms and for the both experimental temperatures, from the dissolved O_2 concentration (mg.L^{-1}) increase in deoxygenated water (Tribe et al., 1995). The flux of O_2 between the water and the air at a given time (t_i, in hours) depends on the height of the water column (H, in m), the saturation concentration (Cs) and the current concentration (C_i) according to:

$$\mathrm{dO_2}/\mathrm{dt} = \mathrm{KL}/\mathrm{H} \times (\mathrm{Cs} - \mathrm{Ci})$$

The integral gives:

$$\mathrm{In}\,(\mathrm{Cs} - \mathrm{Co}/\mathrm{Cs} - \mathrm{Ci}) = \mathrm{KL}/\mathrm{H} \times \mathrm{t}$$ where Co is the concentration at t=0

The slope of the regression between the left term in the above equation versus time, and multiplied by H (0.11m), gives KL in m.hrs^{-1}. In order to obtain KL in m.day^{-1}, the obtained value was multiplied by 24.

Saturation concentration for O_2 was estimated as:

$$\mathrm{CsO_2} = 14.652 - 0.41022 \times \mathrm{T} + 0.007991 \times \mathrm{T}^2 - 7.7774 \times 0.00001 \times \mathrm{T}^3)$$

KL for CO_2 was extrapolated from the ratio between the Schmidt numbers for O_2 and CO_2, both corrected by temperature (Cole & Caraco, 1998), and considering no wind action (n=0.66) (IHA, 2010) according to:

$$KL_{CO_2}/KL_{O_2} = (Sc_{CO_2}/Sc_{O_2})^n$$

Where:

$Sc_{O_2} = -(1800.6 - 120.1 \times T + 3.7818 \times T^2 - 0.047608 \times T^3)$ with water temperature (T) in Celsius

$Sc_{CO_2} = 1911.2 - 118.11 \times T + 3.4527 \times T^2 - 0.04132 \times T^3$ with water temperature (T) in Celsius

ß is the chemical enhancement coefficient (dimensionless) that accounts to the reaction of CO_2aq with OH^- at high water pH conditions (pH > 9) (Bade & Cole, 2006), and it was estimated using the equations below:

$r_{CO_2} = e^{1246.98+(-6.19 \times 10^4)/T-183 \times \log(T)}$ with water temperature (T) in Kelvin. Units s^{-1}

$r_{OH^-} = e^{-930.13+(3.1 \times 10^4)/T-140.9 \times \log(T)}$ with water temperature (T) in Kelvin. Units $mol.dm^{-3}.s^{-1}$

Dw = (999.83952 + 16.945176 x (T /1.00024) - 7.9870401 x (10^{-3}) x ((T /1.00024) ^{2}) - 46.170461 x (10^{-6}) x (T /1.00024) ^{3} + 105.56302 x 10^{-9} x ((T /1.00024)^4) - 280.54253 x 10^{-12} x (T/1.00024)^5) / (1 + 16.87985 x 10^{-3} x (T/1.00024)) Water density in $gr.cm^{-3}$, with water temperature (T) in Celsius

$x0 = -0.864671$ Ctes.

$x1 = 8659.19$

$x2 = -22786.2$

Q = ((Dw/1000)/1) x $e^{(x0+x1 \times ((T)^{-1})}$ + x2 x ((T)-^{2}) x (Dw/1000)$^{2/3}$) with water temperature (T) in Kelvin

$y0 = 0.61415$ Ctes.

$y1 = 48251.33$

$y2 = -67707.93$

$y3 = 10102100$

$pKGw = y0 + y1 \times (T^{-1}) + y2 \times (T^{-2}) + y3 \times (T^{-3})$ with water temperature (T) in Kelvin

$n = 6$ Ctes.

$b0 = 0.642044$

$b1 = -56.8534$

$b2 = -0.375754$

pkw = (-2 x n x (log_{10}(1+Q) -(Q/(Q+1)) x (Dw/1000) x (b0+b1 x (T^{-1}) + b2 x (Dw/1000)))) + pkGW + 2 x log_{10}((1 x 18.015286)/1000)	with water temperature (T) in Kelvin
$Kw = 10^{-pKw}$	Cte.
$[OH^-] = Kw/10^{-pH}$	OH^- concentration in $mol.L^{-1}$
$R = rCO_2 + rOH^- \times [OH^-]$	Cte.
K1 = $10^{-(6320.81 / T-126.3405 + 19.568 \times ln (T))}$	in $mol.L^{-1}$ and with water temperature (T) in Kelvin
K2 = $10^{-(5143.69 / T-90.1833 + 14.613 \times ln (T))}$	in $mol.L^{-1}$ and with water temperature (T) in Kelvin
$T = ((([H^+]^2/K1 \times K2 + K1 \times [H^+]) + 1$	Dimensionless, with K1 and K2 in $mol.L^{-1}$
$D = 0.05019 \times e^{(-19510/8.314 \times T)}$	with water temperature (T) in Kelvin
K = ((1.83) / (599.42/ (1911.1-118.11 x (T) + 3.4527 x (T^2)-0.04132 x (T^3)) $^{-0.5}$))	with water temperature (T) in Celsius
$Z = (D \times 3600)/K$	dimensionless
ß = T/((T-1) + (tanh((R x T x D^{-1})$^{0.5}$ x Z)/((R x T x D^{-1}) $^{0.5}$ x R)))	dimensionless

<u>Equations for estimating total carbon allocation among the different biotic and abiotic components</u>

All the parameters considered were expressed in mgC, and were extrapolated for the total experimental water volume (total aquarium volume, 3.5L) or experimental water surface (water surface in contact with the air, ~0.04m^{-2}) in the case of the carbon exchange (dC).

Carbon content in phytoplankton was estimated by assuming C:Chl ratio ~ 30

$$C \text{ in phyto.} = Chl - a \times 0.001 \times 30 \times 3.5$$

Where chlorophyll-a (Chl-a) was multiplied by 0.001 to convert from µg to mg/L, 30 to convert from Chl-a to C and by 3.5L to convert from 1L to the total water volume.

Carbon content in zooplankton was estimated by assuming that 45% of the dry weight (DW in $mg.L^{-1}$) corresponded to C

$$C \text{ in zoo.} = DW \times 0.45 \times 3.5$$

Where zooplankton DW was multiplied by 0.45 to convert DW into C and by 3.5L to convert from 1L to the total water volume.

Total inorganic carbon dissolved in the water, was assessed from DIC directly estimated for initial and final times:

$$\text{dissolved C} = \text{DIC} \times 0.001 \times 12$$

Where DIC was multiplied by 1e-6 to transform from µmol to mol.L^{-1}, by 12 to transform to g.L^{-1} and by 1000 to transform into mg.L^{-1}.

The total sedimented carbon over the experiment was assessed by assuming that 80% of the Sed. PM was C

$$\text{Sed. C} = \text{Sed. PM} \times 1000 \times (\pi \times (0.06)^2) \times 0.8$$

Where 1000 was used to convert from g to mg, and 0.06m was the radio of the aquarium bottom surface.

The total carbon exchange with the atmosphere over the experiment (ΔC) was assessed as the total diel flux in mgCO_2.m^2 corrected by the total water surface in contact with the air

$$\Delta C = \text{diel } CO_2 \text{ diffusion} \times (\pi \times (0.1175)^2) \times 0.273$$

Where 0.1175m was the radio of the aquarium upper surface and 0.273 correspond to the 27.3% of the molecular weight in CO_2. As the diel CO_2 diffusion has negative sign when considering exchange with the atmosphere, we used the absolute value to account amount of carbon gained by the system.

Results

Table S1. Main effects of factors: time (in days), treatment (treat.: Cya-Control, Cya-Warm, Chlo-Control and Chlo-Warm), period (light versus dark hours) and their interactions, on the different physico-chemical parameters: water temperature (wTemp., in °C), pH, dissolved oxygen (DO, in mg.L^{-1}), total phosphorous (TP, in µg.L^{-1}), total nitrogen (TN, in µg.L^{-1}) and dissolved nutrients (PO_4^{3-}, NO_3^- and NH_4^+, all in in µg.L^{-1}). Water temperature, pH and dissolved O_2 were sampled with every 3 days frequency, total nutrients at initial, middle and final times, and dissolved nutrients at initial and final times. For DO and TN a log transformation was applied, and for TN one outlier (according to Cook´s distance) was removed.

		time	treat	period	time*treat	time*period	treat*period	time*treat*period	% exp. dev.
wTemp.	**F**	329.7	4824.3	0.8	256.4	12.6	5.3	16.0	96.9
	df	518	515	514	511	510	507	504	
	p	***	***	ns	***	ns	**	***	

pH	**F**	1.4	91.9	5.8	18.5	161.1	6.1	2.9	51.1
	df	518	515	514	511	510	507	504	
	p	ns	***	*	***	***	***	*	
DO	**F**	3.2	132.1	107.9	49.1	63.5	14.0	1.8	60.3
	df	518	515	514	511	510	507	504	
	p	ns	***	***	***	***	***	ns	
TP	**F**	286.3	3.2	-	16.4	-	-	-	73.1
	df	133	130	-	127	-	-	-	
	p	***	*	-	***	-	-	-	
TN	**F**	7.02	68.4	-	32.04	-	-	-	71
	df	132	129	-	126	-	-	-	
	p	**	***	-	***	-	-	-	
PO_4^{3-}	**F**	164.4	15.3	-	63.5	-	-	-	84.8
	df	78	75	-	72	-	-	-	
	p	***	***	-	***	-	-	-	
NO_3^-	**F**	62.01	5.3	-	7.4	-	-	-	58.2
	df	78	75	-	72	-	-	-	
	p	***	**	-	***	-	-	-	
NH_4^+	**F**	418.2	10.7	-	26.6	-	-	-	89.7
	df	63	60	-	58	-	-	-	
	p	***	***	-	***	-	-	-	

Statistics extracted from the ANOVA table form the GLMs: F-values, degrees of freedom (d.f.) and p-values: ns: $p>0.05$, *$p \leq 0.05$, **$p< 0.01$, *** $p< 0.001$.

% of explained deviance (% exp. dev.) from the general GLM.

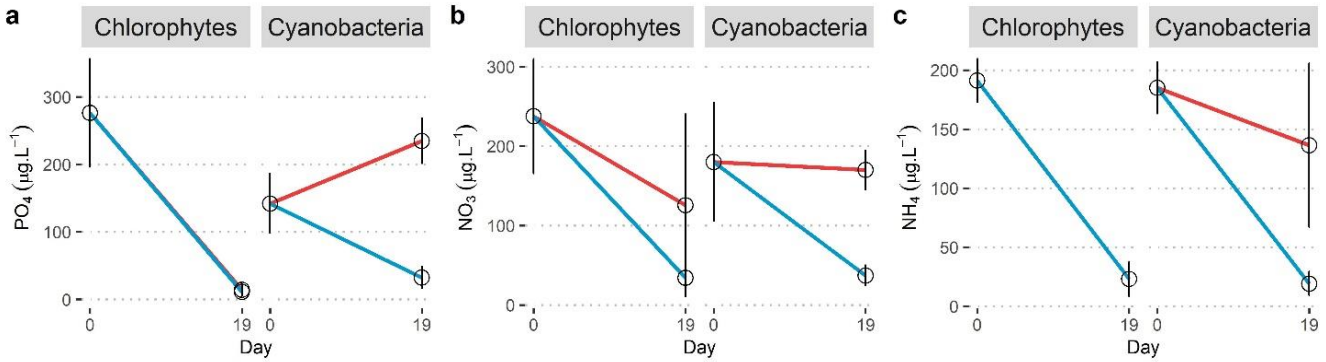

Figure S2. Comparison between phytoplankton communities (chlorophytes versus cyanobacteria) and between temperature conditions (control in sky-blue warm in red) for the change over time for the concentration of dissolved nutrients: a) PO_4^{3-}, c) NO_3^- and d) NH_4^+. Each dot represents the mean value for the 10 replicates and vertical lines the standard deviation.

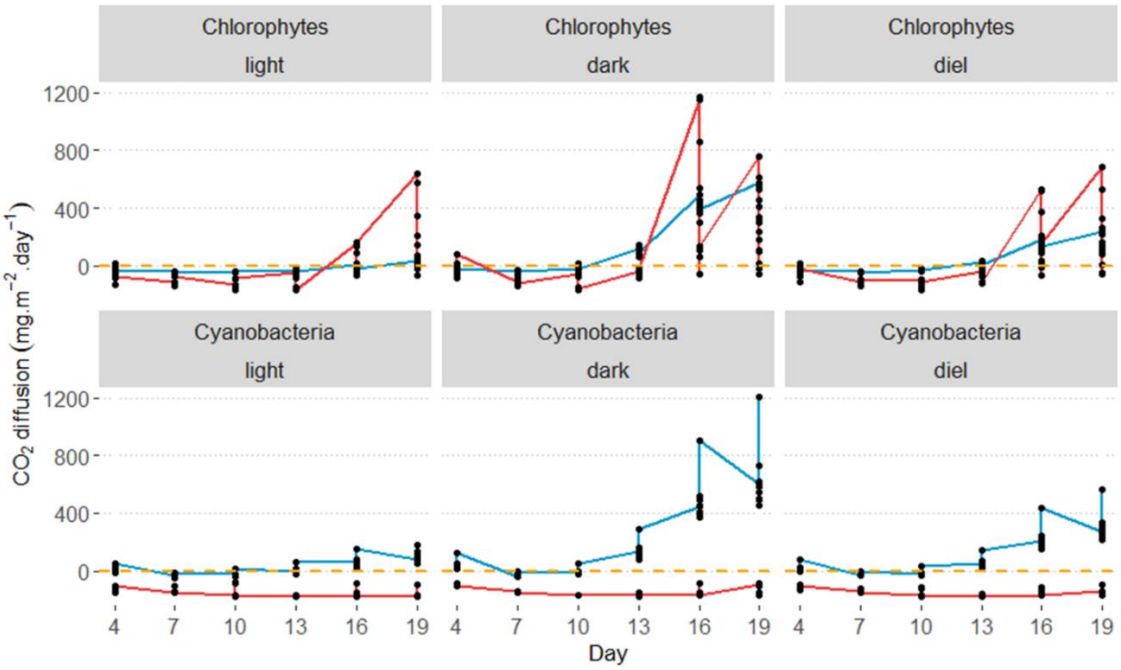

Figure S3. Diffusive CO_2 flux (in $mg.m^{-2}.day^{-1}$) versus time (in days), over the 19 days of the experiment starting at day 4. Chlorophytes-dominated systems are shown in the upper panel and cyanobacteria-dominated systems in the bottom panel. Data for control temperature condition are shown in sky-blue and data for warm temperature condition in red. Fluxes for light and dark hours, and the diel flux estimation are shown in independent columns from left to right. For dark and diel CO_2 diffusion, there are no data on the first sampling date as no dark measurements were conducted on day 1.

CHAPTER 5

GENERAL DISCUSSION

Throughout this thesis, different methodological approaches, with different spatial and temporal scales, were applied to contribute to the understanding of how the combination of physical, chemical, and biological factors drive carbon fluxes (CO_2 and CH_4) in shallow lakes.

Whole ecosystem fluxes of CO_2 and CH_4 in natural subtropical shallow lakes with distinct dominant regimes of primary producers, contrasting in features such as type (i.e., submerged macrophytes versus phytoplankton) and total biomass (i.e., from high to extremely low) were studied and estimated (ecosystem scale, Chapter 2). Controlled indoor experiments were implemented to analyze CO_2 and CH_4 fluxes as driven by processes involving fish and benthic macroinvertebrates, both at the water-sediment interface and at the water column (mesocosm scale, Chapter 3). Controlled experiments were also used to analyze processes driving the balance between CO_2 uptake and efflux in planktonic communities (microcosm scale, Chapter 4). In both experiments, carbon fluxes were compared between community configurations that can be found at low or moderate nutrient levels versus high nutrient levels (such as fish communities with a major role of planktivorous fish and phytoplankton communities dominated by green algae, versus fish communities mainly composed of benthivorous fish, and phytoplankton communities dominated by cyanobacteria, respectively), as a proxy of contrasting levels of anthropogenic impact.

The results extracted from the studies conducted at different spatial and temporal scales support the main hypothesis of this thesis, by indicating that the general regime in shallow lakes, given by the type and total biomass of the dominant primary producer (such as submerged macrophytes, phytoplankton, or extremely low primary production) and the typically distinct structure of the associated biological communities, strongly condition in-lake carbon processing and thereby the total CO_2 and CH_4 fluxes. This occurs likely through the interplay of abiotic factors and biological factors, such as trophic and non-trophic biotic interactions, as discussed below.

Effects of abiotic factors on carbon fluxes

Several abiotic characteristics of the environment either promote or hinder conditions for the production of CO_2 and CH_4. In this section, some of them will briefly described in connection to the findings in the thesis, namely temperature, organic matter quality and quantity, and oxygen availability.

The clear increase in the total biomass of phytoplankton and in the CO_2 uptake found under a +4°C warmer scenario (Chapter 4) is in agreement with the notion that temperature directly impacts the rate of all metabolic processes (such as primary production, respiration, and decomposition), with important ecological consequences (Allen et al., 2005). Besides, in the overall ecosystem analysis we also found a clear effect of temperature on CH_4 emissions, particularly in the clear-vegetated lake (Chapter 2) with higher emissions (via both diffusion and ebullition) of CH_4 in spring and summer than in winter season. A similar pattern was found for

CO_2 fluxes at the littoral zone in this clear-vegetated lake, with higher CO_2 efflux in summer compared to winter. Meanwhile, in the densely vegetated pelagic zone, less CO_2 uptake occurred in the warmest season. These patterns on CO_2 fluxes may be the result of a stronger increase in ecosystem respiration compared to the increase in gross primary production with warming, as it has been previously documented at different experimental scales (Yvon-Durocher et al., 2010, 2011, 2017).

The slightly different results found in the lab experiments, may reflect methodological limitations given by logistic constrains. For instance, the absence of sediments in our microcosm experiment (Chapter 4) might explain the predominant CO_2 uptake with warming, as the microbial respiration of accumulated organic matter at the sediment level has been frequently reported to represent the major proportion of the ecosystem respiration in shallow freshwaters, and to drive the ecosystem CO_2 fluxes (Bachmann et al., 2000; Kortelainen et al., 2006). However, indirect effects of temperature, such as several changes in the structure of biological communities and the reinforcement of eutrophication manifestations (e.g., Meerhoff et al., 2022), have been experimentally identified as having a stronger impact on CO_2 and CH_4 fluxes than the direct warming effects on metabolic rates (Davidson et al., 2015). Results obtained along this thesis agree with this, as discussed in following sections in this chapter.

Organic matter (OM) represents the substrate for CO_2 and CH_4 production. Our findings suggest that, both organic matter quality and quantity may affect total carbon emissions. Primary producers biomass (i.e., macrophytes and phytoplankton) is known to be an important precursor for CH_4 production (Xing et al., 2006; West et al., 2012, 2015; Grasset et al., 2019; Bodmer et al., 2021). In the field study (Chapter 2), the quality of organic matter provided by the diverse plant community composition in the littoral zone of the clear-vegetated lake (i.e., with different life-forms including free-floating, emergent, and submerged macrophytes) most likely contributed to fueling total carbon emissions. Particularly, all the predominant species that were found in the littoral zone of the clear-vegetated lake (i.e., *Pontederia crassipes, Typha* sp., and *Ceratophyllum* sp.) have been experimentally found to fuel CH_4 production (Grasset et al., 2019). In addition, we also found relevant CH_4 emissions in the phytoplankton-turbid ecosystems (Chapter 2). The comparison among lakes, in the whole ecosystem analysis (Chapter 2), showed higher total carbon emissions (CO_2 and CH_4) in the two most productive ecosystems, i.e., the clear-vegetated and the phytoplankton turbid lakes, than in the least productive ecosystem i.e., the sediment-turbid lake. With low autochthonous productivity, carbon processing in the sediment-turbid lake should expectedly be mainly fueled by terrestrial inputs, and allochthonous carbon has been characterized as less labile than autochthonous carbon (Grasset et al., 2018). Besides its origin, also a likely low amount of organic matter (although not tested) seemed to determine a poor substrate for mineralization in the sediment-turbid lake. This translated into moderate CO_2 efflux and into dissolved CH_4 undersaturation at surface waters with CH_4 ecosystem uptake, which seems not to be a common phenomenon as has not been reported in the overview papers so far (Bastviken et al., 2011; Holgerson & Raymond, 2016).

Among abiotic factors, the availability of dissolved oxygen (O_2), likely through its effects on pathways and rates of organic matter mineralization, may play a major role in the carbon processing within aquatic ecosystems. Water column processes linked to the availability of dissolved O_2 that could affect CH_4 fluxes, such as oxidation (Bastviken et al., 2004, 2008) or CH_4 production under oxic conditions (Donis et al., 2017; Bizic et al., 2018; Günthel et al., 2019), were less clearly evidenced in this thesis. However, processes at the water-sediment interface showed strong effects of dissolved O_2 availability on CO_2 and CH_4 fluxes. In the mesocosm experiment (Chapter 3), the presence of tubifex worms supported a well oxygenated sediment-water interface, where oxic organic matter mineralization translated into higher CO_2 production and emissions than in the absence of tubifex worms. High respiration rates and CO_2 emissions in well-oxygenated sediments, due to benthic macroinvertebrates bioirrigation effects, have been previously documented in experimental closed sediment cores (Baranov et al., 2016). On the contrary, in the mesocosms without tubifex worms anoxic organic matter mineralization translated into higher CH_4 emissions than in the mesocosms with tubifex worms, likely due to an increase in CH_4 production and a reduction in CH_4 oxidation (Bastviken et al., 2004, 2008).

Effects of non-trophic interactions on carbon fluxes

As briefly seen above, several processes related to biological activity create or alter conditions for the production or consumption of CO_2 and CH_4. Through their physiology and behavior, living organisms can modify their environment, and the abiotic factors that drive carbon processing, for example, by increasing organic matter, consuming or producing O_2, and even changing temperature dynamics. In this thesis, macrophytes, benthic macroinvertebrates, and fish were shown to impact CO_2 and CH_4 fluxes through non-trophic effects on their immediate environment.

The low total CH_4 emissions commonly reported in the presence of dense submerged macrophyte beds, which was actually observed in the pelagic zone of the clear-vegetated lake in Uruguay (Chapter 2), likely occurs as a consequence of a well-oxygenated water column due to plant photosynthesis (Yoshida et al., 2014), and a well-oxygenated water-sediment interface due to roots' oxygen loss (ROL) effect (Sorrell et al., 2002; Sorrell & Downes, 2004; Bodmer et al., 2021). In contrast, the highest total CH_4 emissions occurred in the phytoplankton-turbid lake (Chapter 2). This is in line with studies where high biomasses of phytoplankton, usually with cyanobacteria as the dominant taxonomic group, promote anoxic conditions and enhance total CH_4 emissions (Yan et al., 2017; Beaulieu et al., 2019; Yang et al., 2019).

Besides, in the mesocosm experiment described in Chapter 3, the penetration depth of O_2 into the water-sediment interface was strongly affected by the activity of benthic macrofauna, through the bioirrigation of tubifex worms on foraging galleries. Tubifex, which live head-down partially buried, pump large volumes of oxygen into the sediments through ingesting sediment

particles and excreting them as fecal pellets at the surface (Palmer, 1968; Lagauzère et al., 2009; Hölker et al., 2015). This effect of tubifex worms on water-sediment interface oxygenation strongly affected the total carbon fluxes in our experiment: the deepest the O_2 penetration, the highest the CO_2 efflux and the lowest the CH_4 ebullition. Similar effects regarding CO_2 and CH_4 fluxes, as a function of the availability of O_2 in freshwater sediments, have been previously reported for other macroinvertebrates, such as larvae of Diptera and Ephemeroptera (Leal et al., 2007; Baranov et al., 2016). On the contrary, a role of facilitators in sediment CH_4 release and in enhancing total CH_4 emissions has been reported for *Chaoborus* larvae and some Polychaeta (Figueiredo-Barros et al., 2009; McGinnis et al., 2017). These contradictory results might be the consequence of different interactions of macroinvertebrate groups with the sediment environment. *Chaoborus* larvae, for instance, typically perform diel vertical migration along the water column and the water-sediment interface, using CH_4 bubbles to facilitate their migration in the water column in addition to physically disturbing the sediments and thus promoting the release of more CH_4 bubbles (McGinnis et al., 2017).

Similar to *Chaoborus*', bioturbation by benthivorous fish implies a direct physical disturbance on the water-sediment interface. From the mesocosm experiment described in Chapter 3, it seems that the net effects of fish bioturbation on CO_2 and CH_4 fluxes depended on the bioturbation pressure (i.e., the frequency and intensity of the disturbance). A short-time increase in CH_4 ebullition was found at moderate bioturbation pressure by carp (moderate due to small body-size of the individuals used and a low frequency of exposure). However, large body-sized fish, disturbing sediments with high frequency (as in the mesocosm experiment conducted by Oliveira Junior et al. 2019), could promote oxygenation of the water-sediment interface and thus similar effects on CO_2 and CH_4 fluxes than those previously mentioned for tubifex. Coinciding with the results presented in Chapter 3, other experimental studies (Booth et al., 2021) have also shown how increasing bioturbation frequency translates into increasing aerobic conditions in the sediments and into increasing CO_2 emissions, with an inverted U-shaped curve in CH_4 emissions. In the experiment of Booth et al. (2021), for instance, different frequencies of bioturbation were simulated by mechanical disturbance of sediments. In our experiment using live carps and analyzing benthic macroinvertebrate effects and trophic interactions between some components of the aquatic fauna, we arrived at similar results.

Effects of trophic interactions on carbon fluxes

Trophic interactions are also highlighted as key drivers of carbon fluxes in shallow freshwaters (Hansson et al., 2012; Devlin et al., 2015; Grasset et al., 2020). In this thesis, we found clear evidence on how trophic interactions in the pelagic (Chapters 3 and 4) and benthic (Chapter 3) habitats, directly or indirectly -through affecting the abiotic environment, translated into different CO_2 and CH_4 fluxes.

A clear predation pressure effect of fish upon zooplankton was evidenced in the mesocosm experiment (Chapter 3), with the almost absence of *Daphnia* spp. in the treatments where fish

were permanently present. However, the consequent release of zooplankton grazing upon phytoplankton did not translate into higher phytoplankton total biomass nor higher CO_2 uptake. In contrast, bottom-up effects on zooplankton composition were observed between palatable (chlorophyte-dominated) versus unpalatable (cyanobacteria-dominated) phytoplankton treatments in the microcosm experimental scale (Chapter 4). Despite the fact that at the +4°C treatment both experimental phytoplankton communities increased their total biomass, the increase was two-fold higher in the cyanobacterial dominated regime than in the chlorophyte-dominated regime, which also translated into a significantly stronger CO_2 uptake in the former. The higher increase in cyanobacterial biomass can be explained due to the typically low grazing pressure by zooplankton on cyanobacteria, as well as due to the negative impacts of cyanobacteria on cladocerans (e.g., evidenced in our experiment by the presence of resting eggs), in agreement with previous research (Ahlgren et al., 1990; DeMott, 1999; Colina et al., 2016).

In agreement with our hypothesis for the mesocosm experimental scale (Chapter 3), pelagic trophic cascading effects of zooplanktivorous fish on zooplankton (shown by the almost complete absence of *Daphnia* spp. with fish presence), led to higher abundances of methane-oxidizing bacteria (MOB) in the water column. Although previous works have found a decrease on CH_4 diffusion due to pelagic trophic cascade effects upon zooplankton (Devlin et al., 2015), likely by indirectly increasing CH_4 oxidation in the water column, this was not evidenced in our experiment. This may have occurred due to the shallow water column in the mesocosms and thus a too-short gas residence time, not allowing for the oxidation of dissolved CH_4 in enough proportion as to substantially affect CH_4 diffusion. In contrast, in the same experiment, the consequences on carbon fluxes of fish trophic activity at the benthic habitat were far more clearly evidenced. Fish predation on tubifex worms hampered sediment oxygenation, reducing CO_2 emissions but enhancing CH_4 emissions.

At the mesocosm experimental scale (Chapter 3), the combined analyses of pelagic and benthic processes allowed us to highlight the coupling between benthic and pelagic habitats and its relevant impact on carbon processing and fluxes. Both fish species, i.e., carp and sticklebacks (mostly benthivores and mostly zooplanktivores, respectively) effectively promoted the above-described pelagic trophic cascading effects, as well as controlled the development of tubifex worms at the water-sediment interface. This benthic-pelagic coupling effect on CO_2 and CH_4 fluxes, point out the relevance of integrating processes between the different habitats in shallow freshwaters ecosystems to properly understand their contributions to the carbon cycle.

Effects of the overall ecosystem regime on carbon fluxes

The overall ecosystem analysis and the meso and microcosm experiments conducted in this thesis provide evidence regarding how the interplay between different components of the abiotic environment and the biological communities affect CO_2 and CH_4 fluxes in shallow

freshwaters. Added to this, different results from this thesis highlight the fundamental role of the coupling between benthic, pelagic, and littoral habitats on carbon fluxes in shallow freshwater.

We found clearly contrasting patterns in CO_2 and CH_4 fluxes between the submerged macrophyte-dominated conditions (particularly the non-littoral or pelagic zone of the clear-vegetated lake, which was covered by submerged plants) and the phytoplankton dominated regimes (i.e., the phytoplankton-turbid lake). These findings highlight that a shift in the composition of such key biological communities and on the general functioning of shallow lakes as expected with eutrophication, likely enhance total carbon emissions (of CO_2 and CH_4). This has been reported by a variety of recent studies conducted for natural ecosystems and in artificial systems at different experimental scales (Xing et al., 2006; Davidson et al., 2015; Jeppesen et al., 2016; Yan et al., 2017; Beaulieu et al., 2019; Yang et al., 2019; Grasset et al., 2020). The low total CH_4 emissions and the occurrence of CO_2 uptake in the pelagic zone of the clear-vegetated lake support the hypothesis that a well-developed community of submerged macrophytes may decrease total carbon emissions from shallow freshwaters (Huss & Wehr, 2004; Xing et al., 2006; Kosten et al., 2010; Natchimuthu et al., 2014; Jeppesen et al., 2016). In contrast, net CO_2 efflux and high CH_4 emissions were found in the phytoplankton-turbid lake (Chapter 2), confirming our hypothesis.

The above-described patterns, linked to different dominant primary producers, can be modified by bioturbation of benthivorous fish or by the bioirrigation by benthic macroinvertebrates. In line with our results, we can hypothesize that in submerged macrophytes-dominated lakes and without significant densities of benthivorous fish that could promote plant uprooting and deplete bioirrigating macroinvertebrates, an intense sediment oxygenation and in consequence low CH_4 emissions would occur. However, the expected high oxic mineralization would also sustain high CO_2 emissions from the water-sediment interface, which may be compensated by macrophyte CO_2 uptake. In contrast, in more eutrophic phytoplankton-dominated lakes fish bioturbation might reinforce CH_4 emissions, which, together with a poorer community of macroinvertebrates due to high fish predation, would contribute to anoxic sediments and further release of CH_4.

Also, littoral and pelagic lake zones were shown to potentially develop different roles regarding total carbon fluxes. In the clear-vegetated lake (Chapter 2), contrary to the pattern observed for the submerged macrophyte-dominated pelagic zone, the littoral zone (in our case mainly covered by emergent and free-floating plants) showed high CO_2 and CH_4 emissions. The different compositions of the primary producer communities in both zones might have promoted different conditions regarding O_2 availability in the water column and at the sediments. In addition, inputs of carbon from the surrounding lands that are received and processed in the littoral zones (Wetzel, 1992; Juutinen et al., 2003; Jansson et al., 2007) might have also contributed to the different observed patterns. In fact, the major proportion of carbon (in CO_2 equivalents) emitted by the clear-vegetated lake occurred at the littoral zone (Fig. EMS3 in Chapter 2).

Besides the differences in carbon processing, the coupling between different lake habitats was also strongly evidenced in this thesis. This occurred mainly by the zooplanktivorous and benthivorous fish consumption of combined pelagic and benthic resources (Chapter 3). In particular, a stronger role of benthic processes on carbon dynamics and CO_2 and CH_4 fluxes, in comparison to pelagic processes, was clear as shown in Chapter 3. Our field estimations could be improved, e.g., by better estimations of CO_2 uptake by free-floating plants and by acknowledging plant-mediated CH_4 fluxes in the vegetated lake. Despite those limitations, however, our field and laboratory results clearly showed the relevance of considering the relative contribution of different habitats or lake zones in order to generate accurate estimations regarding carbon fluxes at the whole ecosystem scale and to contribute to improve estimations of carbon budgets.

Results from Chapter 2 contribute to global inventories of carbon fluxes with data from subtropical ecosystems and from the south hemisphere, which are far less documented than temperate and boreal regions and in general north hemisphere locations (Cole et al., 2007; Holgerson & Raymond, 2016; Aben et al., 2017; Sanches et al., 2019).

In addition, this kind of study can provide relevant insights on how the changes in the composition of biological communities and in general in the functioning of shallow lakes that are expected with climate warming could change carbon fluxes. Particularly, the CO_2 uptake by submerged macrophytes, registered even in winter, and the extremely low concentration of dissolved CO_2 compared to lakes in higher latitudes (Fig. 5, Chapter 2), highlights the potential importance of warmer temperatures and of more intense light radiation on macrophyte-mediated carbon fluxes in subtropical regions. Besides, climate warming (and currently warm climates) seems to reinforce eutrophication and its manifestations in shallow freshwaters (Paerl & Huisman, 2008; Moss, 2010; Kosten et al., 2012; Paerl & Paul, 2012; Lürling et al., 2018). At the same time, the consequences of eutrophication and particularly of a dominance by cyanobacteria seem to positively feedback on climate warming (Moss, 2011; Yan et al., 2017; Bižić et al., 2020; Meerhoff et al., 2022). Evidence found in this thesis support the previous statement. Although net CO_2 uptake was observed at the microcosm scale (Chapter 4) through high primary production by cyanobacteria, a minor proportion of the fixed carbon was apparently incorporated into the classic trophic web (through zooplankton biomass). Therefore, once sedimented, such high organic matter would fuel mineralization. Under high cyanobacterial biomass such process is expected to occur in anoxic conditions, leading to high CH_4 production (Beaulieu et al., 2019; Yan et al., 2019; Li et al., 2021). This was not found in our short-term no-sediments microcosm experiment, but the link between high cyanobacterial biomass and high CH_4 total emissions has already been documented in other works (i.e., phytoplankton organic matter is a suitable substrate for mineralization and CH_4 production (West et al., 2012, 2015), plus the occurrence of CH_4 production by cyanobacteria under oxic conditions (Grossart et al., 2011; Günthel et al., 2019; Bižić et al., 2020)).

CHAPTER 6

CONCLUSIONS AND PERSPECTIVES

Conclusions

In this section, the main conclusions drawn based on the different studies presented in this thesis as well as from the combination of these studies, are highlighted, following the original order of the objectives. Many of these partial conclusions may serve as hypotheses for future work.

Specific objective 1 (Chapter 2):

To estimate and compare CO_2 and CH_4 fluxes among natural subtropical shallow lakes with contrasting regimes (i.e., clear-vegetated lake dominated by submerged macrophytes, phytoplankton-turbid lake, and sediment-turbid lake with extremely low primary production) at the habitat and the ecosystem levels. Secondly, to compare the estimated fluxes in subtropical shallow lakes with already published data for temperate and boreal lakes.

Related conclusions:

1. Different shallow lake regimes manifest different patterns of in-lake carbon processing and ecosystem CO_2 and CH_4 fluxes. Contrasting functional groups (i.e., submerged macrophytes versus phytoplankton) and total biomass (i.e., high versus extremely low), typically occurring under different regimes, and the typically associated distinct trophic web structure, impact CO_2 and CH_4 fluxes.

2. Under submerged-macrophytes dominated conditions, and despite the presence of suitable organic matter for carbon mineralization, the usually well-oxygenated conditions in the water column and water-sediment interface translate into lower CH_4 total emissions than in phytoplankton-dominated lakes.

3. From the comparison of dissolved CO_2 with ecosystems located in temperate and boreal regions, our subtropical clear-vegetated shallow lake (with warmer mean temperatures and more intense light radiation), seems to sustain more unsaturated CO_2 concentrations with respect to the atmosphere, which would potentially translate into stronger CO_2 uptake.

4. Littoral zones can play a major role in carbon processing and emissions. Therefore, the integration of patterns from the pelagic and littoral zones is needed to generate accurate estimations of carbon fluxes at the whole ecosystem level.

Specific objective 2 (Chapter 3):

To experimentally unravel the trophic and non-trophic effects of fish on CO_2 and CH_4 fluxes, analyzing the potential variability of fish impacts on both water column and sediment processes using sticklebacks (mostly zooplanktivorous) and carps (mostly benthivorous). In addition, we

assessed the potential differentiated effects of predation pressure and bioturbation, through the comparison between systems with the permanent presence or intermittent presence of fish.

Related conclusions:

1. Different types of fish impact CO_2 and CH_4 fluxes in varying ways through trophic and non-trophic effects, which is likely related to their different use of space and foraging behavior.

2. The net effects of fish bioturbation depend on its intensity and frequency (namely bioturbation pressure). Low to moderate bioturbation pressure (i.e., from small body-sized fishes and present at low abundances) can increase CH_4 ebullition. In contrast, high bioturbation pressure (i.e., from larger body-sized fish and at high abundances) can decrease total CH_4 emissions by enhancing sediment oxygenation.

3. Fish predation on benthic macroinvertebrates can strongly reduce O_2 penetration into the sediments, by hampering macroinvertebrates bioirrigation.

4. In conditions without or with low predation pressure on benthic macroinvertebrates, well-oxygenated water-sediment interfaces can promote high CO_2 emissions.

5. Trophic cascading effects at the water column can deplete MOB. However, pelagic processes seemed to have a lower relative weight explaining net carbon fluxes than benthic processes.

Specific objective 3 (Chapter 4):

To unravel how the metabolic balance (CO_2 uptake: CO_2 efflux ratio) in pelagic freshwater ecosystems, would change under warmer conditions with a likely higher frequency of cyanobacterial dominance, which is expected to occur in freshwaters world-wide.

Related conclusions:

1. High cyanobacterial biomasses developed under eutrophic and warmer conditions can sustain CO_2 uptake. However, a low proportion of the fixed carbon is expected to be incorporated to the classic trophic web through zooplankton grazing, likely due to cyanobacteria poor quality food for zooplankton.

2. Under cyanobacteria-dominated conditions, large amounts of organic matter are expected to sediment and in part be available for mineralization into CO_2 or CH_4.

General conclusions:

From the general overview of this thesis and the integration of results obtained combining ecosystem, mesocosm and microcosm scale analyses (Fig. 1), it is also possible to extract the following conclusions:

- Under eutrophic and warmer conditions, total carbon emission into the atmosphere, mainly as CH_4, would potentially increase.

- Whole ecosystem considerations, with the integration of littoral, pelagic, and benthic processes are needed to fully predict and understand net carbon fluxes from shallow lakes.

- Combination of field patterns with controlled experiments are needed to elucidate mechanisms and detailed linkages between major players in the system, compensating for the contrasting weaknesses of each approach (simplism versus realism, mechanistic versus descriptive nature, etc.).

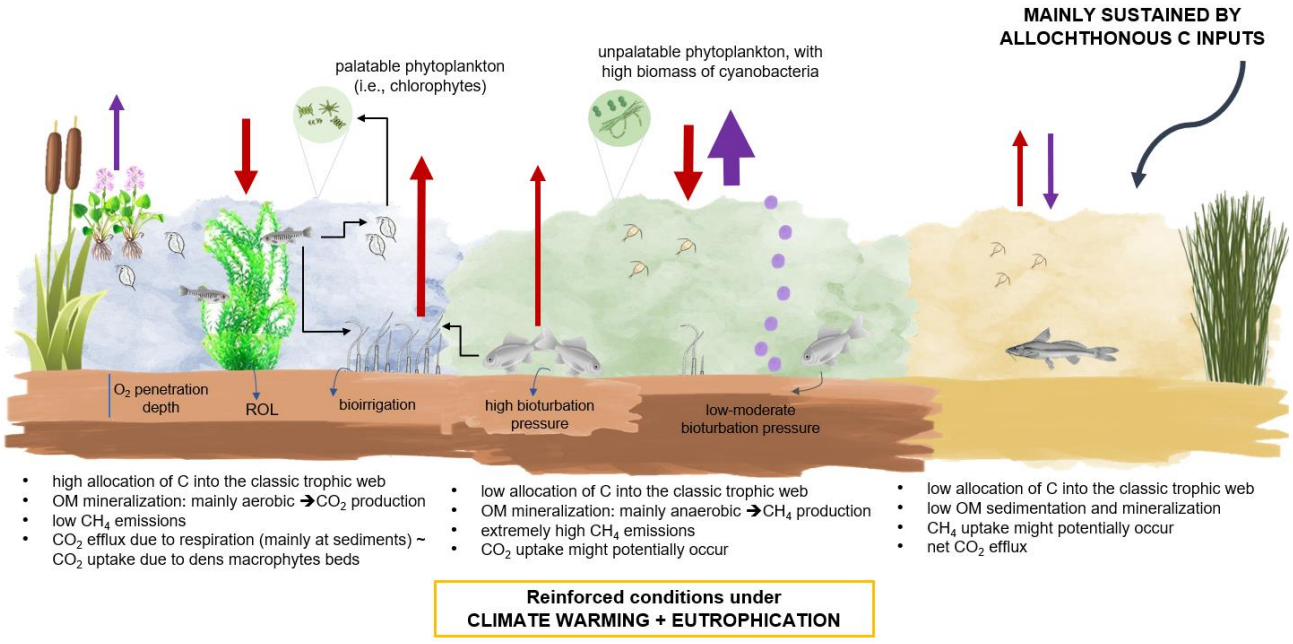

Figure 1. Summary of the main results found or hypothesized based on results in this thesis. Red and violet arrows indicate CO_2 and CH_4 fluxes, respectively, and the width of the arrows indicate the expected relative contribution to the overall amount of GHG exchanged. Thin blue arrows indicate non-trophic effects whereas thin black arrows indicate trophic interactions of biota, both affecting carbon processing.

The knowledge generated in the context of the present thesis, regarding the factors driving CO_2 and CH_4 fluxes in shallow freshwaters, can be potentially used as an input for the development of management practices focused on preventing or mitigating carbon emissions from freshwater ecosystems with different levels of anthropogenic impacts. In this line, possible management practices should focus on: controlling activities that promote eutrophication (e.g.,

limiting production activities that alter flow, natural vegetation, and/or implies fertilization and other agrochemicals in a certain area around the waterbody), as well as introducing or promoting the growth of submerged macrophytes that can enhance the diversity of consumers, sustain clear-water conditions and thereby reduce net carbon emissions.

Perspectives

As mentioned throughout this thesis, shallow ecosystems contribute the most in terms of CO_2 and CH_4 emissions from freshwaters. In particular, a negative correlation between total emissions and surface area has been clearly documented for aquatic ecosystems at different latitudes (Holgerson & Raymond, 2016). A recent definition group lentic freshwaters with a small total surface (covering less than 5 hectares), shallow waters (less than 5m depth), and a clear zone free from emergent vegetation (less than 30% of their surface covered by emergent vegetation) as ponds (Richardson et al., 2022). Even when, ponds are usually considered jointly with shallow lakes when quantifying freshwaters contributions to global carbon emissions, their particular morphology promotes different structures and functioning that may promote distinctive behaviors regarding CO_2 and CH_4 fluxes (Holgerson, 2015; Holgerson & Raymond, 2016; Richardson et al., 2022). Pond´s small surface area and small fletch promote less wind-driven turbulence and in consequence low gas exchange rates (Markfort et al., 2010). In addition, ponds can dramatically warm during the day, which might induce stratification, but they can cool off and completely mix overnight (Martinsen et al., 2019). As a consequence of these diel changes in mixing and temperature, internal nutrient loading and ecosystem respiration can be enhanced (Wilhelm & Adrian, 2008; Staehr et al., 2012). Also, their low water volume : surface ratio makes ponds even more vulnerable to external stressors, such as terrestrial inputs of nutrients, organic matter, and contaminants from anthropogenic origin (Biggs et al., 2017; Hill et al., 2018), the management of surrounding land, or climate change and climate variability. Despite the fact that the role of ponds related to biodiversity reservoirs and ecosystem services has gained increasing attention in the last years (Biggs et al., 2017; Hill et al., 2018; Riley et al., 2018), their contribution to the global carbon budget is still poorly quantified (Holgerson & Raymond, 2016). In many regions around the world, the number of ponds is increasing as they are constructed or re-constructed for different purposes, such as increasing local biodiversity, to control local temperature and floodings, to increase aesthetic value, and, even more often, for productive uses (Downing et al., 2006; Hill et al., 2018; Swartz & Miller, 2021; Cael et al., 2022). Likely given the usually intensive anthropogenic activities in their surroundings, artificial water bodies emit more GHG per unit surface than natural similar ecosystems (Ollivier et al., 2019; Peacock et al., 2019, 2021; Webb et al., 2019; Rosentreter et al., 2021). In the current context of worldwide increasing eutrophication and climate change, it is key to understand how ponds located at different climatic regions and under different levels of anthropogenic impact contribute to the global carbon budget.

Particularly, the construction of artificial ponds in Uruguay is a widespread practice in the rural landscapes, sometimes with aesthetic purposes, but mainly for collecting water for livestock and to supplement the irrigation of agricultural crops in times of drought. Indeed, artificial ponds are perceived as a fundamental element in agricultural production and their construction is been promoted by private initiatives and national authorities (García Petillo et al., 2012). According to gross estimations based on satellite imagery, more than 19.200 ha in Uruguay are currently covered by artificial ponds (Colina, 2022).

We consider that further research is needed to better account for the relative contribution of aquatic systems, not least artificial ponds, to net carbon emissions in Uruguay. In addition to develop management measurements focused on hampering emissions from freshwaters, it is highly important to understand how the main productive activities in the surrounding lands affect the relevant abiotic and biotic potential drivers of carbon identified over this thesis. Thus, a better knowledge about the general conditions of artificial ponds in Uruguay (i.e., trophic state, biodiversity, carbon emissions, etc.), together with the main findings of this thesis, might help elucidate which local and regional management practices, associated to ponds and their surrounding lands, enhance total carbon emissions and which ones promote lower total emissions or even eventually carbon retention.

Such knowledge may also contribute to improve the national estimations of GHG emissions, in accordance with the new guidelines of the IPCC (2019), as a tool to support decision making and environmental management.

REFERENCES

Aben, R. C. H., N. Barros, E. Van Donk, T. Frenken, S. Hilt, G. Kazanjian, L. P. M. Lamers, E. T. H. M. Peeters, J. G. M. Roelofs, L. N. De Senerpont Domis, S. Stephan, M. Velthuis, D. B. Van De Waal, M. Wik, B. F. Thornton, J. Wilkinson, T. Delsontro, & S. Kosten, 2017. Cross continental increase in methane ebullition under climate change. Nature Communications 8: 1–8.

Acuña, V., A. Wolf, U. Uehlinger, & K. Tockner, 2008. Temperature dependence of stream benthic respiration in an Alpine river network under global warming. Freshwater Biology 53: 2076–2088.

Ahlgren, G., L. Lundstedt, M. Brett, & C. Forsberg, 1990. Lipid composition and food quality of some freshwater phytoplankton for cladoceran zooplankters. Journal of Plankton Research 12: 809–818.

Allen, A. P., J. F. Gillooly, & J. H. Brown, 2005. Linking the global carbon cycle to individual metabolism. Functional Ecology 19: 202–213.

Almeida, R. M., G. N. Nóbrega, P. C. Junger, A. V. Figueiredo, A. S. Andrade, C. G. B. de Moura, D. Tonetta, E. S. Oliveira, F. Araújo, F. Rust, J. M. Piñeiro-Guerra, J. R. Mendonça, L. R. Medeiros, L. Pinheiro, M. Miranda, M. R. A. Costa, M. L. Melo, R. L. G. Nobre, T. Benevides, F. Roland, J. de Klein, N. O. Barros, R. Mendonça, V. Becker, V. L. M. Huszar, & S. Kosten, 2016. High primary production contrasts with intense carbon emission in a eutrophic tropical reservoir. Frontiers in Microbiology 7: 1–13.

Angel, R., P. Claus, & R. Conrad, 2012. Methanogenic archaea are globally ubiquitous in aerated soils and become active under wet anoxic conditions. ISME Journal 6: 847–862.

APHA/AWWA/WEF, 2017. 2540 SOLIDS D- Total Suspended Solids Dried at 103–105°C In Rice, E. W., R. B. Baird, & A. D. Eaton (eds), Standard Methods for the Examination of Water and Wastewater: 69.

Arocena, R., L. Aubriot, S. Bonilla, G. Chalar, D. Conde, G. Daners, L. De León, D. Fabían, J. Gorga, N. Mazzeo, & F. Scasso, 1999. Métodos en Ecología de Aguas Continentales.

Attayde, J. L., R. F. Menezes, S. Kosten, G. Lacerot, E. Jeppesen, V. Huszar, C. W. C. Branco, D. da Mota-Marques, C. Kruk, F. Teixeira-de-Mello, J. H. C. Gomes, C. C. C. Machado, M. Meerhoff, & N. Mazzeo, 2021. Potential effects of warming on the trophic structure of shallow lakes in South America: a comparative analysis of subtropical and tropical systems. Hydrobiologia.

Attermeyer, K., S. Flury, R. Jayakumar, P. Fiener, K. Steger, V. Arya, F. Wilken, R. Van Geldern, & K. Premke, 2016. Invasive floating macrophytes reduce greenhouse gas emissions from a small tropical lake. Scientific Reports 6.

Atwood, T. B., E. Hammill, H. S. Greig, P. Kratina, J. B. Shurin, D. S. Srivastava, & J. S. Richardson, 2013. Predator-induced reduction of freshwater carbon dioxide emissions. Nature Geoscience 6: 191–194.

Audet, J., É. M. Neif, Y. Cao, C. C. Hoffmann, T. L. Lauridsen, S. E. Larsen, M. Søndergaard, E. Jeppesen, & T. A. Davidson, 2017. Heat-wave effects on greenhouse gas emissions from shallow lake mesocosms. Freshwater Biology 00: 1–13.

Bachmann, R. W., M. V. Hoyer, & D. E. Canfield, 2000. Internal heterotrophy following the switch from macrophytes to algae in Lake Apopka, Florida. Hydrobiologia 418: 217–227.

Bade, D. L., & J. J. Cole, 2006. Impact of chemically enhanced diffusion on dissolved inorganic carbon stable isotopes in a fertilized lake. J. Geophys. Res 111: 1014.

Balmer, M., & J. Downing, 2011. Carbon dioxide concentrations in eutrophic lakes: undersaturation implies atmospheric uptake. Inland Waters 1: 125–132.

Bansal, S., O. F. Johnson, J. Meier, & X. Zhu, 2020. Vegetation Affects Timing and Location of Wetland Methane Emissions. Journal of Geophysical Research: Biogeosciences 125: e2020JG005777.

Baranov, V., J. Lewandowski, P. Romeijn, G. Singer, & S. Krause, 2016. Effects of bioirrigation of non-biting midges (Diptera: Chironomidae) on lake sediment respiration. Scientific Reports 6.

Bastviken, D., J. J. Cole, M. L. Pace, & M. C. Van de-Bogert, 2008. Fates of methane from different lake habitats: Connecting whole-lake budgets and CH_4 emissions. Journal of Geophysical Research: Biogeosciences 113: 1–13.

Bastviken, D., J. Cole, M. Pace, & L. Tranvik, 2004. Methane emissions from lakes: Dependence of lake characteristics, two regional assessments, and a global estimate. Global Biogeochemical Cycles 18: 1–12.

Bastviken, D., J. Ejelrtsson, I. Sundh, & L. J. Tranvik, 2003. Methane as a source of carbon and energy for chironomid larvae. Ecology 84: 969–981.

Bastviken, D., L. J. Tranvik, J. Downing, J. a Crill, P. M, & A. Enrich-prast, 2011. Freshwater Methane Emissions Offset the Continental Carbon Sink. Science 331: 50.

Battin, T. J., S. Luyssaert, L. A. Kaplan, A. K. Aufdenkampe, A. Richter, & L. J. Tranvik, 2009. The boundless carbon cycle. Nature Geoscience 2: 598–600.

Beaulieu, J. J., T. DelSontro, & J. A. Downing, 2019. Eutrophication will increase methane emissions from lakes and impoundments during the 21st century. Nature Communications 10: 3–7.

Bhattacharyya, P., D. P. Sinhababu, K. S. Roy, P. K. Dash, P. K. Sahu, R. Dandapat, S. Neogi, & S. Mohanty, 2013. Effect of fish species on methane and nitrous oxide emission in relation to soil C, N pools and enzymatic activities in rainfed shallow lowland rice-fish farming system. Agriculture, Ecosystems and Environment 176: 53–62.

Biderre-Petit, C., D. Jézéquel, E. Dugat-Bony, F. Lopes, J. Kuever, G. Borrel, E. Viollier, G. Fonty, & P. Peyret, 2011. Identification of microbial communities involved in the methane cycle of a freshwater meromictic lake. FEMS Microbiology Ecology 77: 533–545.

Biggs, J., S. von Fumetti, & M. Kelly-Quinn, 2017. The importance of small waterbodies for biodiversity and ecosystem services: implications for policy makers. Hydrobiologia 793: 3–39.

Bižić, M., D. Ionescu, M. Günthel, K. Tang, & H.-P. Grossart, 2018. Oxic Methane Cycling: New Evidence for Methane Formation in Oxic Lake Water: 1–22.

Bižić, M., T. Klintzsch, D. Ionescu, M. Y. Hindiyeh, M. Günthel, A. M. Muro-Pastor, W. Eckert, T. Urich, F. Keppler, & H.-P. Grossart, 2020. Aquatic and terrestrial cyanobacteria produce methane. Science Advances 6: eaax5343.

Bodelier, P. L. E., M. Meima-Franke, C. A. Hordijk, A. K. Steenbergh, M. M. Hefting, L. Bodrossy, M. Von Bergen, & J. Seifert, 2013. Microbial minorities modulate methane consumption through niche partitioning. ISME Journal 7: 2214–2228.

Bodmer, P., R. Vroom, T. Stepina, P. A. del Giorgio, & S. Kosten, 2021. Methane Fluxes of Vegetated Areas in Natural Freshwater Ecosystems: Assessments and Global Significance.

Booth, M. T., M. Urbanic, X. Wang, & J. J. Beaulieu, 2021. Bioturbation frequency alters methane emissions from reservoir sediments. Science of the Total Environment 789.

Borges Machado, K., L. Cardoso Galli Vieira, & J. C. Nabot, 2019. Predicting the dynamics of taxonomic and functional phytoplankton compositions in different global warming scenarios. Hydrobiologia 830: 115–134.

Borrel, G., D. Jézéquel, C. Biderre-Petit, N. Morel-Desrosiers, J. P. Morel, P. Peyret, G. Fonty, & A. C. Lehours, 2011. Production and consumption of methane in freshwater lake ecosystems. Research in Microbiology 162: 832–847.

Brasil, J., & V. L. de M. Huszar, 2011. O papel dos traços funcionais na ecologia do fitoplâncton continental. Oecologia Australis 15: 799–834.

Bridgewater, L. L., R. B. Baird, A. D. Eaton, E. W. Rice, American Public Health Association, American Water Works Association, & Water Environment Federation (eds), 2017. Standard methods for the examination of water and wastewater.

Brooks, J. L., & S. I. Dodson, 1965. Predation, body size and composition of plankton. Science 150: 28–35.

Brothers, S. M., S. Hilt, K. Attermeyer, H. P. Grossart, S. Kosten, B. Lischke, T. Mehner, N. Meyer, K. Scharnweber, & J. Kohler, 2013. A regime shift from macrophyte to phytoplankton dominance enhances carbon burial in a shallow, eutrophic lake. Ecosphere 4: art137.

Brown, J. H., 2004. Toward a metabolic theory of ecology. Ecology 85: 1771–1789.

Burks, R. L., D. M. Lodge, E. Jeppesen, & T. L. Lauridsen, 2002. Diel horizontal migration of zooplankton: costs and benefits of inhabiting the littoral: Costs and benefits of DHM. Freshwater Biology 47: 343–365.

Burns, C. W., & B. Hegarty, 1994. Diet selection by copepods in the presence of cyanobacteria. Journal of Plankton Research 16: 1671–1690.

Cadillo-Quiroz, H., S. Bräuer, E. Yashiro, C. Sun, J. Yavitt, & S. Zinder, 2006. Vertical profiles of methanogenesis and methanogens in two contrasting acidic peatlands in central New York State, USA. Environmental Microbiology 8: 1428–1440.

Cael, B. B., J. Biggs, & D. A. Seekell, 2022. The size-distribution of Earth's lakes and ponds: limits to power-law behavior. Frontiers in Ecology and the Environment.

Callieri, C., 2017. Synechococcus plasticity under environmental changes. FEMS Microbiology Letters 364.

Carey, C. C., J. P. Doubek, R. P. McClure, & P. C. Hanson, 2018. Oxygen dynamics control the burial of organic carbon in a eutrophic reservoir. Limnology and Oceanography Letters 293–301.

Carey, C. C., B. W. Ibelings, E. P. Hoffmann, D. P. Hamilton, & J. D. Brookes, 2012. Eco-physiological adaptations that favour freshwater cyanobacteria in a changing climate. Water Research 46: 1394–1407.

Chumchal, M. M., & R. W. Drenner, 2004. Interrelationships between phosphorus loading and common carp in the regulation of phytoplankton biomass. Archiv fur Hydrobiologie 161: 147–158.

Cloern, J., 1995. An empirical model of the phytoplankton chlorophyll: carbon ratio-the conversion factor between productivity an. Limnology and Oceanography 40: 1313–1321.

Cole, Caraco, Kling, & Krat, 1994. Carbon dioxide supersaturation in the surface waters of lake. Science 265: 1568–1570.

Cole, J. J., 2013. Freshwater ecosystems and the carbon cycle. Vol. 146. Oldendorf, Germany: International Ecology Institute.

Cole, J. J., D. L. Bade, D. Bastviken, M. L. Pace, & M. V. D. Bogert, 2010. Multiple approaches to estimating air-water gas exchange in small lakes. Limnology and Oceanography: Methods 8: 285–293.

Cole, J. J., & N. F. Caraco, 1998. Atmospheric Exchange of Carbon Dioxide in a Low-Wind Oligotrophic Lake Measured by the Addition of SF6. Limnology and Oceanography 43: 647–656.

Cole J. J., Caraco N. F., Kling G. W., & Kratz T., 1994. Carbon dioxide supersaturation in the surface waters of lake. Science 265: 1568–1570.

Cole, J. J., S. R. Carpenter, M. L. Pace, M. C. Van de Bogert, J. L. Kitchell, & J. R. Hodgson, 2006. Differential support of lake food webs by three types of terrestrial organic carbon. Ecology Letters 9: 558–568.

Cole, J. J., Y. T. Prairie, N. F. Caraco, W. H. McDowell, L. J. Tranvik, R. G. Striegl, C. M. Duarte, P. Kortelainen, J. A. Downing, J. J. Middelburg, & J. Melack, 2007. Plumbing the global carbon cycle: Integrating inland waters into the terrestrial carbon budget. Ecosystems 10: 171–184.

Colina, M., 2022. Producto 1. Identificación y descripción de las parcelas identificadas como humedales gestionados en Uruguay. IC URU18G31-1227 - Consultoría para generar insumos para la estimación de las emisiones de gases de efecto invernadero en humedales gestionados en Uruguay.

Colina, M., D. Calliari, C. Carballo, & C. Kruk, 2016. A trait-based approach to summarize zooplankton–phytoplankton interactions in freshwaters. Hydrobiologia 767: 221–233.

Colina, M., M. Meerhoff, G. Pérez, A. J. Veraart, P. L. E. Bodelier, & S. Kosten, 2021. Trophic and non-trophic effects of fish and macroinvertebrates on carbon emissions. Freshwater Biology 00: 1–15.

Costello, A. M., & M. E. Lidstrom, 1999. Molecular characterization of functional and phylogenetic genes from natural populations of methanotrophs in lake sediments. Applied and Environmental Microbiology 65: 5066–5074.

Datta, A., D. R. Nayak, D. P. Sinhababu, & T. K. Adhya, 2009. Methane and nitrous oxide emissions from an integrated rainfed rice-fish farming system of Eastern India. Agriculture, Ecosystems and Environment 129: 228–237.

Davidson, T. A., J. Audet, E. Jeppesen, F. Landkildehus, T. L. Lauridsen, M. Søndergaard, & J. Syväranta, 2018. Synergy between nutrients and warming enhances methane ebullition from experimental lakes. Nature Climate Change 8: 156–160.

Davidson, T. A., J. Audet, J. C. Svenning, T. L. Lauridsen, M. Søndergaard, F. Landkildehus, S. E. Larsen, & E. Jeppesen, 2015. Eutrophication effects on greenhouse gas fluxes from shallow-lake mesocosms override those of climate warming. Global Change Biology 21: 4449–4463.

De Senerpont Domis, L. N., W. M. Mooij, & J. Huisman, 2007. Climate-induced shifts in an experimental phytoplankton community: a mechanistic approach. Hydrobiologia 584: 403–413.

de Tezanos Pinto, P., & I. O'Farrell, 2014. Regime shifts between free-floating plants and phytoplankton: A review. Hydrobiologia 740: 13–24.

DelSontro, T., J. J. Beaulieu, & J. A. Downing, 2018. Greenhouse gas emissions from lakes and impoundments: Upscaling in the face of global change. Limnology and Oceanography Letters 64–75.

DelSontro, T., L. Boutet, A. St-Pierre, P. A. del Giorgio, & Y. T. Prairie, 2016. Methane ebullition and diffusion from northern ponds and lakes regulated by the interaction between temperature and system productivity. Limnology and Oceanography 61: S62–S77.

DeMott, W., R. D. Gulati, & E. Van Donk, 2001. Daphniafood limitation in three hypereutrophic Dutch lakes: Evidence for exclusion oflarge-bodied species by interfering filaments of cyanobacteria. Limnology and Oceanography 46: 2054–2060.

DeMott, W. R., 1999. Foraging strategies and growth inhibition in five daphnids feeding on mixtures of a toxic cyanobacterium and a green alga. Freshwater Biology 42: 263–274.

Devlin, S. P., J. Saarenheimo, J. Syväranta, & R. I. Jones, 2015. Top consumer abundance influences lake methane efflux. Nature Communications 6.

Diaz, R. J., & J. H. Trefry, 2006. Comparison of sediment profile image data with profiles of oxygen and Eh from sediment cores. Journal of Marine Systems 62: 164–172.

Doi, H., 2009. Spatial patterns of autochthonous and allochthonous resources in aquatic food webs. Population Ecology 51: 57–64.

Donis, D., S. Flury, A. Stöckli, J. E. Spangenberg, D. Vachon, & D. F. McGinnis, 2017. Full-scale evaluation of methane production under oxic conditions in a mesotrophic lake. Nature Communications 8: 1661.

Downing, J. A., 2010. Emerging global role of small lakes and ponds: Little things mean a lot. Limnetica 29: 9–24.

Downing, J. A., J. J. Cole, J. J. Middelburg, R. G. Striegl, C. M. Duarte, P. Kortelainen, Y. T. Prairie, & K. A. Laube, 2008. Sediment organic carbon burial in agriculturally eutrophic impoundments over the last century. Global Biogeochemical Cycles 22.

Downing, J. A., Y. T. Prairie, J. J. Cole, C. M. Duarte, L. J. Tranvik, R. G. Striegl, W. H. McDowell, P. Kortelainen, N. F. Caraco, J. M. Melack, & J. J. Middelburg, 2006. Abundance and Size Distribution of Lakes, Ponds and Impoundments. Limnology and Oceanography 51: 469–478.

Dumont, H. J., I. Van De Velde, & S. Dumont, 1975. The Dry Weight Estimate of Biomass in a Selection of Cladocera, Copepoda and Rotifera from the Plankton, Periphyton and Benthos of Continental Waters. Oecologia 19: 75–97.

Fallon, R. D., & T. D. Brock, 1980. Planktonic blue-green algae: Production, sedimentation, and decomposition in Lake Mendota, Wisconsin: Blue-green algal sedimentation. Limnology and Oceanography 25: 72–88.

Figueiredo-Barros, M. P., A. Caliman, J. J. F. Leal, R. L. Bozelli, V. F. Farjalla, & F. A. Esteves, 2009. Benthic bioturbator enhances CH_4 fluxes among aquatic compartments and atmosphere in experimental microcosms. Canadian Journal of Fisheries and Aquatic Sciences 66: 1649–1657.

Forbes, S. A., 1887. The lake as a microcosm. Bulletin of Peoria Scientific Association 77–87.

Frei, M., M. A. Razzak, M. M. Hossain, M. Oehme, S. Dewan, & K. Becker, 2007. Methane emissions and related physicochemical soil and water parameters in rice-fish systems in Bangladesh. Agriculture, Ecosystems and Environment 120: 391–398.

García Petillo, M., P. Cánepa, & C. Ronzoni, 2012. Manual para el diseño y la construcción de tajamares de aguada. Ministerio de Agricultura Ganadería y Pesca (MGAP) de Uruguay.

Geerts, A. N., J. Vanoverbeke, B. Vanschoenwinkel, W. Van Doorslaer, H. Feuchtmayr, D. Atkinson, B. Moss, T. A. Davidson, C. D. Sayer, & L. De Meester, 2015. Rapid evolution of thermal tolerance in the water flea Daphnia. Nature Climate Change 5: 665–668.

Ger, K. A., L. A. Hansson, & M. Lürling, 2014. Understanding cyanobacteria-zooplankton interactions in a more eutrophic world. Freshwater Biology 59: 1783–1798.

Geurts, J. J. M., A. J. P. Smolders, A. M. Banach, J. P. M. van de Graaf, J. G. M. Roelofs, & L. P. M. Lamers, 2010. The interaction between decomposition, net N and P mineralization and their mobilization to the surface water in fens. Water Research 44: 3487–3495.

Geurts, J. J. M., A. J. P. Smolders, J. T. A. Verhoeven, J. G. M. Roelofs, & L. P. M. Lamers, 2008. Sediment Fe:PO_4 ratio as a diagnostic and prognostic tool for the restoration of macrophyte biodiversity in fen waters. Freshwater Biology 53: 2101–2116.

Gillooly, J. F., 2000. Effect of body size and temperature on generation time in zooplankton. Journal of Plankton Research 22: 241–251.

Gillooly, J. F., & S. I. Dodson, 2000. Latitudinal patterns in the size distribution and seasonal dynamics of new world, freshwater cladocerans. Limnology and Oceanography 45: 22–30.

Glibert, P. M., 2017. Eutrophication, harmful algae and biodiversity — Challenging paradigms in a world of complex nutrient changes. Marine Pollution Bulletin 124: 591–606.

Grasset, C., G. Abril, R. Mendonça, F. Roland, & S. Sobek, 2019. The transformation of macrophyte-derived organic matter to methane relates to plant water and nutrient contents. Limnology and Oceanography 1–13.

Grasset, C., R. Mendonça, G. Villamor Saucedo, D. Bastviken, F. Roland, & S. Sobek, 2018. Large but variable methane production in anoxic freshwater sediment upon addition of allochthonous and autochthonous organic matter. Limnology and Oceanography 63: 1488–1501.

Grasset, C., S. Sobek, K. Scharnweber, S. Moras, H. Villwock, S. Andersson, C. Hiller, C. Nydahl Anna, F. Chaguaceda, W. Colom, & J. Tranvik Lars, 2020. The CO_2-equivalent balance of freshwater ecosystems is non-linearly related to productivity. Global Change Biology 2: 1–11.

Grossart, H.-P., K. Frindte, C. Dziallas, W. Eckert, & K. W. Tang, 2011. Microbial methane production in oxygenated water column of an oligotrophic lake. Proceedings of the National Academy of Sciences 108: 19657–19661.

Gudasz, C., D. Bastviken, K. Premke, K. Steger, & L. J. Tranvik, 2012. Constrained microbial processing of allochthonous organic carbon in boreal lake sediments. Limnology and Oceanography 57: 163–175.

Gudasz, C., D. Bastviken, K. Steger, K. Premke, S. Sobek, & L. J. Tranvik, 2010. Temperature-controlled organic carbon mineralization in lake sediments. Nature 466: 478–481.

Gudasz, C., S. Sobek, D. Bastviken, B. Koehler, & L. J. Tranvik, 2015. Temperature sensitivity of organic carbon mineralization in contrasting lake sediments. Journal of Geophysical Research G: Biogeosciences 120: 1215–1225.

Günthel, M., D. Donis, G. Kirillin, D. Ionescu, M. Bizic, D. F. McGinnis, H.-P. Grossart, & K. W. Tang, 2019. Contribution of oxic methane production to surface methane emission in lakes and its global importance. Nature Communications 10: 5497.

Gyllström, M., L.-A. Hansson, E. Jeppesen, F. G. Criado, E. Gross, K. Irvine, T. Kairesalo, R. Kornijow, M. R. Miracle, M. Nykänen, T. Nõges, S. Romo, D. Stephen, E. V. Donk, & B. Moss, 2005. The role of climate in shaping zooplankton communities of shallow lakes. Limnology and Oceanography 50: 2008–2021.

Hansson, L.-A., A. Nicolle, W. Granéli, P. Hallgren, E. Kritzberg, A. Persson, J. Björk, P. A. Nilsson, & C. Brönmark, 2012. Food-chain length alters community responses to global change in aquatic systems. Nature Climate Change 2: 1–6.

Havens, K. E., 1993. Responses to experimental fish manipulations in a shallow, hypereutrophic lake: the relative importance of benthic nutrient recycling and trophic cascade. Hydrobiologia 254: 73–80.

Heiri, O., A. F. Lotter, & G. Lemcke, 2001. Loss on Ignition as a Method for Estimating Organic and Carbonate Content in Sediments: Reproducibility and Comparability of Results. Journal of Paleolimnology 25: 101–110.

Hernández, M., R. Conrad, M. Klose, K. Ma, & Y. Lu, 2017. Structure and function of methanogenic microbial communities in soils from flooded rice and upland soybean fields from Sanjiang plain, NE China. Soil Biology and Biochemistry 105: 81–91.

Hessen, D. O., 1992. Nutrient Element Limitation of Zooplankton Production. Source: The American Naturalist 140: 799–814.

Hill, M. J., C. Hassall, B. Oertli, L. Fahrig, B. J. Robson, J. Biggs, M. J. Samways, N. Usio, N. Takamura, J. Krishnaswamy, & P. J. Wood, 2018. New policy directions for global pond conservation. Conservation Letters 11.

Hilt, S., S. Brothers, E. Jeppesen, A. J. Veraart, & S. Kosten, 2017. Translating Regime Shifts in Shallow Lakes into Changes in Ecosystem Functions and Services. BioScience 67: 928–936.

Hofmann, H., L. Federwisch, & F. Peeters, 2010. Wave-induced release of methane: Littoral zones as a source of methane in lakes. Limnology and Oceanography 55: 1990–2000.

Holgerson, M. A., 2015. Drivers of carbon dioxide and methane supersaturation in small, temporary ponds. Biogeochemistry 124: 305–318.

Holgerson, M. A., & P. A. Raymond, 2016. Large contribution to inland water CO_2 and CH_4 emissions from very small ponds. Nature Geoscience 9: 222–226.

Hölker, F., M. J. Vanni, J. J. Kuiper, C. Meile, H.-P. Grossart, R. Adrian, A. Lorke, O. Dellwig, A. Brand, M. Hupfer, G. Nützmann, & J. Lewandowski, 2015. Tube-dwelling invertebrates: tiny ecosystem engineers have large effects in lake ecosystems. Ecological Monographs 85: 333–351.

Hothorn, T., F. Bretz, P. Westfall, & R. M. Heiberger, 2016. Package “multcomp” Title Simultaneous Inference in General Parametric Models. Biometrical Journal 50: 346–363.

Huss, A. A., & J. D. Wehr, 2004. Strong indirect effects of a submersed aquatic macrophyte, Vallisneria americana, on bacterioplankton densities in a mesotrophic lake. Microbial Ecology 47: 305–315.

Iglesias, C., M. Meerhoff, L. S. Johansson, I. González-Bergonzoni, N. Mazzeo, J. P. Pacheco, F. T. de Mello, G. Goyenola, T. L. Lauridsen, M. Søndergaard, T. A. Davidson, & E. Jeppesen, 2017. Stable isotope analysis confirms substantial differences between subtropical and temperate shallow lake food webs. Hydrobiologia 784: 111–123.

IHA, 2010. GHG measurement guidelines for freshwater reservoirs. UNESCO / International Hydropower Association.

IPCC, 2006. Vol. 4 Chapter 7, Wetlands 2006 IPCC Guidelines For National Greenhouse Gas Inventories.

IPCC, 2013. Supplement to the 2006 IPCC guidelines for national greenhouse gas inventories: wetlands: methodological guidance on lands with wet and drained soils, and constructed wetlands for wastewater treatment.

IPCC, 2019. Vol. 4, Chapter 7. Wetlands 2019 Refinement to the 2006 IPCC Guidelines for National Greenhouse Gas Inventories: 52.

IPCC, 2021. Climate Change 2021: The Physical Science Basis. Contribution of Working Group I to the Sixth Assessment Report of the Intergovernmental Panel on Climate Change [Masson-Delmotte, V., P. Zhai, A. Pirani, S. L. Connors, C. Péan, S. Berger, N. Caud, Y. Chen. Cambridge University Press: 3949.

ISO 10260, 1992. Water quality - Measurement of biochemical parameters - Spectrometric determination of the chlorophyll-a concentration Int. Org. Standard, Geneva, 1st ed. 1992-07-15.

Jakobsen, T. S., P. B. Hansen, E. Jeppesen, P. Grønkjær, & M. Søndergaard, 2003. Impact of three-spined stickleback Gasterosteus aculeatus on zooplankton and chl a in shallow, eutrophic, brackish lakes. Marine Ecology Progress Series 262: 277–284.

Jakobsen, T. S., P. B. Hansen, E. Jeppesen, & M. Søndergaard, 2004. Cascading effect of three-spined stickleback Gasterosteus aculeatus on community composition, size, biomass and diversity of phytoplankton in shallow, eutrophic brackish lagoons. Marine Ecology Progress Series 279: 305–309.

Janssen, A. B. G., S. Hilt, S. Kosten, J. J. M. de Klein, H. W. Paerl, & D. B. Van de Waal, 2020. Shifting states, shifting services: Linking regime shifts to changes in ecosystem services of shallow lakes. Freshwater Biology 66: 1–12.

Jansson, M., L. Persson, A. M. De Roos, R. I. Jones, & L. J. Tranvik, 2007. Terrestrial carbon and intraspecific size-variation shape lake ecosystems. Trends in Ecology and Evolution 22: 316–322.

Jeppesen, E., B. Kronvang, M. Meerhoff, M. Søndergaard, K. M. Hansen, H. E. Andersen, T. L. Lauridsen, L. Liboriussen, M. Beklioglu, A. Özen, & J. E. Olesen, 2009. Climate Change Effects on Runoff, Catchment Phosphorus Loading and Lake Ecological State, and Potential Adaptations. Journal of Environmental Quality 38: 1930–1941.

Jeppesen, E., D. Trolle, T. A. Davidson, R. Bjerring, M. Søndergaard, L. S. Johansson, T. L. Lauridsen, A. Nielsen, S. E. Larsen, & M. Meerhoff, 2016. Major changes in CO_2 efflux when shallow lakes shift from a turbid to a clear water state. Hydrobiologia 778: 33–44.

Jones, R. I., & J. Grey, 2011. Biogenic methane in freshwater food webs. Freshwater Biology 56: 213–229.

Junger, P. C., F. dá C. C. Dantas, R. L. G. Nobre, S. Kosten, E. M. Venticinque, F. de C. Araújo, H. Sarmento, R. Angelini, I. Terra, A. Gaudêncio, N. H. They, V. Becker, C. R. Cabral, L. Quesado, L. S. Carneiro, A. Caliman, & A. M. Amado, 2019. Effects of seasonality, trophic state and landscape properties on CO_2 saturation in low-latitude lakes and reservoirs. Science of the Total Environment 664: 283–295.

Juutinen, S., J. Alm, T. Larmola, J. T. Huttunen, M. Morero, P. J. Martikainen, & J. Silvola, 2003. Major implication of the littoral zone for methane release from boreal lakes. Global Biogeochemical Cycles 17.

Kajan, R., & P. Frenzel, 1999. The effect of chironomid larvae on production, oxidation and fluxes of methane in a flooded rice soil. FEMS Microbiology Ecology 28: 121–129.

Keller, P. S., N. Catalán, D. von Schiller, H. P. Grossart, M. Koschorreck, B. Obrador, M. A. Frassl, N. Karakaya, N. Barros, J. A. Howitt, C. Mendoza-Lera, A. Pastor, G. Flaim, R. Aben, T. Riis, M. I. Arce, G. Onandia,

J. R. Paranaíba, A. Linkhorst, R. del Campo, A. M. Amado, S. Cauvy-Fraunié, S. Brothers, J. Condon, R. F. Mendonça, F. Reverey, E. I. Rõõm, T. Datry, F. Roland, A. Laas, U. Obertegger, J. H. Park, H. Wang, S. Kosten, R. Gómez, C. Feijoó, A. Elosegi, M. M. Sánchez-Montoya, C. M. Finlayson, M. Melita, E. S. Oliveira Junior, C. C. Muniz, L. Gómez-Gener, C. Leigh, Q. Zhang, & R. Marcé, 2020. Global CO_2 emissions from dry inland waters share common drivers across ecosystems. Nature Communications 11: 1–8.

Kim, S. Y., A. J. Veraart, M. Meima-Franke, & P. L. E. Bodelier, 2015. Combined effects of carbon, nitrogen and phosphorus on CH_4 production and denitrification in wetland sediments. Geoderma 259–260: 354–361.

Kling, G. W., G. W. Kipphut, & M. C. Miller, 1992. The flux of CO_2 and CH_4 from lakes and rivers in arctic Alaska. Hydrobiologia 240: 23–36.

Kortelainen, P., M. Rantakari, J. T. Huttunen, T. Mattsson, J. Alm, S. Juutinen, T. Larmola, J. Silvola, & P. J. Martikainen, 2006. Sediment respiration and lake trophic state are important predictors of large CO_2 evasion from small boreal lakes. Global Change Biology 12: 1554–1567.

Kosten, S., V. L. M. Huszar, E. Bécares, L. S. Costa, E. van Donk, L. A. Hansson, E. Jeppesen, C. Kruk, G. Lacerot, N. Mazzeo, L. De Meester, B. Moss, M. Lürling, T. Nõges, S. Romo, & M. Scheffer, 2012. Warmer climates boost cyanobacterial dominance in shallow lakes. Global Change Biology 18: 118–126.

Kosten, S., A. Kamarainen, E. Jeppesen, E. H. Van Nes, E. T. H. M. Peeters, N. Mazzeo, L. Sass, J. Hauxwell, N. Hansel-welch, T. L. Lauridsen, M. Søndergaard, R. W. Bachmann, G. Lacerot, & M. Scheffer, 2009a. Climate-related differences in the dominance of submerged macrophytes in shallow lakes. Global Change Biology 15: 2503–2517.

Kosten, S., G. Lacerot, E. Jeppesen, D. Da Motta Marques, E. H. Van Nes, N. Mazzeo, & M. Scheffer, 2009b. Effects of submerged vegetation on water clarity across climates. Ecosystems 12: 1117–1129.

Kosten, S., & M. Meerhoff, 2014. Lake Communities. Encyclopedia of Life Sciences 1–11.

Kosten, S., F. Roland, D. M. L. Da Motta Marques, E. H. Van Nes, N. Mazzeo, L. D. S. L. Sternberg, M. Scheffer, & J. J. Cole, 2010. Climate-dependent CO_2 emissions from lakes. Global Biogeochemical Cycles 24.

Kosten, S., S. van den Berg, R. Mendonça, J. R. Paranaíba, F. Roland, S. Sobek, J. Van Den Hoek, & N. Barros, 2018. Extreme drought boosts CO_2 and CH_4 emissions from reservoir drawdown areas. Inland Waters 8: 329–340.

Kruk, C., L. Rodríguez-Gallego, M. Meerhoff, F. Quintans, G. Lacerot, N. Mazzeo, F. Scasso, J. C. Paggi, E. T. H. M. Peeters, & S. Marten, 2009. Determinants of biodiversity in subtropical shallow lakes (Atlantic coast, Uruguay): Species richness in shallow subtropical lakes. Freshwater Biology 54: 2628–2641.

Kruk, C., L. Rodriguez-Gallego, F. Quintans, G. Lacerot, F. Scasso, N. Mazzeo, M. Meerhoff, & J. C. Paggi, 2006. Biodiversidad y calidad de agua de 18 pequeñas lagunas en la costa sureste de Uruguay Bases para la Conservación y el Manejo de la Costa Uruguaya: 599–610.

Laas, A., P. Nõges, T. Kõiv, & T. Nõges, 2012. High-frequency metabolism study in a large and shallow temperate lake reveals seasonal switching between net autotrophy and net heterotrophy. Hydrobiologia 694: 57–74.

Lacerot, G., S. Kosten, R. Mendonça, E. Jeppesen, J. L. Attayde, N. Mazzeo, F. Teixeira-de-Mello, G. Cabana, M. Arim, J. H. Cantarino Gomes, S. Tserenpil, & M. Scheffer, 2021. Large fish forage lower in the food web and food webs are more truncated in warmer climates. Hydrobiologia 849.17: 3877-3888.

Lagauzère, S., L. Pischedda, P. Cuny, F. Gilbert, G. Stora, & J. M. Bonzom, 2009. Influence of Chironomus riparius (Diptera, Chironomidae) and Tubifex tubifex (Annelida, Oligochaeta) on oxygen uptake by sediments. Consequences of uranium contamination. Environmental Pollution 157: 1234–1242.

Larsen, S., T. Andersen, & D. O. Hessen, 2011. The pCO_2 in boreal lakes: Organic carbon as a universal predictor? Global Biogeochemical Cycles 25: 1–8.

Leal, J. J. F., A. L. Dos Santos Furtado, F. De Assis Esteves, R. L. Bozelli, & M. P. Figueiredo-Barros, 2007. The role of Campsurus notatus (Ephemeroptera: Polymitarcytidae) bioturbation and sediment quality on potential gas fluxes in a tropical lake. Hydrobiologia 586: 143–154.

Lemoine, D. G., F. Mermillod-Blondin, M. H. Barrat-Segretain, C. Massé, & E. Malet, 2012. The ability of aquatic macrophytes to increase root porosity and radial oxygen loss determines their resistance to sediment anoxia. Aquatic Ecology 46: 191–200.

Li, W., X. Xu, J. Yao, N. Tanaka, O. Nishimura, & H. Ma, 2019. Combined effects of elevated carbon dioxide and temperature on phytoplankton-zooplankton link: A multi-influence of climate change on freshwater planktonic communities. Science of the Total Environment 658: 1175–1185.

Li, Y., J. Shang, C. Zhang, W. Zhang, L. Niu, L. Wang, & H. Zhang, 2021. The role of freshwater eutrophication in greenhouse gas emissions: A review. Science of the Total Environment 768.

Liboriussen, L., & E. Jeppesen, 2003. Temporal dynamics in epipelic, pelagic and epiphytic algal production in a clear and a turbid shallow lake: Temporal dynamics algal production in a clear and turbid shallow lake. Freshwater Biology 48: 418–431.

Liboriussen, L., & E. Jeppesen, 2006. Structure, biomass, production and depth distribution of periphyton on artificial substratum in shallow lakes with contrasting nutrient concentrations. Freshwater Biology 51: 95–109.

Litchman, E., P. De, T. Pinto, C. A. Klausmeier, M. K. Thomas, & K. Yoshiyama, 2010. Linking traits to species diversity and community structure in phytoplankton. Fifty years after the ‘‘Homage to Santa Rosalia’’: Old and new paradigms on biodiversity in aquatic ecosystems, 15-28.

Lürling, M., F. Eshetu, E. J. Faassen, S. Kosten, & V. L. M. Huszar, 2013. Comparison of cyanobacterial and green algal growth rates at different temperatures. Freshwater Biology 58: 552–559.

Lürling, M., M. M. Mello, F. van Oosterhout, L. de S. Domis, & M. M. Marinho, 2018. Response of natural cyanobacteria and algae assemblages to a nutrient pulse and elevated temperature. Frontiers in Microbiology 9: 1851.

Ma, Y., L. Sun, C. Liu, X. Yang, W. Zhou, B. Yang, G. Schwenke, & D. L. Liu, 2018. A comparison of methane and nitrous oxide emissions from inland mixed-fish and crab aquaculture ponds. Science of the Total Environment 637–638: 517–523.

Magen, C., L. L. Lapham, J. W. Pohlman, K. Marshall, S. Bosman, M. Casso, & J. P. Chanton, 2014. A simple headspace equilibration method for measuring dissolved methane. Limnology and Oceanography: Methods 12: 637–650.

Maintainer, N., & D. Navarro, 2015. Package “lsr” Type Package Title Companion tò`Learning Statistics with R’’.

Marczak, L. B., R. M. Thompson, & J. S. Richardson, 2007. Meta-analysis: Trophic level, habitat, and productivity shape the food web effects of resource subsidies. Ecology 88: 140–148.

Markfort, C. D., A. L. S. Perez, J. W. Thill, D. A. Jaster, F. Porté-Agel, & H. G. Stefan, 2010. Wind sheltering of a lake by a tree canopy or bluff topography. Water Resources Research 46.

Martinsen, K. T., M. R. Andersen, & K. Sand-Jensen, 2019. Water temperature dynamics and the prevalence of daytime stratification in small temperate shallow lakes. Hydrobiologia 826: 247–262.

Masundire, H. M., 1994. Mean individual dry weight and length-weight regressions of some zooplankton of Lake Kariba. Hydrobiologia 272: 231–238.

McGinnis, D. F., S. Flury, K. W. Tang, & H. P. Grossart, 2017. Porewater methane transport within the gas vesicles of diurnally migrating Chaoborus spp.: An energetic advantage. Scientific Reports 7.

McGraw, K. O., & S. P. Wong, 1992. A Common Language Effect Size Statistic. Psychological Bulletin 111: 361–365.

Mckee, D., D. Atkinson, C. S.E., E. J.W., I. Harvey, T. Heyes, K. Hatton, D. Wilson, & B. Moss, 2002. Macro-zooplankter responses to simulated climate warming in experimental freshwater microcosms. Freshwater Biology 47: 1557–1570.

Meerhoff, M., J. Audet, T. A. Davidson, L. De Meester, S. Hilt, S. Kosten, Z. Liu, N. Mazzeo, H. Paerl, M. Scheffer, & E. Jeppesen, 2022. Feedbacks between climate change and eutrophication: revisiting the allied attack concept and how to strike back. Inland Waters 1–42.

Meerhoff, M., J. M. Clemente, F. T. de Mello, C. Iglesias, A. R. Pedersen, & E. Jeppesen, 2007a. Can warm climate-related structure of littoral predator assemblies weaken the clear water state in shallow lakes? Global Change Biology 13: 1888–1897.

Meerhoff, M., C. Fosalba, C. Bruzzone, N. Mazzeo, W. Noordoven, & E. Jeppesen, 2006. An experimental study of habitat choice by *Daphnia*: Plants signal danger more than refuge in subtropical lakes. Freshwater Biology 51: 1320–1330.

Meerhoff, M., C. Iglesias, F. T. De Mello, J. M. Clemente, E. Jensen, T. L. Lauridsen, & E. Jeppesen, 2007b. Effects of habitat complexity on community structure and predator avoidance behaviour of littoral zooplankton in temperate versus subtropical shallow lakes. Freshwater Biology 52: 1009–1021.

Meerhoff, M., & E. Jeppesen, 2009. Shallow Lakes and Ponds Encyclopedia of Inland Waters: 645–655.

Meerhoff, M., F. T. Mello, C. Kruk, C. Alonso, I. González-bergonzoni, J. P. Pacheco, G. Lacerot, M. Arim, M. Beklio, S. Brucet, G. Goyenola, C. Iglesias, N. Mazzeo, S. Kosten, & E. Jeppesen, 2012. Environmental Warming in Shallow Lakes: A Review of Potential Changes in Community Structure as Evidenced from Space-for-Time Substitution Approaches. Advances in Ecological Research 46: 259–349.

Montoya, J. M., & D. Raffaelli, 2010. Climate change, biotic interactions and ecosystem services. Philosophical Transactions of the Royal Society B: Biological Sciences 365: 2013–2018.

Mooij, W. M., S. Hülsmann, L. N. De Senerpont Domis, B. A. Nolet, P. L. E. Bodelier, P. C. M. Boers, L. M. Dionisio Pires, H. J. Gons, B. W. Ibelings, R. Noordhuis, R. Portielje, K. Wolfstein, & E. H. R. R. Lammens, 2005. The impact of climate change on lakes in the Netherlands: A review. Aquatic Ecology 39: 381–400.

Morales-Williams, A. M., A. D. Wanamaker, C. J. Williams, & J. A. Downing, 2021. Eutrophication Drives Extreme Seasonal CO_2 Flux in Lake Ecosystems. Ecosystems 24: 434–450.

Moresco, G., L. Cabrera, & M. Meerhoff, (in.prep.). Influência do aquecimento global na comunidade fitoplânctonica e seus impactos no ciclo do Carbono.

Moss, B., 2010. Climate change, nutrient pollution and the bargain of Dr Faustus. Freshwater Biology 55: 175–187.

Moss, B., 2011. Allied attack: climate change and eutrophication. Inland Waters 1: 101–105.

Moss, B., S. Kosten, M. Meerhoff, R. Battarbee, E. Jeppesen, N. Mazzeo, K. Havens, G. Lacerot, Z. Liu, L. De Meester, H. Pearl, & M. Scheffer, 2011. Allied attack: climate change and eutrophication. Inland Waters 1: 101–105.

Myhre, G., D. Shindell, F. Bréon, W. Collins, J. Fuglestvedt, J. Huang, D. Koch, J. Lamarque, D. Lee, B. Mendoza, T. Nakajima, A. Robock, G. Stephens, T. Takemura, & H. Zhan, 2013. Anthropogenic and Natural Radiative Forcing: In Climate Change 2013: The Physical Science Basis. Contribution of Working Group I to the Fifth Assessment Report of the Intergovernmental Panel on Climate Change. Cambridge University Press, Cambridge, United Kingdom and New York, NY, USA 659–740.

Nakagawa, S., & I. C. Cuthill, 2007. Effect size, confidence interval and statistical significance: A practical guide for biologists. Biological Reviews 82: 591–605.

Natchimuthu, S., B. Panneer Selvam, & D. Bastviken, 2014. Influence of weather variables on methane and carbon dioxide flux from a shallow pond. Biogeochemistry 119: 403–413.

Nõges, T., R. Laugaste, P. Nõges, & I. Tõnno, 2008. Critical N:P ratio for cyanobacteria and N_2-fixing species in the large shallow temperate lakes Peipsi and Võrtsjärv, North-East Europe. Hydrobiologia 599: 77–86.

Ockenden, M. C., W. Tych, K. J. Beven, A. L. Collins, R. Evans, P. D. Falloon, K. J. Forber, K. M. Hiscock, M. J. Hollaway, R. Kahana, C. J. A. Macleod, M. L. Villamizar, C. Wearing, P. J. A. Withers, J. G. Zhou, C. McW. H. Benskin, S. Burke, R. J. Cooper, J. E. Freer, & P. M. Haygarth, 2017. Prediction of storm transfers and annual loads with data-based mechanistic models using high-frequency data. Hydrology and Earth System Sciences 21: 6425–6444.

Odum, H. T., 1956. Primary Production in Flowing Waters. Limnology and Oceanography 1: 102–117.

Oliveira Junior, E. S., R. J. M. Temmink, B. F. Buhler, R. M. Souza, N. Resende, T. Spanings, C. C. Muniz, L. P. M. Lamers, & S. Kosten, 2019. Benthivorous fish bioturbation reduces methane emissions, but increases total greenhouse gas emissions. Freshwater Biology 64: 197–207.

Oliveira Junior, E., T. van Bergen, J. Nauta, A. Budiša, R. Aben, S. Weideveld, C. Souza, C. Muniz, J. Roelofs, L. Lamers, & S. Kosten, 2020. Water Hyacinth's Effect on Greenhouse Gas Fluxes: A Field Study in a Wide Variety of Tropical Water Bodies. Ecosystems 24: 988-1004.

Ollivier, Q. R., D. T. Maher, C. Pitfield, & P. I. Macreadie, 2019. Punching above their weight: Large release of greenhouse gases from small agricultural dams. Global Change Biology 25: 721–732.

O'Neil, J. M., T. W. Davis, M. A. Burford, & C. J. Gobler, 2012. The rise of harmful cyanobacteria blooms: The potential roles of eutrophication and climate change. Harmful Algae 14: 313–334.

Pacheco, F. S., F. Roland, & J. A. Downing, 2014. Eutrophication reverses whole-lake carbon budgets. Inland Waters 4: 41–48.

Pacheco, J. P., C. Iglesias, M. Meerhoff, C. Fosalba, G. Goyenola, F. Teixeira-de Mello, S. García, M. Gelós, & F. García-Rodríguez, 2010. Phytoplankton community structure in five subtropical shallow lakes with different trophic status (Uruguay): A morphology-based approach. Hydrobiologia 646: 187–197.

Pacheco, J. P., C. Iglesias Frizzera, G. Goyenola, F. Teixeira de-Mello, C. Fosalba, A. Baattrup-Pedersen, M. Meerhoff, & E. Jeppesen, 2021. Invasion of *Ceratium furcoides* in subtropical lakes in Uruguay: Environmental drivers and fish kill record during its bloom. Biological Invasions 23: 3597-3612.

Paerl, H. W., N. S. Hall, & E. S. Calandrino, 2011. Controlling harmful cyanobacterial blooms in a world experiencing anthropogenic and climatic-induced change. Science of the Total Environment 409: 1739–1745.

Paerl, H. W., & J. Huisman, 2008. Climate: Blooms like it hot. Science 320: 57–58.

Paerl, H. W., & V. J. Paul, 2012. Climate change: Links to global expansion of harmful cyanobacteria. Water Research 46: 1349–1363.

Palma-Silva, C., C. C. Marinho, E. F. Albertoni, I. B. Giacomini, M. P. Figueiredo Barros, L. M. Furlanetto, C. R. T. Trindade, & F. de A. Esteves, 2013. Methane emissions in two small shallow neotropical lakes: The role of temperature and trophic level. Atmospheric Environment 81: 373–379.

Palmer, M. F., 1968. Aspects of the respiratory physiology of Tubifex tubifex in relation to its ecology. Journal of Zoology 154: 463–473.

Peacock, M., J. Audet, D. Bastviken, S. Cook, C. D. Evans, A. Grinham, M. A. Holgerson, L. Högbom, A. E. Pickard, P. Zieliński, & M. N. Futter, 2021. Small artificial waterbodies are widespread and persistent emitters of methane and carbon dioxide. Global Change Biology 27: 5109–5123.

Peacock, M., J. Audet, S. Jordan, J. Smeds, & M. B. Wallin, 2019. Greenhouse gas emissions from urban ponds are driven by nutrient status and hydrology. Ecosphere 10: e02643.

Postel, L., H. Fock, & W. Hagen, 2000. Biomass and abundance - Abundance ans species identification In Harris, R. P., P. Wiebe, J. Lenz, H. R. Skjoldan, & M. Huntley (eds), ICES Zooplankton Methodology Manual: 147–153.

Rahman, M. M., 2015. Role of common carp (Cyprinus carpio) in aquaculture production systems. Frontiers in Life Science 8: 399–410.

Rahman, M. M., 2015b. Effects of co-cultured common carp on nutrients and food web dynamics in rohu aquaculture ponds. Aquaculture Environment Interactions 6: 223–232.

Reynolds, C., 2006. Ecology of Phytoplankton. Cambridge University Press.

Rice, E. W., R. B. Baird, & A. D. Eaton, 2017. Standard Methods for the Examination of Water and Wastewater. American Public Health Association.

Richardson, D. C., M. A. Holgerson, M. J. Farragher, K. K. Hoffman, K. B. S. King, M. B. Alfonso, M. R. Andersen, K. S. Cheruveil, K. A. Coleman, M. J. Farruggia, R. L. Fernandez, K. L. Hondula, G. A. López Moreira Mazacotte, K. Paul, B. L. Peierls, J. S. Rabaey, S. Sadro, M. L. Sánchez, R. L. Smyth, & J. N. Sweetman, 2022. A functional definition to distinguish ponds from lakes and wetlands. Scientific Reports 12: 10472.

Riley, W. D., E. C. E. Potter, J. Biggs, A. L. Collins, H. P. Jarvie, J. I. Jones, M. Kelly-Quinn, S. J. Ormerod, D. A. Sear, R. L. Wilby, S. Broadmeadow, C. D. Brown, P. Chanin, G. H. Copp, I. G. Cowx, A. Grogan, D. D. Hornby, D. Huggett, M. G. Kelly, M. Naura, J. R. Newman, & G. M. Siriwardena, 2018. Small Water

Bodies in Great Britain and Ireland: Ecosystem function, human-generated degradation, and options for restorative action. Science of the Total Environment 645: 1598–1616.

Rosentreter, J. A., A. V. Borges, B. R. Deemer, M. A. Holgerson, S. Liu, C. Song, J. Melack, P. A. Raymond, C. M. Duarte, G. H. Allen, D. Olefeldt, B. Poulter, T. I. Battin, & B. D. Eyre, 2021. Half of global methane emissions come from highly variable aquatic ecosystem sources. Nature Geoscience 14: 225–230.

RStudio Team, 2018. RStudio: Integrated Development Environment for R.

Salonen, K., K. Kononen, & L. Arvola, 1983. Respiration of plankton in two small, polyhumic lakes. Hydrobiologia 101: 65–70.

Sanches, L. F., B. Guenet, C. C. Marinho, N. Barros, & F. de Assis Esteves, 2019. Global regulation of methane emission from natural lakes. Scientific Reports 9: 255.

Sander, R., 2015. Compilation of Henry's law constants (version 4.0) for water as solvent. Atmospheric Chemistry and Physics 15: 4399–4981.

Sanseverino, A. M., D. Bastviken, I. Sundh, J. Pickova, & A. Enrich-Prast, 2012. Methane Carbon Support Aquatic Food Webs to the Fish Level. PLoS ONE 7: 1–8.

Sarmento, H., 2012. New paradigms in tropical limnology: the importance of the microbial food web. Hydrobiologia 686: 1–14.

Schallenberg, M., M. D. De Winton, P. Verburg, D. J. Kelly, K. D. Hamill, & D. P. Hamilton, 2013. Ecosystem Services of Lakes. Ecosystem services in New Zealand - Conditions and trends 203–225.

Scheffer, M., 2004. Ecology of Shallow Lakes. Springer, Dordrecht.

Scheffer, M., S. Hosper, M. Meijer, B. Moss, & E. Jeppesen, 1993. Alternative equilibria in shallow lakes. Trends in Ecology and Evolution 8: 275–279.

Scheffer, M., S. Szabo, A. Gragnani, E. H. van Nes, S. Rinaldi, N. Kautsky, J. Norberg, R. M. M. Roijackers, & R. J. M. Franken, 2003. Floating plant dominance as a stable state. Proceedings of the National Academy of Sciences 100: 4040–4045.

Schindler, D. E., 1997. Influence of Food Web Structure on Carbon Exchange Between Lakes and the Atmosphere. Science 277: 248–251.

Schindler, D. E., & M. D. Scheuerell, 2002. Habitat coupling in lake ecosystems. Oikos 98: 177–189.

Schneider, E. L., & S. Carlquist, 1996. Conductive tissue in Ceratophyllum demersus (Ceratophyllaceae). SIDA, Contributions to Botany 17: 437–443.

Signorell, A., A. Alfons, N. Andreregg, T. Aragon, A. Arppe, A. Baddeley, K. Barton, B. Bolker, H. Borchers, F. Caeiro, S. Champely, D. Chessel, & L. Chhay, 2019. DescTools: Tools for Descriptive Statistics.

Smith, V. H., 1998. Cultural Eutrophication of Inland, Estuarine, and Coastal Waters Successes, Limitations, and Frontiers in Ecosystem Science: 7–49.

Smith, V. H., G. D. Tilman, & J. C. Nekola, 1999. Eutrophication: impacts of excess nutrient inputs on freshwater, marine, and terrestrial ecosystems. Environmental Pollution 100: 179–196.

Sobek, S., T. DelSontro, N. Wongfun, & B. Wehrli, 2012. Extreme organic carbon burial fuels intense methane bubbling in a temperate reservoir. Geophysical Research Letters 39.

Sobek, S., E. Durisch-Kaiser, R. Zurbrü, N. Wongfun, M. Wessels, N. Pasche, & B. Wehrli, 2009. Organic carbon burial efficiency in lake sediments controlled by oxygen exposure time and sediment source. Limnology and Oceanography 54: 2243–2254.

Søndergaard, M., R. Bjerring, & E. Jeppesen, 2013. Persistent internal phosphorus loading during summer in shallow eutrophic lakes. Hydrobiologia 710: 95–107.

Sorrell, B. K., & M. T. Downes, 2004. Water velocity and irradiance effects on internal transport and metabolism of methane in submerged Isoetes alpinus and Potamogeton crispus. Aquatic Botany 79: 189–202.

Sorrell, B. K., M. T. Downes, & C. L. Stanger, 2002. Methanotrophic bacteria and their activity on submerged aquatic macrophytes. Aquatic Botany 72: 107–119.

Staehr, P. A., L. Baastrup-Spohr, K. Sand-Jensen, & C. Stedmon, 2012. Lake metabolism scales with lake morphometry and catchment conditions. Aquatic Sciences 74: 155–169.

Steenbergh, A. K., M. M. Meima, M. Kamst, & P. L. E. Bodelier, 2010. Biphasic kinetics of a methanotrophic community is a combination of growth and increased activity per cell. FEMS Microbiology Ecology 71: 12–22.

Steinberg, L. M., & J. M. Regan, 2008. Phylogenetic comparison of the methanogenic communities from an acidic, oligotrophic fen and an anaerobic digester treating municipal wastewater sludge. Applied and Environmental Microbiology 74: 6663–6671.

Stewart, R. I. A., M. Dossena, D. A. Bohan, E. Jeppesen, R. L. Kordas, M. E. Ledger, M. Meerhoff, B. Moss, C. Mulder, J. B. Shurin, B. Suttle, R. Thompson, M. Trimmer, & G. Woodward, 2013. Mesocosm Experiments as a Tool for Ecological Climate-Change Research Advances in Ecological Research: 71–181.

Swartz, T. M., & J. R. Miller, 2021. The American Pond Belt: an untold story of conservation challenges and opportunities. Frontiers in Ecology and the Environment 19: 501–509.

Teixeira de Mello, F., M. Meerhoff, Z. Pekcan-Hekim, & E. Jeppesen, 2009. Substantial differences in littoral fish community structure and dynamics in subtropical and temperate shallow lakes. Freshwater Biology 54: 1202–1215.

Tranvik, L. J., 1988. Availability of dissolved organic carbon for planktonic bacteria in oligotrophic lakes of differing humic content. Microbial Ecology 16: 311–322.

Tranvik, L. J., J. J. Cole, & Y. T. Prairie, 2018. The study of carbon in inland waters — from isolated ecosystems to players in the global carbon cycle. Limnology and Oceanography Letters 3: 41–48.

Tranvik, L. J., J. A. Downing, J. B. Cotner, S. A. Loiselle, R. G. Striegl, T. J. Ballatore, P. Dillon, K. Finlay, K. Fortino, L. B. Knoll, P. L. Kortelainen, T. Kutser, S. Larsen, I. Laurion, D. M. Leech, S. L. McCallister, D. M. McKnight, J. M. Melack, E. Overholt, J. A. Porter, Y. Prairie, W. H. Renwick, F. Roland, B. S. Sherman, D. W. Schindler, S. Sobek, A. Tremblay, M. J. Vanni, A. M. Verschoor, E. von Wachenfeldt, & G. A. Weyhenmeyer, 2009. Lakes and reservoirs as regulators of carbon cycling and climate. Limnology and Oceanography 54: 2298–2314.

Tribe, L. A., C. L. Briens, & A. Margaritis, 1995. Determination of the volumetric mass transfer coefficient (kLa) using the dynamic “gas out–gas in” method: Analysis of errors caused by dissolved oxygen probes. Biotechnology and Bioengineering 46: 388–392.

Trolle, D., P. a. Staehr, T. a. Davidson, R. Bjerring, T. L. Lauridsen, M. Søndergaard, & E. Jeppesen, 2012. Seasonal Dynamics of CO_2 Flux Across the Surface of Shallow Temperate Lakes. Ecosystems 15: 336–347.

Vadeboncoeur, Y., M. J. Vander Zanden, & D. M. Lodge, 2002. Putting the Lake Back Together: Reintegrating Benthic Pathways into Lake Food Web Models. BioScience 52: 44.

Valderrama, J. C., 1981. The simultaneous analysis of total nitrogen and total phosphorus in natural waters. Marine Chemistry 10: 109–122.

Van Bergen, T. J. H. M., N. Barros, R. Mendonça, R. C. H. Aben, I. H. J. Althuizen, V. Huszar, L. P. M. Lamers, M. Lürling, F. Roland, & S. Kosten, 2019. Seasonal and diel variation in greenhouse gas emissions from an urban pond and its major drivers. Limnology and Oceanography 64: 2129–2139.

Van de Bogert, M. C., S. R. Carpenter, J. J. Cole, & M. L. Pace, 2007. Assessing pelagic and benthic metabolism using free water measurements. Limnology and Oceanography-Methods 5: 145–155.

Van Kruistum, H., P. L. E. Bodelier, A. Ho, M. Meima-Franke, & A. J. Veraart, 2018. Resistance and Recovery of Methane-Oxidizing Communities Depends on Stress Regime and History; A Microcosm Study. Frontiers in Microbiology 9: 1714.

Vander Zanden, M. J., & Y. Vandeboncoeur, 2002. Fishes as integrators of benthic and pelagic food webs in lakes. Ecology 83: 2152–2161.

Verpoorter, C., T. Kutser, D. A. Seekell, & L. J. Tranvik, 2014. A global inventory of lakes based on high-resolution satellite imagery. Geophysical Research Letters 41: 6396–6402.

Verreycken, H., G. Van Thuyne, & C. Belpaire, 2011. Length-weight relationships of 40 freshwater fish species from two decades of monitoring in Flanders (Belgium). Journal of Applied Ichthyology: 1416–1421.

Villa, J. A., Y. Ju, T. Stephen, C. Rey-Sanchez, K. C. Wrighton, & G. Bohrer, 2020. Plant-mediated methane transport in emergent and floating-leaved species of a temperate freshwater mineral-soil wetland. Limnology and Oceanography 65: 1635–1650.

Visser, P. M., J. M. H. Verspagen, G. Sandrini, L. J. Stal, H. C. P. Matthijs, T. W. Davis, H. W. Paerl, & J. Huisman, 2016. How rising CO_2 and global warming may stimulate harmful cyanobacterial blooms. Harmful Algae 54: 145–159.

Wanninkhof, R., 2014. Relationship between wind speed and gas exchange over the ocean revisited. Limnology and Oceanography: Methods 12: 351–362.

Wanninkhof, R. H., 1992. Relationship between wind speed and gas exchange. Journal of Geophysical Research 97: 7373–7382.

Webb, J. R., P. R. Leavitt, G. L. Simpson, H. M. Baulch, H. A. Haig, K. R. Hodder, & K. Finlay, 2019. Regulation of carbon dioxide and methane in small agricultural reservoirs: Optimizing potential for greenhouse gas uptake. Biogeosciences 16: 4211–4227.

West, W. E., J. J. Coloso, & S. E. Jones, 2012. Effects of algal and terrestrial carbon on methane production rates and methanogen community structure in a temperate lake sediment. Freshwater Biology 57: 949–955.

West, W. E., S. M. McCarthy, & S. E. Jones, 2015. Phytoplankton lipid content influences freshwater lake methanogenesis. Freshwater Biology 60: 2261–2269.

Wetzel, R. G., 1992. Gradient-dominated ecosystems: sources and regulatory functions of dissolved organic matter in freshwater ecosystems. Hydrobiologia 229: 181–198.

Wetzel, R. G., 2001. Limnology: lake and river ecosystems. Gulf professional publishing

Weyhenmeyer, G. A., S. Kosten, M. B. Wallin, L. J. Tranvik, E. Jeppesen, & F. Roland, 2015. Significant fraction of CO_2 emissions from boreal lakes derived from hydrologic inorganic carbon inputs. Nature Geoscience 8: 933–936.

Wilhelm, S., & R. Adrian, 2008. Impact of summer warming on the thermal characteristics of a polymictic lake and consequences for oxygen, nutrients and phytoplankton. Freshwater Biology 53: 226–237.

Williamson, C. E., J. E. Saros, W. F. Vincent, & J. P. Smol, 2009. Lakes and reservoirs as sentinels, integrators, and regulators of climate change. Limnology and Oceanography 54: 2273–2282.

Xing, Y., P. Xie, H. Yang, A. Wu, & L. Ni, 2006. The change of gaseous carbon fluxes following the switch of dominant producers from macrophytes to algae in a shallow subtropical lake of China. Atmospheric Environment 40: 8034–8043.

Xiong, J., J. T. Huang, L. Nie, & B. D. Xiao, 2013. The effects of nutrient concentration on purification ability and eco-physiology of Ceratophyllum demersum. Acta Hydrobiologica Sinica 37: 1066–1072.

Yan, X., X. Xu, M. Ji, Z. Zhang, M. Wang, S. Wu, G. Wang, C. Zhang, & H. Liu, 2019. Cyanobacteria blooms: A neglected facilitator of CH_4 production in eutrophic lakes. Science of the Total Environment 651: 466–474.

Yan, X., X. Xu, M. Wang, G. Wang, S. Wu, Z. Li, H. Sun, A. Shi, & Y. Yang, 2017. Climate warming and cyanobacteria blooms: Looks at their relationships from a new perspective. Water Research 125: 449–457.

Yang, H., T. Andersen, P. Dörsch, K. Tominaga, J. E. Thrane, & D. O. Hessen, 2015. Greenhouse gas metabolism in Nordic boreal lakes. Biogeochemistry 126: 211–225.

Yang, Y., J. Chen, T. Tong, B. Li, T. He, Y. Liu, & S. Xie, 2019. Eutrophication influences methanotrophic activity, abundance and community structure in freshwater lakes. Science of the Total Environment 662: 863–872.

Yoshida, N., H. Iguchi, H. Yurimoto, A. Murakami, & Y. Sakai, 2014. Aquatic plant surface as a niche for methanotrophs. Frontiers in Microbiology 5: 30.

Yvon-Durocher, G., A. P. Allen, D. Bastviken, R. Conrad, C. Gudasz, A. St-Pierre, N. Thanh-Duc, & P. A. Del Giorgio, 2014. Methane fluxes show consistent temperature dependence across microbial to ecosystem scales. Nature 507: 488–491.

Yvon-Durocher, G., C. J. Hulatt, G. Woodward, & M. Trimmer, 2017. Long-term warming amplifies shifts in the carbon cycle of experimental ponds. Nature Climate Change 7: 209–213.

Yvon-Durocher, G., J. I. Jones, M. Trimmer, G. Woodward, & J. M. Montoya, 2010. Warming alters the metabolic balance of ecosystems. Philosophical Transactions of the Royal Society B: Biological Sciences 365: 2117–2126.

Yvon-Durocher, G., J. M. Montoya, G. Woodward, J. I. Jones, & M. Trimmer, 2011. Warming increases the proportion of primary production emitted as methane from freshwater mesocosms. Global Change Biology 17: 1225–1234.

Zambrano, L., M. Scheffer, M. Martínez-ramos, & M. Martinez-ramos, 2001. Catastrophic Response of Lakes to Benthivorous Fish Introduction. Oikos 94: 344–350.

Zheng, H., Z. Fu, J. Zhong, & W. Long, 2018. Low methane emission in rice cultivars with high radial oxygen loss. Plant and Soil 431: 1–10.